Méthodes de commande extrémale avec action anticipative: application à des systèmes d'énergie renouvelable soumis à des perturbations mesurables

par

Anouer KEBIR

THÈSE PAR ARTICLES PRÉSENTÉE À L'ÉCOLE DE TECHNOLOGIE SUPÉRIEURE COMME EXIGENCE PARTIELLEÀ L'OBTENTION DU DOCTORAT EN GÉNIE
Ph. D.

MONTRÉAL, LE 19 OCTOBRE 2018

ÉCOLE DE TECHNOLOGIE SUPÉRIEURE
UNIVERSITÉ DU QUÉBEC

PRÉSENTATION DU JURY

CETTE THÈSE A ÉTÉ ÉVALUÉE

PAR UN JURY COMPOSÉ DE :

Mme Lyne Woodward, directeur de thèse
Département de génie électrique à l'École de technologie supérieure

Mme Ouassima Akhrif, codirecteur de thèse
Département de génie électrique à l'École de technologie supérieure

M. Éric David, président du jury
Département de génie mécanique à l'École de technologie supérieure

M. Guy Gauthier, membre du jury
Département de génie de la production automatisée à l'École de technologie supérieure

M. Michel Perrier, examinateur externe
Département de génie à l'École polytechnique de Montréal

IL A FAIT L'OBJET D'UNE SOUTENANCE DEVANT JURY ET PUBLIC

LE 28 SEPTEMBRE 2018

À L'ÉCOLE DE TECHNOLOGIE SUPÉRIEURE

DÉDICACE

À la mémoire de mon grand-père Ahmed Bou Othmane.

REMERCIEMENTS

Je tiens tout d'abord à exprimer mes sincères remerciements à ma directrice de recherche, professeure Lyne Woodward pour son dévouement, son enthousiasme, et sa grande disponibilité. Merci pour votre patience, vos lectures et relectures des différentes parties de ce travail et votre soutien tout au long de la réalisation de ce projet.

J'exprime également ma profonde gratitude à ma codirectrice, professeure Ouassima Akhrif pour son écoute, ses précieux conseils et sa contribution importante au niveau théorique. Merci pour vos encouragements, vos lectures attentives et votre contribution à l'aboutissement de cette thèse.

Je suis aussi reconnaissant pour l'appui financier qui m'a été accordé par le conseil de recherches en sciences naturelles et en génie du canada (CRSNG) et qui a contribué énormément au bon déroulement de cette thèse.

J'aimerais ensuite remercier les membres de jury d'avoir accepté d'évaluer cette thèse et contribuer à l'amélioration de mon travail.

Un grand merci aussi aux membres du Groupe de Recherche en Électronique de Puissance et Commande Industrielle (GREPCI) pour leur support matériel et avec qui j'ai partagé ma passion de recherche et échangé des discussions intéressantes et constructives.

Mes remerciements chaleureux vont à mes parents, à ma sœur Amira et mes frères Anis et Omar pour leur amour inconditionnel, leurs encouragements et leur présence malgré la distance.

Je souhaite aussi remercier mes amis qui m'ont accompagné et soutenu au cours de ces années, particulièrement mon ami Moslem et mon amie Darine.

Enfin, un grand merci à mon épouse Amal qui a toujours cru en moi et m’a supporté tout au long de ce parcours, je t’aime !

MÉTHODES DE COMMANDE EXTRÉMALE AVEC ACTION ANTICIPATIVE: APPLICATION À DES SYSTÈMES D'ÉNERGIE RENOUVELABLES SOUMIS À DES PERTURBATIONS MESURABLES

Anouer KEBIR

RÉSUMÉ

L'optimisation en temps réel a pour objectif d'amener et de maintenir un système à son point d'opération optimal et ce, indépendamment des perturbations externes pouvant faire varier ce point optimal. Dans de nombreuses situations, ces systèmes sont non-linéaires et ont une dynamique méconnue. Aussi, l'utilisation d'une méthode d'optimisation en temps réel qui ne se base pas sur un modèle dynamique fondamental tout en tenant compte du temps de réponse du système est nécessaire. La commande extrémale est une approche possible pour optimiser un tel type de système en temps réel. Un modèle empirique est alors utilisé pour estimer le gradient de la fonction objectif et ensuite, le commander à zéro, point optimal de la fonction objectif. Toutefois, cette méthode d'optimisation ne converge pas rapidement et/ou précisément vers le point de fonctionnement optimal désiré lorsque le système est soumis régulièrement à des perturbations externes.

Notre projet de recherche vise à développer de nouvelles approches pour la commande extrémale afin qu'elle amène un système dont la dynamique est inconnue à converger rapidement et précisément vers le point de fonctionnement optimal et ce, malgré la présence de perturbations externes. Dans le cadre de cette thèse, trois approches sont développées. L'idée de base de ces approches consiste à intégrer dans la commande extrémale une action anticipative à base d'un réseau de neurones multicouches qui donne une estimation de la position du point de fonctionnement optimal du système lorsqu'il est soumis à l'effet de perturbations externes. Cette estimation est une information précieuse permettant d'adapter en temps réel les paramètres de la commande extrémale afin d'améliorer sa précision et sa vitesse de convergence en présence de perturbations externes. Les trois approches proposent trois différentes façons de contrôler les paramètres de la commande extrémale. Les deux premières approches améliorent la performance de la commande extrémale lorsque le système est soumis à des perturbations mesurables. La première approche utilise l'optimum du système estimé par l'action anticipative comme une condition initiale pour la commande extrémale afin de pousser rapidement le système au voisinage de son optimum et par la suite contrôler le système en boucle fermée avec la commande extrémale pour converger vers l'optimum réel. La deuxième approche adapte l'amplitude du signal d'excitation de la commande extrémale en fonction de l'optimum du système estimé par l'action anticipative afin d'assurer le maximum de vitesse de convergence tout en garantissant une meilleure précision autour de l'optimum. La troisième approche améliore la performance de la commande extrémale malgré la présence des perturbations mesurables et/ou non mesurables avec l'utilisation d'un modèle par réseau de neurones adaptatif dans l'action anticipative qui ajuste en temps réel les paramètres de la commande extrémale.

Une étude théorique approfondie des approches proposées est effectuée. Celle-ci permet à la fois d'établir la preuve de stabilité pour 2 des trois approches proposées et également de formuler théoriquement le gain en termes de temps de convergence des approches par rapport à la méthode de perturbation. L'amélioration de la performance de la commande extrémale avec les trois approches est validée en simulation, dans le cas de l'optimisation d'une pile à combustible microbienne et, expérimentalement dans le cas de l'optimisation d'un système photovoltaïque. Les résultats expérimentaux montrent que l'efficacité de suivi de l'optimum d'un système perturbé optimisé en utilisant chacune des trois approches proposées augmente respectivement jusqu'à 30 %, 20% et 15 % en comparaison avec la méthode de perturbation.

Mots-clés: Optimisation en temps réel, commande extrémale, réseau de neurones, système photovoltaïque, pile à combustible microbienne.

EXTREMUM-SEEKING CONTROL METHODS WITH ANTICIPATIVE ACTION: APPLICATION TO RENEWABLE ENERGY SYSTEMS SUBJECT TO MEASURABLE DISTURBANCES

Anouer KEBIR

ABSTRACT

Real-time optimization aims to bring and maintain a system at its optimum point of operation, regardless of external disturbances that may affect this optimal point. In many situations, these systems are non-linear and have an unknown dynamic. Also, the use of a real-time optimization method which does not require a fundamental dynamic model and takes into account the response time of the system is necessary. Extremum-seeking control is one approach able to optimize in real time such a type of system. It only requires an empirical model to estimate the gradient of the objective function prior to control it at zero, the optimum of the objective function. However, this optimization method does not converge quickly and/or precisely to the desired optimum operating point when the system is regularly exposed to external disturbances.

Our research project aims to develop new approaches to make the extremum-seeking control scheme able to bring a system with unknown dynamics to converge quickly and accurately to its optimal operating point, despite the presence of external disturbances. In this thesis, three approaches are developed. The basic idea of these approaches is to integrate in the extremum-seeking control method an anticipative action based on a multilayer neural network model which gives an estimate of the position of the optimal operating point of the system with regards to the external disturbances to which it is submitted. This estimate is used to adapt in real time the parameters of the extremum seeking control in order to improve its accuracy and reduce its time of convergence under external disturbances. The three approaches offer three different ways to control the parameters of the extremum-seeking control scheme. The first two approaches improve the performance of the extremum seeking control loop when the system faces measurable disturbances. The first approach uses the estimation of the system's optimum provided by the anticipative action as an initial condition for the extremum-seeking controller in order to quickly push the system close to its optimum and then fine tune this position using the extremum seeking control loop. The second approach adapts the amplitude of the excitation signal of the extremum-seeking control loop according to the system optimum estimated by the anticipative action in order to ensure the maximum speed of convergence while guaranteeing a better precision around the optimum. The third approach improves the performance of the extremum-seeking control scheme despite the presence of measurable and/or unmeasurable disturbances by adapting online the neural network model used in the anticipative.

A detailed theoretical study of the proposed approaches is provided. This study establishes the stability of two approaches. Moreover, it formulates the gain obtained with the proposed methods in terms of time of convergence compared with the perturbation method. The improvement of the performance of the approaches is validated through simulations of a microbial fuel cell. It is also validated experimentally using a photovoltaic system. The results of this experimental study show that the optimum tracking efficiency of each of the three proposed methods is improved up to 30%, 20% and 15% respectively compared to the perturbation method.

Keywords: Real-time optimization, extremum-seeking control, neural network, photovoltaic system, microbial fuel cell.

TABLE DES MATIÈRES

Page

LISTE DES TABLEAUX

Page

LISTE DES FIGURES

Page

LISTE DES ABRÉVIATIONS, SIGLES ET ACRONYMES

BFCS	Broyden, Fletcher, Goldfard and Shanno
ESC	Extremum-seeking control
ESC_{aa}	Extremum-seeking control with anticipative action
ESC_{a}	Extremum-seeking control with adaptive excitation
ESC_{ad}	Extremum-seeking control with adaptive anticipative action
MFC	Microbial fuel cell
PV	Photovoltaic panel
PID	Proportional-integral-derivative controller
RTO	Real-time optimisation
RES	Renewable energy sources
NN	Neural network

LISTE DES SYMBOLES ET UNITÉS DE MESURE

UITÉS DE MESURE

kΩ	Kiloohm
Ω	Ohm
L	Litre
s	Seconde
S	Substrat
mg	Milligramme
W	Watt
mW	Milliwatt
rad	Radian
J	Joule
Hz	Hertz

SYMBOLES

Scalaires

a	amplitude du signal d'excitation
a_{min}	amplitude minimale du signal d'excitation
a_{max}	amplitude maximale du signal d'excitation
b	nombre de neurones d'entrée
c	nombre de neurones dans la couche cachée
D_a	nombre de lignes dans la base de données
e_{max}	erreur maximale
E	erreur quadratique
E_{av}	erreur quadratique moyenne
g	gradient
$\hat{g}$	gradient estimé
$\widehat{g_{\varepsilon}}_{av}$	gradient moyen estimé
G	radiation

J	fonction objectif
J^*	optimum de la fonction objectif
k	gain
k_{ESC}	gain ESC
k_{ESC_a}	gain ESC_a
m_{NN}	pente de la fonction tangente hyperbolique
N_p	nombre de périodes du signal d'excitation
N_g	nombre total de points utilisés pour le test de généralisation
N_D	nombre maximal de lignes
P_s^*	puissance de sortie maximale
P_s	puissance de sortie
P_{pvc}	puissance de sortie de petite cellule photovoltaïque
p	modèle empirique
R_{ph}	valeur de la photorésistance
R_{in}	résistance interne
R_{ex}	charge externe
$\hat{R}_{in}$	résistance interne estimée
R_{sh}	résistance Shunt
R_{cst}	résistance constante
S_0	concentration du substrat
T_c	temps de convergence
T_{eff}	efficacité de suivi
T_{acc}	précision à l'équilibre
T_{ESC}	temps de convergence de ESC
$T_{\mathrm{ESC_{aa}}}$	temps de convergence de ESC_{aa}
$T_{ESC_{NN}}$	temps de convergence du NN
$T_{ESC_{\mathrm{a}}}$	temps de convergence de ESC_a
T_{PID}	temps de réponse du contrôleur PID

T_e	température anodique
T_{MFC}	temps de réponse le plus long de la MFC
T_P	temps de réponse du potentiomètre numérique
u	entrée du système
V_{ex}	tension de sortie du système PV
V_{sh}	tension de la résistance Shunt
V_p	tension de sortie du gradateur numérique
ω_h	fréquence de coupure du filtre passe-haut
ω_l	fréquence de coupure du filtre passe-bas
ω	fréquence d'excitation
y	sortie du système
y^*	sortie optimale du système
α	loi de commande
β	référence générée par la commande
β^*	référence optimale
$\widehat{\beta^*}$	référence optimale estimée
β_0	condition initiale de la référence
$\hat{\beta}_{av}$	référence moyenne
ε^*	erreur d'estimation
ε	erreur
η	moyenne de J
ϕ	fonction d'activation
σ	loi de commutation
μ	paramètre de réglage
γ	gain variable
Δ_g	retard
ϑ_g	tolérance

Vecteurs, Matrices

A	matrice jacobienne
d_u	perturbations non mesurables
d_m	perturbations mesurables
$d_{m_{av}}$	moyenne de perturbations mesurables
d	perturbations externes
f	dynamique du système
x	variables d’état
W_1	poids synaptiques entre le neurone d'entrée et la couche cachée
W_2	poids synaptiques entre la couche cachée et le neurone de sortie

INTRODUCTION

L'un des principaux défis dans l'industrie est de savoir comment exploiter un système au meilleur de sa performance malgré les changements de ses conditions d'opération ou de fonctionnement au cours du temps. L'index de performance d'un système peut être maximisé ou minimisé selon le cas. Par exemple, on peut vouloir maximiser la puissance de sortie d'une source d'énergie renouvelable (un panneau photovoltaïque, une éolienne, une pile à combustible microbienne, etc.) et ce, malgré les perturbations auxquelles est soumis ce système (ensoleillement, vent, concentration du substrat d'alimentation etc.). Un autre exemple est la minimisation du coût de construction d'un produit dans une chaîne de production. Par conséquent, dans de nombreuses applications d'ingénierie, le système doit opérer à proximité d'un point de fonctionnement optimal. En d'autres termes, un point de fonctionnement qui maximise ou minimise une fonction objectif ou fonction coût. Toutefois, si les conditions de fonctionnement du système changent à cause des perturbations externes, la fonction objectif quantifiant la performance de ce système change et conséquemment, son point de fonctionnement optimal varie aussi. Dans certaines situations, le point de fonctionnement optimal du système varie incidemment, car le système n'est soumis à une perturbation externe qu'accidentellement. Par exemple, dans le cas d'optimisation d'une chaîne de production, il est possible que l'une des machines tombe en panne. Ainsi, il faut intervenir occasionnellement afin de ramener le système autour de son point de fonctionnement optimal malgré cette défaillance. Dans ces situations, on peut utiliser des méthodes d'optimisation qui ne sont pas exécutées en temps réel comme les méthodes de recherche opérationnelle (Taha, 2017; Yadav & Malik) pour résoudre ce genre de problème. En revanche, il y a d'autres situations où le système est, en permanence, soumis à des perturbations externes qui ont pour effet de faire varier fréquemment son point de fonctionnement optimal. Ce genre de situation survient dans les systèmes à énergie renouvelable (Hatti, 2018). Par exemple, la meilleure performance d'un panneau photovoltaïque (PV) en terme de production de puissance électrique est fortement liée au niveau de radiation du soleil et à la température externe (Giovanni, Carlos Andres, & Giovanni, 2016). Ces deux perturbations externes varient constamment en fonction du temps, ce qui cause la variation continuelle du point de fonctionnement optimal du système PV. Ainsi, il faut contrôler le système PV afin de suivre en temps réel son maximum de puissance malgré la présence des perturbations externes (Bhatnagar & Nema, 2013; Ram, Rajasekar, & Miyatake, 2017; Verma, Nema, Shandilya, & Dash, 2016). Dans ce genre de situation, le recours à une méthode d’optimisation en temps réel (RTO) (Bonvin, 2017) est indispensable afin de ramener le système autour de son point de fonctionnement optimal à chaque fois qu’une perturbation externe survient. Dans la littérature, on trouve plusieurs choix de méthodes d’optimisation en temps réel (Bonvin, 2017). La complexité du système à commander est un facteur primordial dans le choix de la méthode d’optimisation. Par exemple, dans le cas de l’optimisation d’un système pouvant être modélisé par un modèle fondamental, une méthode d’optimisation dite avec modèle peut être utilisée pour ramener le système autour de son point de fonctionnement optimal (Gao, Hernández, & Engell, 2016; Golden & Ydstie, 1989; Roberts, 1979). Cependant, quand le système à optimiser est fortement non linéaire et possède une dynamique très complexe à modéliser par un modèle fondamental, une méthode d’optimisation dite sans modèle est plus adéquate pour commander ce type de système. En outre, la fonction objectif peut ne pas être disponible analytiquement pour le concepteur. La complexité croissante des systèmes d'ingénierie a conduit à de nombreux défis d'optimisation puisque les solutions analytiques aux problèmes d’optimisation non linéaires et aux systèmes de dimension infinie sont difficiles, voire impossibles à obtenir. Par exemple, dans le cas d’optimisation d’un système chimique comme la pile à combustible microbienne (Dicks & Rand, 2018; Nikhil, Chaitanya, Srikanth, Swamy, & Mohan, 2018), la puissance optimale produite par ce système dépend de la valeur de sa charge interne. Si on souhaite extraire la puissance maximale produite par la pile, il faut que la charge externe égale la charge interne qui varie selon les variations de la concentration et du débit de substrat d’alimentation, de la température, etc. Toutefois, il est impossible d’effectuer une mesure directe de la charge interne à partir d’un capteur ou analytiquement grâce à un modèle, car la pile à combustible microbienne est un système chimique avec une dynamique complexe difficile à modéliser par les lois physiques dans toutes ses conditions de fonctionnement (Xia, Zhang, Pedrycz, Zhu, & Guo, 2018).

Dans le cadre de cette thèse, notre centre d'intérêt est l'optimisation d'un système fortement non linéaire avec une dynamique complexe à modéliser par un modèle fondamental et soumis en permanence à l'effet de perturbations externes. De ce fait, l'utilisation d'une méthode d'optimisation en temps réel à base d'un modèle fondamental mènerait à des solutions sous-optimales en raison de l'incertitude du modèle. Ainsi, à partir des spécifications de ce type de système, notre étude est focalisée sur les méthodes d'optimisation à base d'un modèle empirique où le procédé à optimiser est considéré comme une boîte noire. Ces méthodes d'optimisation sont connues sous le nom de commande extrémale (Ariyur & Krstić, 2003).

La commande extrémale par la méthode de perturbation (C. Zhang & Ordóñez, 2011) est parmi les méthodes d'optimisation en temps réel les plus populaires dans les situations où le modèle et/ou l'expression analytique de la fonction coût du système à optimiser ne sont pas disponibles pour le concepteur. Elle ne nécessite que la disponibilité des mesures de signaux d'entrée et de sortie du système à contrôler. Cette méthode est caractérisée par sa robustesse, mais sa principale limite de performance est sa vitesse de convergence vers le point de fonctionnement optimal qui peut être particulièrement lente pour un système dont la dynamique est elle-même très lente. Ainsi, lorsque le processus est soumis à l'effet d'une perturbation externe rapide, la méthode d'optimisation en temps réel peut converger vers un point de fonctionnement sous-optimal.

Le but de cette thèse est de proposer une nouvelle approche qui améliore la performance de la commande extrémale avec la méthode de perturbation en termes de précision et de temps de convergence dans le cas de l'optimisation d'un système complexe inconnu soumis à l'effet d'une perturbation externe rapide. L'idée de base consiste à intégrer une action anticipative à base d'un réseau de neurones dans la méthode de perturbation qui permet l'adaptation des paramètres de la commande extrémale. La performance des approches proposées sera formulée théoriquement dans le cas d'optimisation d'un système quelconque avant d'être validée expérimentalement dans le cas d'optimisation d'un système PV et par des simulations dans le cas d'optimisation d'une pile à combustible microbienne. De plus, une nouvelle preuve de stabilité sera établie pour les approches développées.

Le rapport est présenté sous forme d'une thèse par articles. Ainsi, les trois derniers chapitres sont consacrés à la présentation des approches proposées sous forme de trois articles de journaux dont deux sont soumis et un est publié dans une revue scientifique.

La thèse est constituée de quatre chapitres. Dans le premier chapitre, le problème d'optimisation en temps réel (RTO) est défini avant de présenter une étude bibliographique sur la commande extrémale avec la méthode de perturbation et un survol des différentes approches proposées dans les revues afin d'améliorer la performance en termes de temps et de précision de convergence. Ensuite, on définit l'objectif principal, les objectifs spécifiques et la méthodologie du projet. Enfin, on met en évidence la contribution et l'originalité des approches proposées dans cette thèse afin d'améliorer la performance de la commande extrémale.

Dans le deuxième chapitre, on propose une amélioration de la performance de la commande extrémale dans le cas où le système est soumis à l'effet des perturbations externes mesurables rapides. L'approche consiste à intégrer une action anticipative à base d'un réseau de neurones qui estime le point de fonctionnement optimal à partir de la mesure de la perturbation externe afin d'amener rapidement le système dans une région proche du point optimal. La commande extrémale pourra ensuite éliminer l'erreur entre le point optimal estimé par le modèle de réseaux de neurones et l'optimum réel du système. La performance de l'approche proposée est évaluée théoriquement pour un système quelconque avant d'être évaluée en simulation dans un contexte d'optimisation d'une pile à combustible microbienne et expérimentalement dans le cas de l'optimisation d'un système PV.

Le troisième chapitre introduit une autre approche qui permet la commande adaptative de l'amplitude du signal d'excitation dans la commande extrémale afin de converger rapidement et précisément vers l'optimum d'un système soumis à l'effet d'une perturbation externe mesurable rapide. Cette approche représente une autre méthode d'intégration de l'action anticipative présentée dans le deuxième chapitre afin de contrôler les paramètres de la commande extrémale. La stabilité de l'approche est démontrée. L'amélioration de performance est validée théoriquement dans le cas d'optimisation d'un système quelconque et expérimentalement dans le cas de l'optimisation d'un système PV.

Le quatrième chapitre propose une amélioration de la performance de la commande extrémale en termes de temps de convergence et de précision lorsque le système est soumis à l'effet de perturbations externes mesurables et non-mesurables. L'idée générale est inspirée de l'approche proposée dans le deuxième chapitre, mais dans cette situation, une nouvelle structure de la commande extrémale est proposée afin d'intégrer un réseau de neurones dont l'apprentissage est effectué en temps réel et qui peut tenir compte des perturbations mesurables et non-mesurables dans son estimation de l'optimum du système. La stabilité de l'approche proposée est démontrée. L'amélioration de performance est prouvée expérimentalement dans le cas de l'optimisation d'un système PV.

CHAPITRE 1

REVUE DE LITTÉRATURE ET CONTRIBUTIONS

Dans le présent chapitre, on définit tout d'abord le problème d'optimisation en temps réel avant de présenter une étude bibliographique sur le développement théorique de la commande extrémale au cours des deux dernières décennies. Plus spécifiquement, on focalise notre étude sur la commande extrémale basée sur la méthode de perturbation et les différentes approches proposées afin d'améliorer la performance de cette méthode en termes de temps de convergence et/ou de précision. Subséquemment, on fixe l'objectif principal et les objectifs spécifiques de la thèse. Enfin, on termine en présentant la méthodologie et la contribution des approches proposées dans cette thèse visant à améliorer la performance de la commande extrémale.

1.1 Définition du problème d'optimisation en temps réel

On considère l'optimisation en temps réel d'un système dynamique soumis à l'effet de perturbations externes et décrit par l'équation suivante :

$$\begin{aligned} \dot{x} &= f(x,u,d) \\ y &= h(x) \end{aligned} \tag{1.1}$$

avec f, la dynamique du système considérée comme inconnue, $x \in \mathbb{R}^n$, le vecteur d'états, $y \in \mathbb{R}$, la sortie du système, $d \in \mathbb{R}^v$, le vecteur des perturbations externes et $u \in \mathbb{R}$, l'entrée du système commandée par une loi de commande lisse α paramétrée par $\beta \in \mathbb{R}$ en boucle fermée:

$$u = \alpha(x,\beta). \tag{1.2}$$

Ainsi, d'après (1.2) la dynamique du système en boucle fermée est décrite par l'équation suivante :

$$\dot{x} = f(x, \beta, d). \tag{1.3}$$

Le paramètre β est la référence générée par la méthode d'optimisation en temps réel devant être suivie par l'entrée u avec la loi de commande α (par exemple un contrôleur PID) afin de maximiser ou minimiser la sortie du système y en régime statique :

$$\begin{gathered} \max_{\beta} y \\ t.q.\ \dot{x} = f(x, \beta, d) = 0 \end{gathered} . \tag{1.4}$$

En définissant J comme la relation statique entre la fonction objectif et le paramètre β le problème devient :

$$\max_{\beta} J. \tag{1.5}$$

Ainsi, afin de converger précisément vers l'optimum de la fonction objectif J d'un système dynamique perturbé, il faut que la référence β soit ajustée en temps réel alors que le système (1.3) est dans son régime permanent ($\dot{x} = f(x, d, \beta) = 0$).

Dans la présente thèse, la commande extrémale est choisie comme méthode d'optimisation en temps réel de par sa capacité à résoudre le problème d'optimisation (1.5) tout en supposant que la fonction f est inconnue et que seule la mesure de y est disponible.

1.2 Développement théorique de la commande extrémale

La commande extrémale est l'une des premières méthodes de commandes adaptatives. En 1922, Leblanc a proposé la commande extrémale avec la méthode de perturbation (Leblanc, 1922) pour maximiser la puissance transférée d'une ligne de transport électrique aérienne à une voiture de tramway. Toutefois, cette étude ne fait aucune mention d'une validation expérimentale. Pendant la deuxième guerre mondiale, les russes ont porté un intérêt considérable au développement de la commande extrémale (Kazakevich, 1944). La première étude scientifique de la commande extrémale a vu le jour dans le monde occidental avec la publication de (Draper & Li, 1951). L'étude consiste à maximiser la puissance de sortie d'un moteur à combustion interne en contrôlant le temps d'allumage à l'aide de la commande extrémale. À partir de cette publication, l'optimisation de la combustion d'un moteur est le domaine le plus populaire de l'application de la commande extrémale. D'après (Åström & Wittenmark, 2013), les années entre 1950 et 1960 sont des années fertiles pour le développement de la commande adaptative, ce qui est aussi le cas pour la commande extrémale. Dans ces années, le nombre de publications portant sur la commande extrémale a augmenté considérablement et la méthode a connu de nombreuses appellations pendant ses débuts (Y Tan, Moase, Manzie, Nešić, & Mareels, 2010). On trouve par exemple: système de contrôle optimal (optimalizing control system) (Draper & Li, 1951), régulateur de recherche d'extremum (extremum seeking regulator) (Ostrovskii, 1957), systèmes d'escalade de colline (hill-climbing systems) (Y Tan et al., 2010), mais l'appellation la plus populaire dans ces deux dernières décennies est commande extrémale (extremum seeking control) (Ariyur & Krstić, 2003). Dans ces années, la plupart des résultats ont porté sur la description des algorithmes de commande extrémale et l'exploration de leurs performances dans des problèmes d'optimisation très particuliers. Néanmoins, les chercheurs ont fait face à la difficulté de formuler mathématiquement un modèle qui est assez général pour décrire le cas d'optimisation d'une grande classe de systèmes, tout en démontrant la stabilité. Au cours des quatre décennies qui suivent (1960-2000), les chercheurs vont s'orienter vers d'autres méthodes d'optimisation.

L'activité de recherche sur la commande extrémale dans le cas où le système à optimiser est considéré comme une boîte noire tout en supposant qu'il n'appartienne à aucune classe bien précise de systèmes a été relancée dans les années 2000 par la publication de (Krstić & Wang, 2000). Sans prédéfinir la structure du système, les auteurs ont prouvé que la commande extrémale avec la méthode de perturbation est localement stable si elle satisfait certaines hypothèses et conditions sur le choix des paramètres de commande. À partir de cette preuve de stabilité, il a été établi que la commande extrémale peut être appliquée à une grande classe de systèmes. Aussi, le nombre de publications au sujet de la commande extrémale a augmenté exponentiellement dans ces deux dernière décennies (en passant de quelques centaines à quelques milliers de publications) et ce, grâce à la performance de la commande extrémale dans de nombreux domaines comme décrit dans (C. Zhang & Ordóñez, 2011). La stabilité semi-globale de la commande extrémale avec la méthode de perturbation a été démontrée par (Ying Tan, Nešić, & Mareels, 2006), ce qui prouve la robustesse de la méthode face aux perturbations externes. Ainsi, dans ces deux dernières décennies, le développement théorique et pratique de la commande extrémale a connu une croissance exponentielle (Ariyur & Krstić, 2003; Brunton, Rowley, Kulkarni, & Clarkson, 2010; Dong, Li, Salsbury, House, & Wu, 2018; Guay, Dochain, & Perrier, 2004; Krstić, 2013; Leyva et al., 2006; Oliveira, Krstić, & Tsubakino, 2017; Peterson & Stefanopoulou, 2004; Toloue & Moallem, 2017; Yin, Chen, & Zhong, 2014).

Une multitude de classifications des méthodes d'optimisation en temps réel avec la commande extrémale a été publiée dans ces deux dernières décennies dans le but de présenter le développement théorique de la commande (Haring, 2016; Larsson, 2001; Ryan, 2012; Y Tan et al., 2010). D'après ces revues de littérature, on peut constater qu'il y a toujours une tendance à classifier les méthodes de commande extrémale principalement en deux catégories. La première catégorie rassemble les méthodes de commande extrémale qui considèrent le système et la fonction objectif à optimiser comme inconnus (Ghaffari, Krstić, & Nešić, 2012; Khong, Nešić, Manzie, & Tan, 2013; Khong, NešIć, Tan, & Manzie, 2013; Krstić & Wang, 2000). Dans cette catégorie, la méthode de perturbation est la plus utilisée parmi toutes les méthodes de commande extrémale (C. Zhang & Ordóñez, 2011). Cette méthode est caractérisée par sa robustesse car elle requiert peu d'informations sur le système afin de l'optimiser. Toutefois, cette approche est caractérisée par une vitesse de convergence très lente et une précision qui décroit si le système est soumis à l'effet d'une perturbation externe rapide (Krstić, 2000). La deuxième classe est constituée principalement des méthodes (que nous appellerons ci-après méthodes paramétriques) qui paramètrent la fonction objectif et/ou la dynamique du système afin d'améliorer la performance de la commande extrémale par la méthode de perturbation en termes de vitesse de convergence et/ou de précision (Clarke & Godfrey, 1966; Haber, 1986; Michalowsky & Ebenbauer, 2015; Mohammadi, Manzie, & Nešić, 2014; Sharafi, Moase, & Manzie, 2015).

Dans le cadre de cette thèse, puisque notre but est également d'améliorer la vitesse de convergence et la précision de la commande extrémale par la méthode de perturbation, on va présenter le principe de fonctionnement de cette méthode d'optimisation en temps réel et identifier sa principale limite de performance. Par la suite, on va présenter une étude bibliographique des méthodes qui poursuivent le même objectif, soit l'amélioration de la performance de la commande extrémale en termes de vitesse de convergence et/ou de précision.

1.2.1 La commande extrémale basée sur la méthode de perturbation

L'idée de base de cette approche consiste à superposer un signal d'excitation avec une faible fréquence et une faible amplitude à l'entrée du système afin d'observer l'impact de ce dernier sur la sortie du système y en régime statique, soit sur la fonction objectif J. En fonction de la variation de la sortie par rapport à l'entrée, il sera décidé dans quel sens et de combien il faut bouger l'entrée de commande. De nombreuses méthodes adoptent cette approche (L Woodward, Perrier, Srinivasan, Pinto, & Tartakovsky, 2010). La méthode d'estimation de gradient avec la méthode de perturbation est l'une des méthodes les plus connues et les plus anciennes. Dans cette méthode, le gradient g de la fonction objectif J par rapport à la référence β ($g = \frac{\partial J}{\partial \beta}$) est estimé afin de commander la référence β pour ramener le système autour de son point de fonctionnement optimal, y^*=J^*=$J(\beta^*)$. La Figure 1.1 illustre le lien existant entre le gradient et la position de l'entrée du système par rapport à son point de fonctionnement optimal. Ainsi, pour une fonction objectif J strictement concave si $\beta > \beta^*$, le gradient est négatif; si $\beta < \beta^*$, le gradient est positif et, finalement, si $\beta = \beta^*$, le gradient est nul.

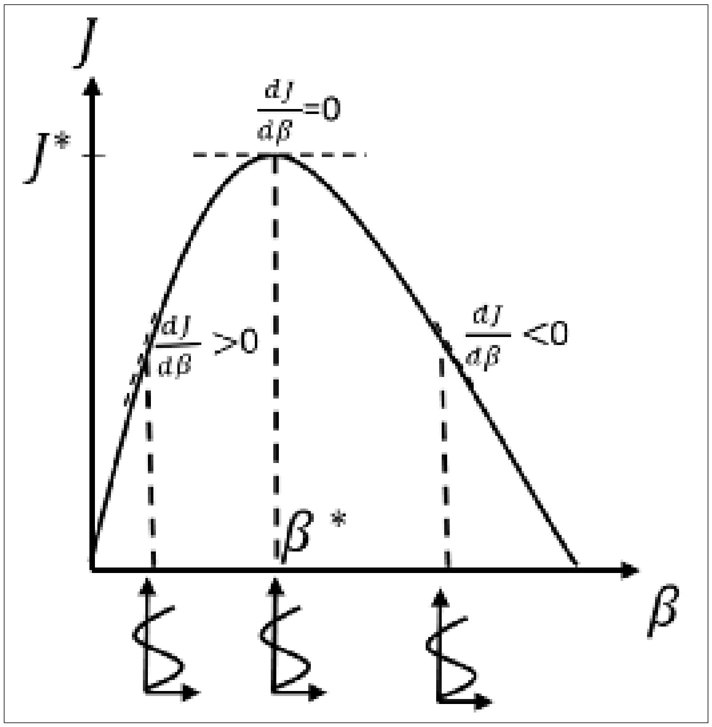

Figure 1.1 Illustration du comportement du gradient de la fonction objectif Jen fonction de la référence β

La méthode de perturbation estime le gradient $\hat{g}$ en utilisant le principe de modulation et de démodulation (Ryan, 2012). D'après la Figure 1.2, la méthode consiste à ajouter un signal d'excitation sinusoïdal avec une faible fréquence ω et une faible amplitude a à l'entrée du système afin de mesurer la sortie du système y en régime permanent, ce qui représente une mesure indirecte de la fonction de performance du système J. Un filtre passe-haut avec une fréquence de coupure ω_h est utilisé par la suite pour supprimer la partie constante η de la sortie du système. Puis, la sortie du filtre passe-haut est multipliée avec le même signal d'excitation avant d'être traitée par un filtre passe-bas avec une fréquence de coupure ω_l afin de supprimer la partie haute fréquence et ne garder que la partie constante qui représente une estimation du gradient $\hat{g}$ de la fonction objectif. Enfin, un intégrateur est utilisé pour contrôler ce gradient à zéro et ainsi ramener le système vers son point de fonctionnement optimal $\beta = \beta^*$.

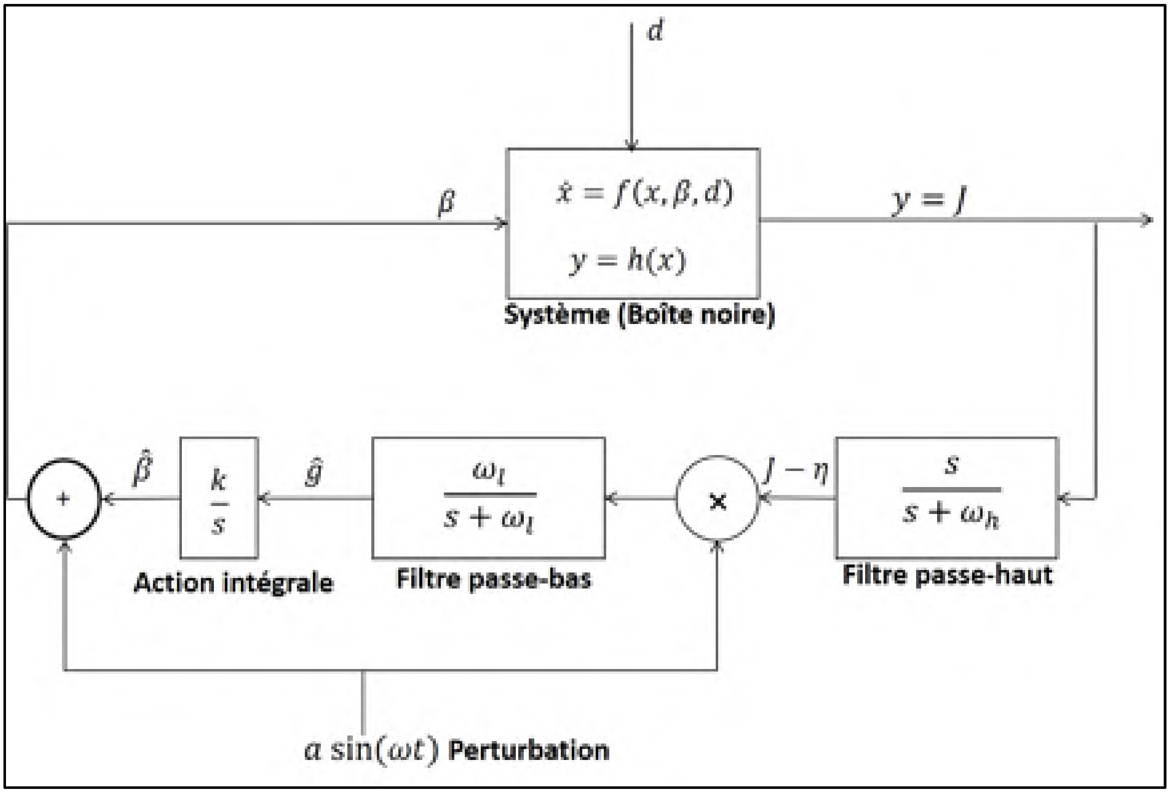

Figure 1.2 Schéma de la méthode de perturbation

Bien que le signal sinusoïdal soit généralement choisi comme un signal d'excitation dans la méthode de perturbation, (Nesic, Tan, & Mareels, 2006; Ying Tan, Nešić, & Mareels, 2008) ont démontré que le choix de la forme du signal d'excitation a un effet direct sur la vitesse de convergence et la précision de la méthode de perturbation. L'étude montre que la commande extrémale avec un signal d'excitation rectangulaire est plus rapide qu'avec un signal sinusoïdal ou triangulaire et légèrement moins précise avec un signal rectangulaire qu'avec un signal sinusoïdal ou triangulaire (Nesic et al., 2006; Ying Tan et al., 2008). En plus, d'autres schémas synoptiques simplifiés de la commande extrémale avec la méthode de perturbation sont présentés dans (Ying Tan et al., 2006).

D'après (Krstić & Wang, 2000), afin de garantir la convergence et la stabilité de la commande extrémale, un certain nombre d'hypothèses sur le système et de conditions sur les choix des paramètres de commande doivent être considérées. L'une de ces hypothèses est que le système soit stable en boucle ouverte (ces hypothèses vont être présentées en détails dans les chapitres qui suivent). Quant aux conditions sur les paramètres, on a deux conditions à respecter. Premièrement, il faut que l'amplitude de signal d'excitation soit faible. Deuxièmement, afin de s'assurer de résoudre le problème statique (1.5), il est nécessaire d'isoler la dynamique du système de l'adaptation elle-même. Pour ce faire, une condition de séparation d'échelle de temps exige que la variation du signal d'excitation soit beaucoup plus lente que la dynamique du système et que les filtres soient beaucoup plus lents que la variation du signal d'excitation. La condition de séparation d'échelle de temps est indispensable pour garantir l'optimisation du système dans son régime statique afin de garantir la convergence vers l'optimum désiré. Or, lorsque cette condition est respectée, le temps de convergence de la commande extrémale dépend de la dynamique du système à optimiser. Par conséquent, si le régime transitoire du système est lent, le temps de convergence de la commande extrémale vers l'optimum sera excessivement lent (Krstić, 2000). De plus, si le point de fonctionnement optimal du système varie très rapidement à cause des perturbations externes, il est possible que la commande extrémale n'arrive pas à converger vers l'optimum désiré.

D'autres études ont été effectuées pour analyser et discuter du choix des paramètres de la commande extrémale avec la méthode de perturbation. (Chioua, 2008) a montré que dans certaines situations, la méthode de perturbation peut ne pas converger vers l'optimum, mais plutôt vers un voisinage de l'optimum. L'erreur de convergence d'un système dynamique non linéaire est proportionnelle non seulement au carré de l'amplitude d'excitation, mais également au carré de la fréquence d'excitation. Il a prouvé que la fréquence d'optimisation doit être nécessairement lente non seulement pour des raisons de stabilité, mais aussi pour la précision. En conclusion, il a montré que la fréquence d'excitation doit être faible, ce qui rend l'optimisation plus lente si la précision est requise.

1.2.2 Les méthodes de commande extrémale améliorées

Afin de réduire ou éliminer l'impact de la séparation d'échelles de temps sur la vitesse de convergence et/ou la précision de la commande extrémale, plusieurs autres types de commande extrémale sont proposés. Dans ces approches, les méthodes paramétriques sont largement utilisées pour améliorer la performance de la commande extrémale avec la méthode de perturbation.

Les méthodes de commande extrémale qui utilisent un modèle paramétré du système sont appelées dans la littérature « méthodes boîte grise » (Grey-box method) (Khong, Nešić, Manzie, et al., 2013; Mohammadi et al., 2014) ou «méthodes à base de modèle» (model-based method) (Michalowsky & Ebenbauer, 2015; Sharafi et al., 2015). D'après (Ryan, 2012), les méthodes paramétriques regroupant les techniques qui paramètrent la fonction objectif et/ou la dynamique du système pour estimer le gradient, le Hessien ou l'optimum de la fonction de performance comprennent des techniques qui utilisent des estimateurs d'états (ex : le filtre de Kalman), la méthode de Newton, etc. Dans le cas où seule la fonction objectif est paramétrée et dont certains paramètres sont inconnus, les dérivées de cette fonction peuvent être calculées à partir des paramètres estimés, rendant ainsi possible l'application des méthodes d'optimisation utilisant les dérivées calculées pour converger rapidement vers un optimum local (Mohammadi et al., 2014; Dragan Nešić, Tan, Manzie, Mohammadi, & Moase, 2012). Par exemple, dans (Banavar, 2002; Speyer, Banavar, Chichka, & Rhee, 2000), une schématisation différente de la commande extrémale avec la méthode de perturbation permettant d'éviter la condition de séparation d'échelles de temps a été proposée. Dans cette approche, la fonction objectif est approximée par une fonction quadratique ou une fonction exponentielle. Les paramètres de la fonction de performance sont supposés varier lentement par rapport à la dynamique du système et sont estimés en temps réel. Un compensateur est alors élaboré afin d'amener le gradient à converger vers zéro. Un large choix de méthodes d'estimation peut être utilisé pour estimer les paramètres du modèle de la fonction objectif (Nesic, Mohammadi, & Manzie, 2013). Dans (Bo & Larsson, 2005), la fonction objectif est décrite par un modèle non-linéaire simple et un estimateur récursif par moindres carrés est utilisé pour estimer les paramètres de la fonction. La méthode de Newton est alors utilisée pour l'optimisation donnant ainsi la possibilité de converger avec précision vers l'optimum désiré. Cette précision est rendue possible par l'utilisation du Hessien qui tient compte de la courbure de la fonction objectif autour de l'optimum, ce qui n'est pas le cas de la méthode de perturbation dont la précision autour de l'optimum dépend du choix d'amplitude de signal d'excitation.

Dans le cas où la dynamique du système de même que la fonction objectif sont tous deux paramétrés, les états du système peuvent également être estimés et utilisés pour optimiser la performance du système en régime permanent (Adetola & Guay, 2006; Nesic et al., 2013). Dans (Moase, Manzie, & Brear, 2009a, 2009b, 2010), un observateur d'états est utilisé pour estimer le gradient et le Hessien d'une fonction de performance et une loi d'adaptation avec la méthode Newton est utilisée en remplacement de la méthode de la plus forte pente. D'autres méthodes de commande extrémale qui donnent la possibilité d'estimer le Hessien de la fonction objectif de sorte que des méthodes d'optimisation de type Newton puissent être appliquées sont également proposées (Ghaffari et al., 2012; Moase et al., 2010; Dragan Nešić et al., 2012; D Nešić, Tan, Moase, & Manzie, 2010).

Récemment, de nouvelles méthodes de commande ont été proposées pour réduire et/ou éliminer l'impact de la séparation d'échelles de temps sur la performance de l'ESC grâce à une paramétrisation plus générale de la fonction objectif tout en supposant que la dynamique du système est inconnue. Comme décrit à la section 1.2.1, l'implémentation de la méthode de perturbation impose deux séparations d'échelles de temps: la première est causée par l'utilisation d'une perturbation sinusoïdale plus lente que la dynamique du système et la deuxième découle de l'utilisation de filtres plus lents que la perturbation utilisée. De plus, l'utilisation d'une action intégrale dans la loi de commande contribue également à la lenteur de la méthode. Dans (Martin Guay, 2014), une méthode plus efficace d'estimation du gradient a été mise au point afin d'éliminer la condition de séparation d'échelles de temps associée aux filtres. Cette méthode consiste à considérer le gradient comme un paramètre variable inconnu à déterminer en fonction du temps avec les techniques de filtrage adaptatif. Cette approche a été validée en simulation pour un système de compression de vapeur (Burns, Weiss, & Guay, 2015). Comme amélioration à cette méthode, en plus d'éliminer la séparation d'échelles de temps associée aux filtres, un contrôleur proportionnel intégral est ajouté à l'ESC dans (M Guay, 2015; Martin Guay & Dochain, 2017). L'approche a encore une fois été validée en simulation pour un système de compression de vapeur (Burns, Laughman, & Guay, 2016). Bien que ces méthodes améliorent significativement la performance de l'ESC en termes de temps de convergence et de précision, leur application demeure limitée à des systèmes dont la dynamique a une structure particulière.

Une autre méthode de détermination du gradient a été proposée aussi dans (E. Moshksar, Ghanbari, Samet, & Guay, 2018) afin d'éliminer la condition de séparation d'échelles de temps relative aux filtres. La méthode repose sur une technique d'identification de paramètres variant dans le temps, basée sur le concept de géométrie presqu'invariante (E Moshksar & Guay, 2016). Dans le cadre de cette étude l'approche est proposée spécialement pour l'optimisation d'un système PV. L'approche proposée permet une convergence rapide vers l'optimum désiré malgré la présence de perturbations externes. Toutefois, l'un des paramètres de la méthode d'optimisation est calculé à partir d'un modèle fondamental du système PV dont on souhaite maximiser la puissance et l'ajustement de ce paramètre pour un système général n'est pas discuté.

Dans (Chichka, Speyer, Fanti, & Park, 2006; Ryan & Speyer, 2010; Walsh, Forbes, Chee, & Ryan, 2017), le gradient et/ou le Hessien de la fonction de performance sont estimés par l'utilisation d'un filtre de Kalman. La principale amélioration par rapport à la méthode de perturbation est que l'utilisation de filtre du Kalman donne la possibilité de filtrer le bruit de mesure pendant l'estimation de gradient et ainsi de converger avec précision vers l'optimum désiré. Cette méthode a été proposée spécialement pour les systèmes statiques ou ayant une dynamique très rapide.

D'autres méthodes de commande extrémale donnent la possibilité de remplacer le signal d'excitation lent dans la méthode de perturbation par un autre signal d'excitation beaucoup plus rapide tout en optimisant le système en régime permanent (Moase & Manzie, 2012a, 2012b; Scheinker & Krstić, 2013; C. Zhang & Ordonez, 2007). Grâce à ce changement, la vitesse de la commande extrémale est nettement améliorée par rapport à la méthode de perturbation et à d'autres méthodes. Aussi, ces méthodes ont la capacité de stabiliser les systèmes instables en boucle ouverte (Moase & Manzie, 2012a, 2012b; Scheinker & Krstić, 2013; C. Zhang, Siranosian, & Krstić, 2007) (Moase et Manzie, 2012b, Scheinker et Krstić, 2013, Zhang et al., 2007b) contrairement à la méthode de (Krstić & Wang, 2000) qui suppose que le système soit stable en boucle ouverte. Les applications de ces méthodes sont destinées à l'optimisation de systèmes qui peuvent être modélisés sous la forme d'un système de type Hammerstein ou Wiener-Hammerstein (Moase & Manzie, 2012a, 2012b) ou des systèmes affines selon l'entrée (Dürr, Krstić, Scheinker, & Ebenbauer, 2015; Dürr, Stanković, Ebenbauer, & Johansson, 2013; Scheinker & Krstić, 2013; Scheinker & Krstić, 2014).

D'autres approches sont proposées afin d'améliorer la performance de la commande extrémale sans nécessairement paramétrer la fonction de performance ou la dynamique du système. Parmi ces approches, on trouve la commande extrémale avec la méthode multi-unité (B Srinivasan, 2007). L'idée de base de cette approche est de supposer que le système global est constitué de sous-systèmes ou d'unités identiques, comme par exemple une centrale électrique qui est constituée par des sources d'énergies renouvelables de même type tels que les panneaux photovoltaïques ou les éoliennes. Ainsi, le gradient est estimé par différence finie entre les sorties des unités identiques excitées à des entrées décalées par une perturbation constante. Un contrôleur intégral comme dans la méthode de perturbation oblige la convergence du gradient à zéro, forçant chaque unité à converger vers son point de fonctionnement optimal. Ainsi, le système global fonctionne à son optimum. L'originalité de la méthode multi-unités est dans l'estimation du gradient par différence finie qui a pour avantage de tenir compte de la dynamique du système sans nécessiter une séparation d'échelles de temps. Conséquemment, la dynamique du système étant éliminée par la différence finie, l'adaptation se fait dans le même ordre de grandeur que la dynamique du système elle-même et la vitesse de convergence est plus rapide que celle obtenue par la méthode de perturbation. Le problème de cette approche est qu'elle exige que le système soit constitué par des unités identiques, ce qui est une hypothèse très limitante pour son application à un système réel, ce dernier pouvant contenir des unités similaires, mais rarement identiques. Ainsi, s'il y a une implémentation expérimentale de l'approche, le système converge vers un point de fonctionnement sous-optimal. Dans (Lyne Woodward, Perrier, & Srinivasan, 2009; L Woodward et al., 2010), une solution intéressante a été proposée afin d'optimiser un système constitué d' unités similaires avec la méthode multi-unité. La solution consiste à ajouter des correcteurs qui compensent les différences entre les unités. Deux types d'adaptation ont été proposés: une approche séquentielle (Lyne Woodward et al., 2009) selon laquelle l'adaptation multi-unités et la correction ont été effectuées séparément, et une approche simultanée (L Woodward et al., 2010) où les deux adaptations ont été réalisées simultanément. Ces correcteurs donnent la possibilité à la méthode multi-unités de converger exactement vers l'optimum de chaque unité et automatiquement de converger vers le point de fonctionnement du système global. L'ajout des correcteurs améliore significativement la précision de la commande avec la méthode multi-unités, mais en contrepartie son temps de convergence devient plus lent à cause du temps d'adaptation consacré aux correcteurs. En plus, le fait de supposer que le système est constitué par des unités similaires est une limitation en soi. On trouve d'autres approches (Azar, Perrier, & Srinivasan, 2011; Esmaeil-Zadeh-Azar, 2010; Khong, Nešić, Manzie, et al., 2013; Khong, NešIć, Tan, et al., 2013) qui améliorent la vitesse de convergence de la commande extrémale avec la méthode de perturbation et qui supposent que le système est constitué par des sous-systèmes semblables.

Dans la suite de ce chapitre, la commande extrémale avec la méthode de perturbation sera appelée tout simplement la commande extrémale (ESC) (extremum seeking control) en raison de sa popularité et vu le nombre élevé de publications scientifiques utilisant la méthode de perturbation dans un contexte de commande extrémale.

1.3 Objectif principal et objectifs spécifiques

D'après le survol effectué des différentes solutions proposées afin d'améliorer la vitesse de convergence et/ou la précision de l'ESC, on constate que celles-ci limitent l'application de l'ESC à des situations restreintes, que ce soit par la paramétrisation de la fonction objectif, la fixation du type, ou encore de la structure du système. Or, le point fort qui caractérise l'ESC est l'optimisation de la performance du système quelle que soit sa complexité en le considérant comme une boîte noire. Ainsi, à partir de ce constat, l'objectif principal de la thèse est de proposer une nouvelle méthode de commande extrémale qui permet de converger précisément et rapidement vers le point de fonctionnement optimal d'un système boîte noire soumis à l'effet d'une perturbation externe rapide sans restriction sur type ou la structure du système.

La séparation multiple des échelles de temps (entre la dynamique du système, la fréquence de la perturbation et la vitesse d'adaptation) est un objectif visé lors du choix des paramètres de l'ESC et ce, afin d'assurer l'optimisation d'un système de type boîte noire dans son régime statique quelle que soit sa dynamique (lente ou rapide). Par contre, le fait de fixer les paramètres afin de respecter cette condition, ne garantit pas la convergence vers le point de fonctionnement optimal si le système est perturbé. Une adaptation des paramètres de l'ESC est alors essentielle pour assurer une bonne précision et une convergence rapide vers l'optimum. Dans ce cas, une loi de commande adaptative capable d'ajuster les paramètres de l'ESC est préférable pour converger rapidement et précisément si la fréquence de la perturbation externe est importante. À partir de cette idée, on a fixé les objectifs spécifiques suivants:

- Proposer une approche qui permet le contrôle adaptatif des paramètres de l'ESC afin de converger rapidement et précisément vers l'optimum désiré malgré la présence de perturbations externes rapides tout en supposant que le système soit une boîte noire.
- Prouver théoriquement qu'avec l'approche proposée, la performance de l'ESC est améliorée dans le cas d'optimisation d'un système quelconque.
- Démontrer la stabilité de l'approche proposée.
- Valider en simulation l'amélioration de performance de l'ESC avec l'approche proposée dans le cas d'optimisation d'un système lent soumis à l'effet d'une perturbation externe rapide.
- Valider expérimentalement l'amélioration de performance de l'ESC dans le cas d'optimisation d'un système rapide soumis à l'effet d'une perturbation externe rapide.

1.4 Méthodologie

1.4.1 Plateforme de simulation et expérimentale

Afin d'évaluer la performance des approches développées, on a choisi deux types de systèmes complexes perturbés en permanence: la pile à combustible microbienne "MFC" (Microbial fuel cell) qui est un système chimique avec une dynamique lente (le régime transitoire est en terme d'heures) et le panneau photovoltaïque (PV) qui est un système électrique avec une dynamique plus rapide (le régime transitoire est en terme de secondes). Le modèle de (Pinto, Srinivasan, Manuel, & Tartakovsky, 2010) est choisi parmi les modèles qui simulent le plus fidèlement le comportement d'une MFC afin d'évaluer la performance de l'ESC dans le cas de l'optimisation de la puissance produite par une MFC soumise en permanence à une variation de la concentration de substrat d'alimentation (S_0). Une plateforme expérimentale est créée afin de tester la performance des approches proposées dans le cas d'optimisation d'un système PV soumis en permanence à l'effet d'une perturbation de radiation (G) (Figure 1.3).

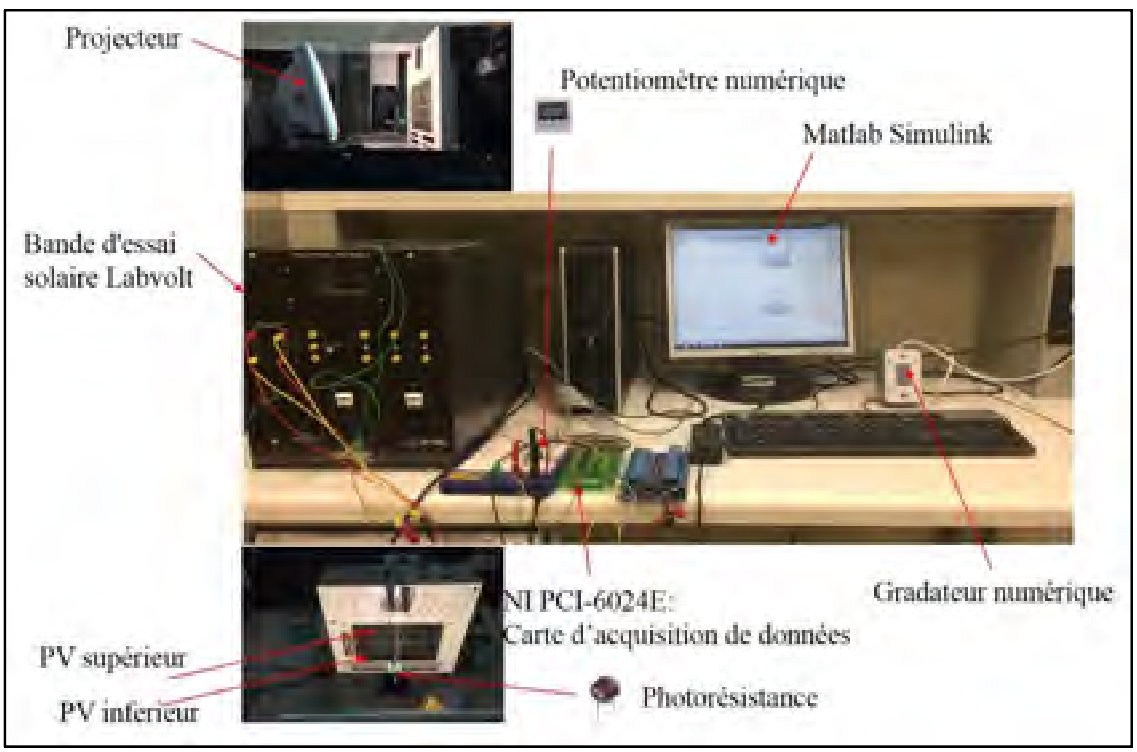

Figure 1.3 Plateforme expérimentale d'un système PV

1.4.2 Les approches proposées

Dans la majorité des cas, les perturbations externes d auxquelles le système est soumis sont des perturbations mesurables $d = d_m$ avec la technologie des capteurs existants sur le marché. Ainsi, si nous incluons une action anticipative dans l'ESC capable de fournir une approximation ou une estimation de la position du point de fonctionnement optimal du système $\widehat{\beta^*} \simeq \beta^*$ à partir de la mesure des perturbations externes d_m, il est possible d'adapter les paramètres de l'ESC afin d'améliorer sa performance en termes de vitesse et de précision lorsque le système est soumis à des perturbations externes mesurables. Dans notre cas, le réseau de neurones multicouche (Shanmuganathan, & Samarasinghe, 2016) est choisi afin de modéliser la relation entre la perturbation externe mesurable d_m et le point de fonctionnement optimal β^*. Le réseau de neurones est caractérisé par sa capacité à modéliser avec précision les systèmes non linéaires complexes tout en considérant ces derniers comme une boîte noire (K. Liu & Zhu, 2015). Il suffit d'avoir une base de données constituée de quelques mesures des perturbations externes d_m et du point de fonctionnement optimal β^* correspondant à chacune de ces mesures afin d'avoir un modèle empirique $\widehat{\beta^*} = p(d_m)$ capable de fournir une estimation du point de fonctionnement optimal $\widehat{\beta^*}$ pour chaque mesure de d_m. Afin d'améliorer la performance de l'ESC dans le cas de l'optimisation d'un système soumis à l'effet des perturbations mesurables (1.6), deux approches sont proposées. Celles-ci ont l'avantage d'adapter les paramètres de l'ESC par une action anticipative.

$$\left.\begin{array}{c}\max\limits_{\beta} y \\ t.q.\ \dot{x} = f(x,\beta,d_m) = 0\end{array}\right\} \Leftrightarrow \max_{\beta} J. \tag{1.6}$$

a. La première approche consiste principalement à utiliser l'action anticipative pour contrôler automatiquement la condition initiale β_{ini} de la commande extrémale. En fait, lorsque le système est soumis à l'effet d'une perturbation externe causant une variation très importante du point de fonctionnement optimal, la condition initiale β_{ini} de la boucle l'ESC risque d'être très loin de l'optimum à chaque variation de d_m. Dans ce cas, si la fréquence de variation de d_m est importante, il est possible

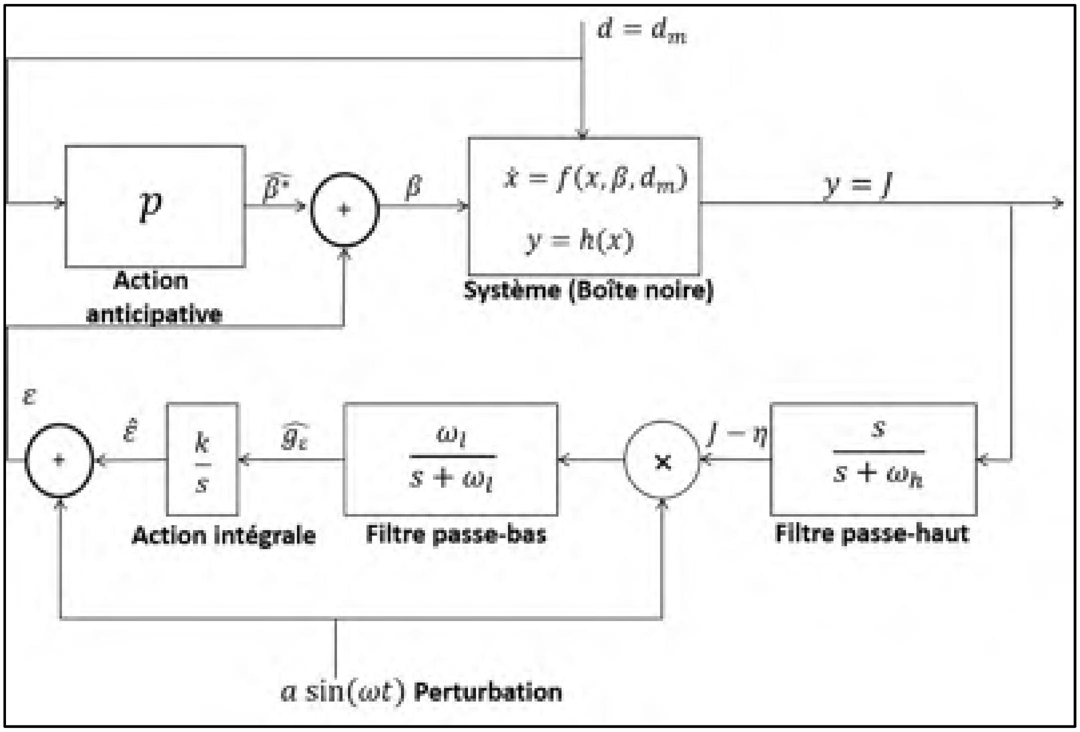

Figure 1.4 Principe de la commande extrémale avec
action anticipative

que l'ESC n'arrive pas à converger vers l'optimum. Pour résoudre ce problème, un bloc d'action anticipative à base d'un modèle par réseau de neurones est ajouté à l'ESC (Figure 1.4). Celle-ci rend possible l'estimation en temps réel du point de fonctionnement optimal selon la mesure de d_m. Cette estimation sera utilisée comme point de départ (ou condition initiale $\beta_{ini} = \widehat{\beta^*}$) pour l'ESC à chaque variation de d_m et ce afin d'amener le système rapidement et précisément vers le point de fonctionnement optimal réel β^*. Dans cette approche, le rôle principal de l'ESC est de compenser l'erreur d'estimation du réseau de neurones avec le contrôle de $\varepsilon = \beta - \widehat{\beta^*}$ vers ε^*=$\beta^* - \widehat{\beta^*}$, ce qui réduit l'effort de commande de l'ESC et permet de converger rapidement vers l'optimum. Une comparaison théorique de la performance de l'approche proposée et de l'ESC est réalisée grâce à la formulation analytique du temps de convergence de chaque méthode dans le cas d'optimisation d'un système quelconque. Aussi, une comparaison entre la performance de l'approche proposée et de l'ESC est effectuée dans un contexte de simulation d'une MFC soumise à l'effet d'une perturbation rapide de concentration de substrat d'alimentation (S_0) et expérimentalement dans le cas d'optimisation d'un PV soumis à l'effet d'une perturbation rapide de radiation G. Cette comparaison est effectuée grâce à la détermination des facteurs de performance comme l'efficacité de suivi (T_{eff}), la précision en régime statique (T_{acc}) et le temps de convergence (T_c). Le temps de convergence est le temps requis pour atteindre 5% de l'optimum réel, J^*. L'efficacité de suivi et la précision en régime statique sont évalués en utilisant les formules suivantes :

$$T_{eff} = \frac{1}{N_T} \sum_{i=1}^{N_T} \frac{y(i) \times 100}{J^*(i)} \tag{1.7}$$

$$T_{acc} = \frac{1}{N_F - N_I} \sum_{i=N_I}^{N_F} \frac{y(i) \times 100}{J^*(i)} \tag{1.8}$$

avec N_T le nombre total d'échantillons et $[N_I \; N_F]$ une fenêtre d'échantillons définie par l'expert dans laquelle la sortie du système est autour de l'optimum.

b. La deuxième approche consiste à utiliser l'action anticipative pour adapter l'amplitude du signal d'excitation. L'amplitude du signal d'excitation a un impact très important sur la performance de l'ESC. Plus l'amplitude est grande, plus la vitesse de convergence est rapide et plus l'oscillation autour de l'optimum est importante (une mauvaise précision) et vice versa. Dans la majorité des cas, le choix d'amplitude est effectué de façon à faire un compromis entre la vitesse et la précision de convergence, mais on ne peut pas garantir ces deux performances en même temps. Ceci conduit l'ESC, dans certaines situations, vers un point de fonctionnement sous-optimal. Ainsi, afin de converger aussi bien rapidement que précisément vers le point de fonctionnement optimal sans faire de compromis entre ces deux critères de performance, une commande adaptative à base de modèle par réseau de neurones est ajoutée à l'ESC afin de contrôler l'amplitude du signal d'excitation (Figure 1.5). Le principe de base de la méthode proposée consiste à ajuster cette amplitude en fonction de l'erreur entre le point de fonctionnement optimal estimé par l'action anticipative et la position actuelle de l'ESC de l'entrée $\hat{\beta}$. À partir de cette erreur e, un bloc ajuste l'amplitude du signal d'excitation. Si l'erreur est supérieure à un seuil fixé par l'expert e_{max} , le système est excité avec une amplitude importante, a_{max}. Dans le cas contraire, le système est excité avec une faible amplitude a_{min}. La stabilité de l'approche proposée est étudiée car le système global bascule entre deux sous-systèmes en boucle fermée et la méthode de perturbation singulière est alors utilisée pour la preuve de stabilité. Une étude théorique détaillée comparant la vitesse de convergence et la précision de l'approche proposée à celle de l'ESC. La performance est évaluée tout d'abord par la simulation d'une MFC et, expérimentalement dans le cas d'optimisation d'un système PV, tout comme ce fut le cas avec notre première approche.

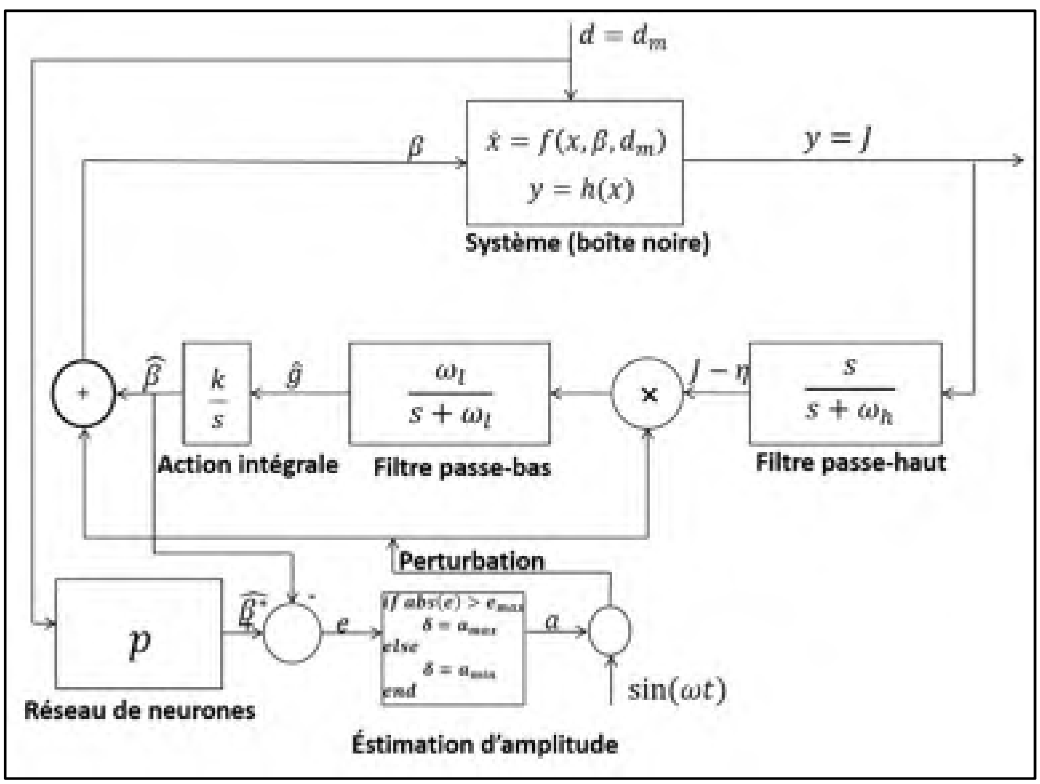

Figure 1.5 Principe de la commande extrémale avec excitation adaptative

Parfois, le système est également soumis à des perturbations non-mesurables ($d = d_u$). Celles-ci qui sont généralement moins fréquentes (par exemple, la détérioration d'une partie du système) que les perturbations mesurables (d_m), mais peuvent changer radicalement le point de fonctionnement optimal du système. Dans un tel cas, il faut que l'action anticipative puisse tenir compte des perturbations non-mesurables d_u dans son estimation afin de garantir la meilleure performance possible en termes de vitesse de convergence et de précision. Ainsi, pour résoudre le problème d'optimisation (1.7), une troisième approche est proposée.

$$\left.\begin{array}{c}\max\limits_{\beta} y \\ t.q.\, \dot{x} = f(x, \beta, d_m, d_u) = 0\end{array}\right\} \Leftrightarrow \max_{\beta} J. \tag{1.7}$$

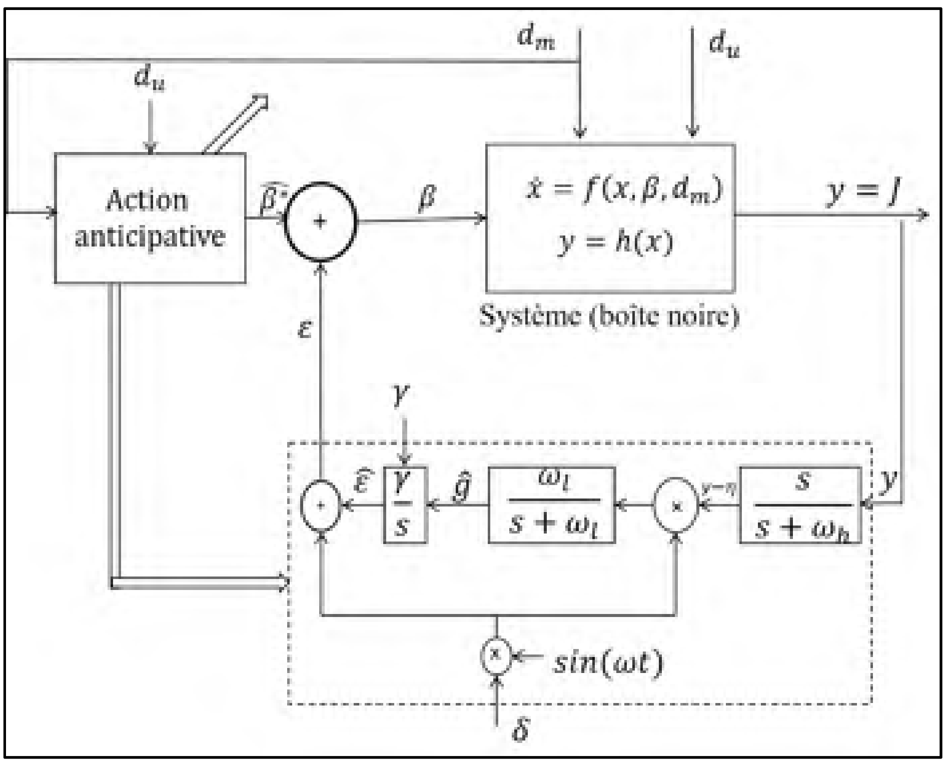

Figure 1.6 Principe de la commande extrémale avec une action anticipative qui tient compte des perturbations mesurables et non-mesurables

c. Dans la troisième approche (Figure 1.6), le principe de base est inspiré par la première approche qui consiste à contrôler autrement la condition initiale dans la commande extrémale. Cependant un nouveau schéma est proposé afin que l'action anticipative donne une bonne estimation du point de fonctionnement optimal $\widehat{\beta^*}$ malgré la présence de la perturbation non-mesurable d_u. L'idée consiste à intégrer un modèle par réseau de neurones dont l'apprentissage est effectué en ligne. Ceci permet la mise à jour du modèle empirique $\widehat{\beta^*} = p(d_m)$ décrivant la relation qui relie la perturbation mesurable d_m et le point de fonctionnement optimal β^* lorsqu'une perturbation non-mesurable d_u survient. L'apprentissage en ligne du réseau de neurones est effectué grâce à l'ajout de nouveaux blocs qui permettent l'intégration d'une base de données dynamique d'apprentissage. La stabilité de l'approche proposée est étudiée avec la méthode de perturbation singulière et les facteurs de performance de l'ESC et de la méthode proposée sont comparés expérimentalement dans le cas d'optimisation d'un PV soumis à l'effet d'une perturbation mesurable rapide, soit la perturbation de radiation G et d'une perturbation non-mesurable simulée par une défaillance d'une partie du système.

1.5 Contributions et originalité de recherche

L'objectif de la recherche est d'améliorer la performance de l'ESC en termes de précision et de vitesse de convergence dans le cas d'optimisation d'un système soumis en permanence à l'effet des perturbations externes. Dans la littérature, différentes méthodes sont proposées afin d'améliorer la vitesse de convergence et/ou la précision de l'ESC, mais dans la majorité des cas, l'application de ces approches est limitée à des conditions restreintes qui nous privent de l'une des performances qui caractérise l'ESC et qui consiste à optimiser un système inconnu. Contrairement à ces travaux, dans le cadre de cette thèse, trois nouvelles méthodes de commande extrémale permettent la convergence rapide et précise vers le point de fonctionnement optimal d'un système perturbé sans la connaissance du modèle ni même de la structure de ce dernier.

a. Dans la première méthode, une intégration d'action anticipative à base d'un réseau de neurones permet l'estimation en temps réel d'une condition initiale pour l'ESC au voisinage du point de fonctionnement optimal à chaque fois que le système est soumis à l'effet d'une perturbation mesurable. Il a été démontré théoriquement, dans le cas de l'optimisation d'un système quelconque, que le temps de convergence de l'ESC avec action anticipative est beaucoup plus rapide que celui de l'ESC sans action anticipative. Le résultat de cette étude a été validé en simulation dans le cas d'optimisation de la puissance de sortie d'une pile à combustible microbienne soumise à l'effet d'une perturbation de concentration de substrat S_0 (A. Kebir, Woodward, & Akhrif, 2015) et expérimentalement dans le cas d'optimisation d'un PV soumis à l'effet de perturbation de radiation G. Le modèle de réseau de neurones proposé en action anticipative augmente significativement la vitesse de convergence de l'ESC. Cette augmentation de vitesse, combinée à la précision de convergence de la boucle ESC elle-même, contribue à une efficacité de suivi accrue du point de fonctionnement optimal d'un système lent comme la MFC ou rapide comme le PV en comparaison avec l'ESC sans action anticipative qui n'arrive pas dans certaines situations à converger vers l'optimum désiré si la fréquence de perturbation mesurable est grande. Dans notre situation, seulement la perturbation de S_0 et la perturbation de G sont choisies comme perturbations mesurables respectivement pour la MFC et le PV. Toutefois, l'action anticipative à base d'un réseau de neurones peut être étendue afin d'ingérer d'autres perturbations mesurables, ce qui peut augmenter la robustesse de l'action anticipative en termes de précision d'estimation de l'optimum du système contre les perturbations externes. L'approche proposée peut être appliquée sur d'autres systèmes tels que les systèmes à énergie renouvelable (éolienne, pile à hydrogène, etc.), les systèmes mécaniques (frein ABS, moteur, etc.), etc.

Les premiers résultats de cette étude ont été publiés dans un article de conférence (MED 2015). Cette étude a également mené à la soumission d'un article de journal tel que présenté ci-après:

Kebir, A., Woodward, L., & Akhrif, O. (2015). Extremum-seeking control with anticipative action of microbial fuel cell's power. Dans *Control and Automation (MED), 2015 23th Mediterranean Conference on* (pp. 933-939). IEEE.

Kebir, A., Woodward, L., & Akhrif, O. (2018). Real-time optimization of PV and MFC power using neural network based anticipative extremum-seeking control. *Renewable Energy. Manuscript submitted for publication.*

b. Dans la deuxième méthode, le contrôle adaptatif de l'amplitude du signal d'excitation dans l'ESC grâce à l'intégration de l'action anticipative à base d'un réseau de neurones donne la possibilité de converger en même temps rapidement et précisément vers l'optimum d'un système soumis à l'effet d'une perturbation mesurable sans faire un compromis entre la précision et le temps de convergence. La stabilité de l'approche est validée et l'amélioration de performance de l'ESC est démontrée avec une étude théorique détaillée qui compare le temps de convergence et la précision de l'ESC avec et sans excitation adaptative dans le cas d'optimisation d'un système quelconque. Les résultats de l'étude théorique sont validés dans le cas du suivi du point de fonctionnement optimal d'une MFC (Anouer Kebir, Akhrif, & Woodward, 2016) et d'un PV (Anouer Kebir, Woodward, & Akhrif, 2018) soumis respectivement à l'effet des perturbations mesurables S_0 et G. Les résultats de simulation et expérimentaux ont montré que cette approche réduit de manière significative les effets indésirables de la condition de séparation d'échelle de temps sur les performances du système en boucle fermée tout en augmentant l'efficacité de suivi du point de fonctionnement optimal. Cette méthode peut contribuer à obtenir une efficacité de suivi importante de l'optimum d'une source d'énergie renouvelable ou tout système soumis à des perturbations externes mesurables devant être optimisé.

Cette étude a fait l'objet de deux publications, soit un article de conférence et un article de journal:

Kebir, A., Akhrif, O., & Woodward, L. (2016). Extremum-seeking control of a microbial fuel cell power using adaptive excitation. Dans *Industrial Electronics Society, IECON 2016-42nd Annual Conference of the IEEE* (pp. 4127-4132). IEEE.

Kebir, A., Woodward, L., & Akhrif, O. (2018). Extremum-seeking control with adaptive excitation: application to a photovoltaic system. *IEEE Transactions on Industrial Electronics, 65*(3), 2507-2517.

c. Dans la troisième et dernière méthode, la performance de l’ESC en termes de temps de convergence et de précision est améliorée lorsque le système est soumis à des perturbations mesurables et non-mesurables. Une nouvelle structure de l’ESC est proposée afin d’intégrer dans l’action anticipative un modèle de réseau de neurones adaptatif qui estime avec une bonne précision le point de fonctionnement optimal malgré la présence de perturbations mesurables et non-mesurables. La stabilité de l'approche proposée est établie et l'amélioration des performances de l’ESC est confirmée expérimentalement dans le cas de l'optimisation de la puissance de sortie d'un système PV. Les résultats obtenus ont montré que l’ESC avec une action anticipative à base d’un réseau de neurones adaptatif est plus efficace pour suivre la puissance optimale soumise à l’effet des perturbations mesurables comme la radiation et non mesurables comme la défaillance d'une partie du système PV. Par conséquent, cette méthode augmente significativement la robustesse de l’ESC en termes de suivi du point de fonctionnement optimal et en terme d’application sur une large gamme d’autres systèmes.

Cette étude a permis la soumission de l’article de journal suivant:

Kebir, A., Akhrif, O., & Woodward, L. (2018). Extremum-seeking control with adaptive neural-network-based anticipative action to maximize the power of a photovoltaic system. *IEEE Transactions on Industrial Electronics. Manuscript submitted for publication.*

CHAPITRE 2

REAL-TIME OPTIMIZATION OF RENEWABLE ENERGY SOURCES POWER USING NEURAL NETWORK-BASED ANTICIPATIVE EXTREMUM-SEEKING CONTROL

Anouer Kebir [a], Ouassima Akhrif [a] and Lyne Woodward [a]

[a] Department of Electrical Engineering, École de Technologie Supérieure,
1100 Notre-Dame Ouest, Montréal, Québec, Canada H3C 1K3

Submitted in Renewable Energy, July, 2018

Abstract

This paper presents a fast and accurate real-time optimization (RTO) technique that can be applied to different types of renewable energy sources (RES). Two RES with very different dynamics in terms of complexity and convergence time towards the static regime have been chosen for this study: photovoltaic panels (PV) and microbial fuel cell (MFC). The maximum power generated by these two RES is prone to vary when the system is subjected to various external disturbances. Extremum-seeking control (ESC) is a RTO method that has the ability to optimize the performance of a RES whatever its complexity. However, when the external disturbances affecting the RES result in fast variations of its optimal operating point, the slow convergence of ESC will induce a lack of precision. This paper proposes the addition of a neural network-based anticipative action to the existing ESC scheme to improve its performance in terms of speed and accuracy if the system is subjected to the effect of measurable disturbances. The performance improvement of ESC is demonstrated theoretically for general systems, via simulation for an MFC and experimentally in the case of a PV.

Keywords: Extremum-seeking control, Neural networks, Real-time optimization, Photovoltaic system, microbial fuel cell.

2.1 INTRODUCTION

During the annual United Nation climate change conference, governments promote the development of solutions based on renewable energy (Energy, Renewables, & Energy, 2016). Among emerging options, organic matter and solar energy offer important growth potential, as they are free, abundant, and easily convertible. Photovoltaic systems (PVs) can provide a valuable source of power (e.g., the project Noor in Ouarzazate in Morocco can produce up to 580MW (Laaroussi, Ajana, Bakkali, Faraj, & Cherkaoui, 2017)) . At the same time, microbial fuel cells (MFCs) may offer the advantage of generating electricity while significantly reducing the amount of energy used for pumping in sewage treatment plants through the degradation of organic matter in activated sludge and wastewater. The strengths of these two sources of renewable energy can become a potential solution to solving one of the major 21st century problems such as increasing access to drinking water and renewable energy.

RES such as PVs and MFCs systems present several similarities: they show high non-linear behavior, which is a function of many parameters (e.g., characteristics of materials), and are constantly subjected to external disturbances (e.g., temperature and light irradiance variations for PV system and inlet substrate concentration and pH for MFC). These disturbances affect their internal resistance which in turn leads to variations in their optimal point of operation. Consequently, without any impedance adaptation, the energy recovered from such systems is not necessarily maximal. On the other hand, the model complexity and the speed dynamics may vary considerably from one RES to the other. For example, an MFC has much more complex and much slower dynamics than a PV (the convergence time towards the static regime of an MFC is in terms of days as compared to seconds for a PV). Thus, the optimization methods that are applicable for a PV system are not necessarily usable for the optimization of an MFC. The choice of an appropriate control strategy is essential for RES to work at full power despite external disturbances (Reisi, Moradi, & Jamasb, 2013).

Many approaches have been proposed to track the optimal power point of RES in real time (Ahmed & Salam, 2015; Eltawil & Zhao, 2013; Fathabadi, 2016a; Mamarelis, Petrone, & Spagnuolo, 2014). These different real-time optimization methods can be classified in three categories (Reisi et al., 2013). The first one brings together the model-based or offline methods for which the control signal is determined using technical data or physical specifications of the system. While model-based methods are able to identify the MPP rapidly, even in the case of slow systems (Eltawil & Zhao, 2013; Fathabadi, 2016b), they suffer from a lack of precision due to the model uncertainty. The second category includes online or non-model-based methods which use available measurements instead of a priori knowledge of the system to track the maximum power point (MPP). The use of online techniques to track the optimum leads to better precision, but also to a slower convergence (Bhatnagar & Nema, 2013) if one takes into account the dynamic or response time of a slow system such as an MFC. Since the tracking efficiency of real-time optimization methods depends on a combination of good precision and rapid convergence, hybrid approaches have been proposed in order to take advantage of the rapidity of the offline methods and the precision of the online methods. Not surprisingly, these have shown a better tracking efficiency than online or offline methods alone (Reisi et al., 2013). The RTO problem being a static one, the hybrid optimization method must necessarily take into account the system's dynamics in order to reach the real static optimal point, rather than another sub-optimal point regardless if one is dealing with a PV or an MFC. Thus, our objective in this work is to develop a general-type of hybrid real-time optimization method that allows RES to work at their optimum whatever their model complexity and their response time and in the presence of external disturbances which continuously affect the optimum.

Among the online methods applied to RES in the literature, the Extremum-Seeking Control (ESC) method (Ariyur & Krstić, 2003), which will be studied in the present paper, has shown a relatively good performance in terms of accuracy (Reisi et al., 2013). In an ESC structure, the gradient of the objective function is estimated using a simple static empirical model, and is driven to zero (Krstić & Wang, 2000). The use of a static model is sufficient to solve the (static) real-time optimization problem. However, to obtain such a static empirical model in the case of a dynamic system, one must isolate the dynamics of the system optimization problem. This can be accomplished by adjusting the ESC scheme parameters in order to guarantee a time scale separation between the system dynamics and the adaptation itself. The tracking efficiency of the ESC method is however limited by its slow convergence to the desired optimal operating point (B. Srinivasan, 2007), which is due to this time scale separation, especially if the system has slow dynamics or is submitted to frequent external disturbances: the performance achieved will then be sub-optimal (A. Kebir et al., 2015). Sometimes, such disturbances may be detected before they affect the system, in which case this detection could be used to improve the optimization results. Indeed, if the optimization method uses this disturbance measurement to predict its effect on the optimal point of operation in real time, it can act in advance to reduce the error between the operating point and the optimal value of the system under control. This approach is used to design a hybrid optimization method by augmenting the ESC (online method) with an offline method part in order to obtain a faster convergence to the desired optimal operating point and a better tracking efficiency.

A hybrid method using an offline calculation of the open circuit voltage together with the P/O method has been proposed for PV systems (Moradi & Reisi, 2011). While the simplicity of this approach is suitable for real applications, it has shown a lower tracking efficiency in the presence of rapid variations of light intensity. This is due to the use of temperature measurement (instead of light intensity measurement) in the offline set point calculation. Since the temperature normally varies more slowly than the light irradiance (Bahr, Jokiel, & Rodgers, 2016), it would appear to be more convenient to use the light irradiance measurement in the offline part of the hybrid method while leaving the temperature perturbation to be managed by the slower, but more precise part of the method, namely, the online part. In addition, the method proposed by (Moradi & Reisi, 2011) is specified only for the optimization of a PV system, hence this approach is not applicable for optimizing an MFC.

The hybrid approach proposed in this paper consequently consists in adding an anticipative block to the feedback ESC structure in order to provide faster convergence toward the optimum in the presence of rapid measurable disturbance variations. This anticipative action block models the relationship between the measurable external disturbance and the corresponding optimal operating point of the system. The proposed anticipative action is based on a neural network (NN) model which can offer good estimation without any knowledge of the system model (A. Kebir et al., 2015; Reisi et al., 2013) if trained properly.

To validate the proposed approach, this paper presents a comparison between the performance of the ESC method with and without anticipative action in the context of the power optimization of two types of RES, an MFC and a PV source. Both RES are DC sources that may be subjected to variations of measurable but rapid external disturbances, namely, light irradiation in the case of PV system and inlet substrate concentration in the case of MFC system. They present on the other hand different model complexity and are at both ends of the spectrum as far as their dynamics time response. Note that this comparison is performed using simulation results in the case of the MFC and using experimental results in the case of the PV system, where the light radiations are assumed to vary uniformly. Consequently, the proposed hybrid scheme is seeking a local optimum, and the problem of partial shading in PV is not part of the scope of this study.

The impact of the proposed modification on the time of convergence of the ESC scheme is evaluated theoretically, via simulations and experimentally. A comparison of the simulation and experimental results obtained for the classic ESC and the proposed anticipative ESC scheme is performed based on the following performance criteria: i) the time of convergence (T_c), also expressed as the number of dither periods (N_p), ii) the tracking efficiency (T_{eff}) (Mamarelis et al., 2014) and iii) the tracking accuracy in steady state (T_{acc})(Bizon, 2013; Y.-H. Liu, Liu, Huang, & Chen, 2013).

The paper is organized as follows. After an introduction, Section 2.2 presents the optimization problem. In Section 2.3, the traditional ESC scheme is presented. The proposed anticipative ESC approach is explained in Section 2.4. Its performance is then evaluated through a comparative mathematical analysis in Section 2.5, and through simulation and experimental results in Section 2.6 and Section 2.7. Finally, conclusions of the paper are presented in Section 2.8.

2.2 Optimization problem formulation

Consider a SISO nonlinear system described by the following model:

$$\dot{x} = f(x, u, d_m) \tag{2.1}$$

$$y = h(x) \tag{2.2}$$

where $u \in R$ is the input, $y \in R$ is the output, $d_m \in \mathbb{R}^q$ is the measurable disturbances vector, $x \in \mathbb{R}^n$ is the state, and $f: \mathbb{R}^n \times \mathbb{R} \times \mathbb{R}^q \to \mathbb{R}^n$ and $h: \mathbb{R}^n \to \mathbb{R}$ are smooth functions. Let us assume a smooth control law:

$$u = \alpha(x, \beta), \tag{2.3}$$

parameterized by the scalar β. The dynamics of the overall closed-loop system is described by:

$$\dot{x} = f(x, \alpha(x, \beta), d_m). \tag{2.4}$$

The following assumptions are made about this closed-loop system.

Assumption 1: There exists a smooth function $l: \mathbb{R} \to \mathbb{R}^n$ such that $f(x, \alpha(x, \beta), d_m) = 0$, if and only if $x = l(\beta)$.

Assumption 2: For each $\beta \in \mathbb{R}$, the equilibrium state $x = l(\beta)$ of the system is locally exponentially stable with uniform decay and overshoot constants in β.

According to these assumptions, a control law which does not require the knowledge of $f(x, \alpha(x, \beta), d_m)$ or $l(\beta)$ can be designed for local stabilization (Krstić & Wang, 2000).

As our objective is to control our system such that it operates around its optimal operating point, a third assumption will be considered.

Assumption 3: There exists $\beta^* \in \mathbb{R}$ such that

$$(h \circ l)'(\beta^*) = 0, \tag{2.5}$$

$$(h \circ l)''(\beta^*) < 0. \tag{2.6}$$

This third assumption is required to ensure that the function $y = h(l(\beta))$ is maximal at $\beta = \beta^*$. In order to simplify the formulation of the problem presented hereafter, let $J(\beta)$ be a representation of $(h \circ l)(\beta)$.

Considering Assumptions 1, 2 and 3, the optimization problem can be mathematically formulated as follows:

$$\left.\begin{array}{c} \max\limits_{\beta} y \\ s.t. \quad \dot{x} = f(x, \alpha(x,\beta), d_m) = 0 \end{array}\right\} \Leftrightarrow \max_{\beta} J. \tag{2.7}$$

2.3 The ESC scheme

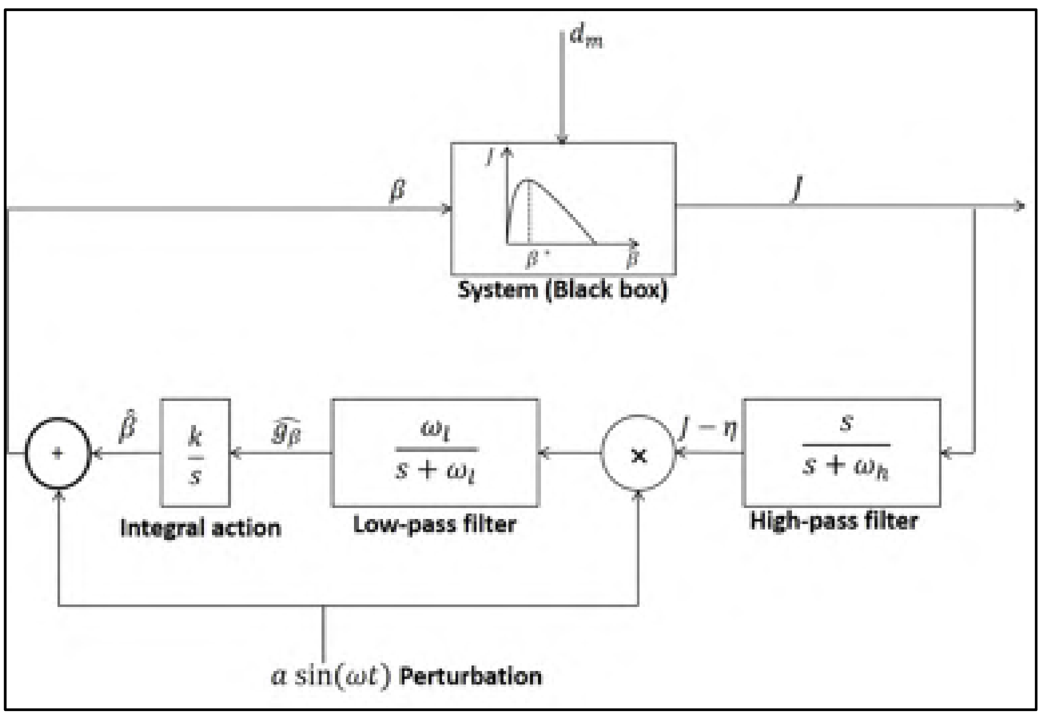

Figure 2.1 Block diagram of the ESC loop

The ESC approach solves the optimization problem (2.7) by converting it into a control problem of the estimated gradient to zero, according to the necessary conditions of optimality defined in Assumption 3 (Krstić & Wang, 2000). The input of the system is thus adjusted to follow the gradient direction, as in the steepest descent algorithm. The estimated gradient is obtained by adding a periodic exogenous perturbation to the system input and observing the effect of this perturbation on the system output (see Figure 2.1). The local stability of the ESC scheme scheme has been demonstrated in (Krstić & Wang, 2000) using the averaging and singular perturbation theories.

The ESC scheme first uses a high-pass filter with a cut off frequency ω_h in order to extract the resulting oscillating part of the exogenous perturbation, which has a frequency ω, from the output signal J. Then, a correlation between the perturbation and the output of the high-pass filter is performed. Finally, a low-pass filter with a cutoff frequency ω_l is used to obtain the average value of the correlation. Thus, the control laws of the ESC loop are:

$$\beta = \hat{\beta} + a sin(\omega t) \tag{2.8}$$

$$\dot{\hat{\beta}} = k\hat{g}_\beta \tag{2.9}$$

$$\dot{\hat{g}}_\beta = -\omega_l \hat{g}_\beta + \omega_l (J - \eta) a\, sin(\omega t) \tag{2.10}$$

$$\dot{\eta} = -\omega_h \eta + \omega_h J \tag{2.11}$$

with $k > 0$, $\hat{g}_\beta$ the estimated gradient, and η, the average value of J. The equality constraint of the optimization problem (2.7) is taken into account by choosing the perturbation and filter frequencies in order to guarantee a time scale separation between the system dynamics, the perturbation signal and the filtered signals. The perturbation frequency is therefore adjusted to be slower than the system dynamics, and the filter cut off frequencies are chosen to be smaller than the perturbation one. As a result, the system controlled by the ESC loop appears to be in a steady state.

However, this time scale separation causes a slow convergence to the optimum and can lead to a sub-optimal performance when the system is submitted to disturbances causing fast variations of its optimal point of operation (Anouer Kebir et al., 2018).

The slow convergence of the ESC loop under fast variations of external disturbances can also be explained by its feedback structure. If disturbances occur, i.e., d_m varies (Fig. 2.1), the ESC scheme will have to detect the effect of these disturbances on the measurable static gradient $\hat{g}_{\beta}$, and then react by controlling the input of the system, β.

2.4 Proposed approach: ESC with anticipative action (denoted ESC_{aa})

2.4.1 Structure of the Anticipative ESC_{aa} scheme

Assuming that i) the external disturbances are available from measurements, and ii) the perturbation method is provided with some information about the effect of these external disturbances on the position of the optimal operating point of the system, an anticipative action can be added to the ESC feedback structure in order to make it able to converge more quickly towards the desired optimum.

Let us assume a function $p: \mathbb{R}^q \to \mathbb{R}$ providing an estimate $\widehat{\beta^*}$ of β^* using the measurement d_m:

$$\widehat{\beta^*} = p(\, d_m) \tag{2.12}$$

and let us define ε to be:

$$\varepsilon = \beta - \widehat{\beta^*}. \tag{2.13}$$

Considering (2.12) and (2.13), the control law (2.3) can be rewritten as follows:

$$u \ = \alpha(x, p(\, d_m) + \varepsilon) \tag{2.14}$$

$$= r(x, \varepsilon,\, d_m) \tag{2.15}$$

with r being the new control law.

From a ESC feedback loop perspective, the optimal input estimate $\widehat{\beta^*}$ can be seen as a constant offset and, consequently, (2.5-2.6) can be written in the new coordinate ε :

$$(h \circ l)'(\varepsilon^*) = 0, \tag{2.16}$$

$$(h \circ l)''(\varepsilon^*) < 0, \tag{2.17}$$

where:

$$\varepsilon^* = \beta^* - \widehat{\beta^*}. \tag{2.18}$$

The ESC$_{aa}$ scheme (Figure 2.2) solves the following optimization problem defined using ε as the new control parameter:

$$\left.\begin{array}{c} \max\limits_{\varepsilon} y \\ s.t. \quad \dot{x} = f(x, r(x,\varepsilon,\ d_m), d_m) = 0 \end{array}\right\} \Leftrightarrow \max\limits_{\varepsilon} J \tag{2.19}$$

with, $J(\varepsilon) \equiv (h \circ l)(\varepsilon)$,

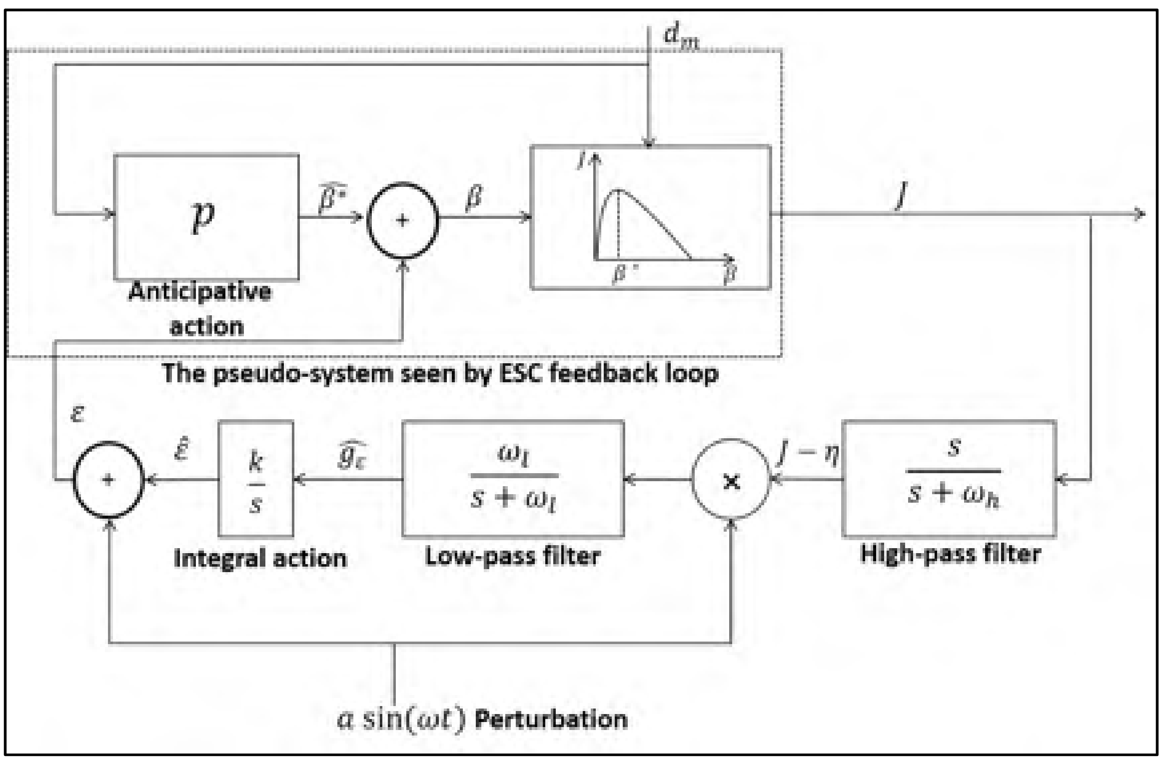

Figure 2.2 Block diagram of the proposed ESC$_a$ scheme.

and is described by the following equations:

$$\beta = \hat{\beta}^* + \varepsilon \tag{2.20}$$

$$\varepsilon = \hat{\varepsilon} + a\sin(\omega t) \tag{2.21}$$

$$\dot{\hat{\varepsilon}} = k\hat{g}_\varepsilon \tag{2.22}$$

$$\dot{\hat{g}}_\varepsilon = -\omega_l \hat{g}_\varepsilon + \omega_l (J - \eta) a \, sin(\omega t) \tag{2.23}$$

$$\dot{\eta} = -\omega_h \eta + \omega_h J. \tag{2.24}$$

2.4.2 Anticipative action: use of a Neural Network model

Most often, for real systems, the function p that attempts to describe the relationship between the disturbances d_m and the optimal operating point of the system β^* is a highly non-linear relationship, which is difficult to describe mathematically using physical laws. This led us to use a modeling technique that does not require explicit knowledge of physical laws, but which uses input-output data. Thus, a neural network model is used, since it is able to successfully model complex systems (Bishop, 1995; Ebrahimi-Moghadam, Mohseni-Gharyehsafa, & Farzaneh-Gord, 2018; Fadare, 2009; Gürgen, Ünver, & Altın, 2018; Heng, Asako, Suwa, & Nagasaka, 2018; Manobel et al., 2018; Mohandes, Rehman, & Halawani, 1998). Moreover, it is a non-linear and multivariable tool, which can be configured by learning from experimental data.

The NN-model is characterized by its architecture, its learning mode (supervised or unsupervised) and its learning algorithm (Bishop, 1995) (backpropagation, Quasi-Newton, BFGS, etc.).

In this study, a static architecture and multilayer perceptron with a hyperbolic activation function was used for modeling. Moreover, since the input and output measurements are readily available, a supervised learning was performed. The multilayer perceptron is usually comprised of two or three layers of fully connected neurons in a setup in which information propagates in one direction, namely, from the input layer to the output layer. The backpropagation method is used in the network learning phase (Bishop, 1995), and thus, the output error of the network is backward-propagated to the hidden layers. The method is used in order to find a set of synaptic coefficients which minimize a given cost function (optimization criterion).

The static neural network model is described as follows:

$$p(d_m) = \widehat{\beta^*} = \left(\frac{1-e^{-m_{NN}*W_2^T*\phi_2}}{1+e^{-m_{NN}*W_2^T*\phi_2}}\right), \tag{2.25}$$

where:

$$\phi_2 = \begin{bmatrix} bias \\ \chi \end{bmatrix}, \tag{2.26}$$

χ is the vector of length c with the i^{th} element defined by the activation function of each neuron of the hidden layer, i.e.,

$$\chi(i) = \left(\frac{1-e^{-m_{NN}\psi(i)}}{1+e^{-m_{NN}\psi(i)}}\right), \tag{2.27}$$

$$\psi = W_1^T\phi_1 \tag{2.28}$$

$$\phi_1 = \begin{bmatrix} bias \\ d_m \end{bmatrix}, \tag{2.29}$$

and $W_1 \in \mathbb{R}^{b\text{ x }c}$ and $W_2 \in \mathbb{R}^{\lambda\text{ x }1}$ are respectively the sets of synaptic weights between the input neuron and the hidden layer and between the hidden layer and the output neuron set after learning; $m_{NN} \in \mathbb{R}$ is the slope of the hyperbolic tangent activation functions ϕ_1 and ϕ_2; $b = q + 1$ since the number of input neurons is equal to the number of measurable disturbances; $\lambda = c + 1$ with c being the number of neurons in the hidden layer chosen by the expert; $bias$ is a constant value chosen by the expert.

2.5 Comparative analysis of the Time of convergence of ESC and ESC_{aa} schemes

The NN model provides an estimate ($\widehat{\beta^*}$) of the real optimal input (β^*) according to the measurable disturbances value (d_m). The error of estimation (ε^*) will be compensated by the ESC feedback loop, which will control the input ε. Thus, the ESC loop will refine the estimated optimal point, as well as compensate the effect of any other unmeasurable disturbances that may affect the optimal point of operation. For any measurable external disturbances included in the model used in the anticipative action, the effort needed by the ESC loop to push the system to its optimal operating point will be reduced. This will be demonstrated by the following mathematical analysis.

2.5.1 Convergence analysis of the ESC scheme

Considering the average model of the closed loop system (Ariyur & Krstić, 2003; Krstić & Wang, 2000), the gradient of the performance index, $\hat{g}_{\beta}$, can be approximated as follows:

$$\hat{g}_{\beta} \backsimeq \frac{a^2}{2} J'(\hat{\beta}). \tag{2.30}$$

Consequently, the time derivative of the unperturbed part of the input, $\dot{\hat{\beta}}$, is described by:

$$\dot{\hat{\beta}} \backsimeq (ka^2/2) J'(\hat{\beta}). \tag{2.31}$$

Considering a first-order Taylor series expansion of the derivative $J'(\hat{\beta})$ around the optimum β^*:

$$\dot{\hat{\beta}} \backsimeq m(\hat{\beta} - \beta^*), \tag{2.32}$$

with $m = \frac{ka^2}{2} \frac{\partial^2 J}{\partial \hat{\beta}^2}\Big|_{\beta^*} < 0$, one can provide a linear expression to characterize the evolution of $\hat{\beta}$:

$$\hat{\beta}(t) \backsimeq (\beta_0 - \beta^*) e^{mt} + \beta^*. \tag{2.33}$$

Let us define T_{ESC} as the time needed, starting from an initial input β_0 for the ESC loop to approach the optimum β^* within a precision of 5%. Note that this initial condition is assumed to be chosen in the neighborhood of the optimum in order to validate the Taylor series expansion made previously. Thus,

$$\hat{\beta}(T_{ESC}) \backsimeq (\beta_0 - \beta^*) e^{mT_{esc}} + \beta^* = \beta^* \pm 0.05\, \beta^*. \tag{2.34}$$

Assuming that β_0 and $\beta^*$are of the same sign, the time needed for the ESC loop to approach the optimum within a precision of 5%, can be described as follows:

$$T_{ESC} \backsimeq m^{-1} ln\left(\frac{|0.05\beta^*|}{|\beta_0 - \beta^*|}\right). \tag{2.35}$$

2.5.2 Convergence analysis of the proposed ESCaa scheme

Let us now consider the proposed ESCaa scheme with the initial condition $\varepsilon_0 = 0$ at $t = t_0 = 0$. Since, by definition, such an initial condition corresponds to an initial value of $\widehat{\beta^*} \approx \beta^*$, from (2.33) by generalization, $\hat{\varepsilon}$ is described by:

$$\hat{\varepsilon}(t) \backsimeq (\varepsilon_0 - \varepsilon^*)e^{mt} + \varepsilon^*. \tag{2.36}$$

Using (2.18):

$$\hat{\varepsilon}(t) \backsimeq \left(\widehat{\beta^*} - \beta^*\right)e^{mt} + \beta^* - \widehat{\beta^*}. \tag{2.37}$$

Hence, using (2.8), (2.13) and (2.21) it can be concluded that,

$$\hat{\beta}(t) \backsimeq \left(\widehat{\beta^*} - \beta^*\right)e^{mt} + \beta^*. \tag{2.38}$$

Defining $\mathrm{T_{ESC_{aa}}}$ as the time needed for the ESCaa scheme to converge towards the optimum within a precision of 5%, we have:

$$\hat{\beta}\left(T_{ESC_{aa}}\right) = \left(\widehat{\beta^*} - \beta^*\right)e^{mt} + \beta^* = \beta^* \pm 0.05\,\beta^*. \tag{2.39}$$

Assuming that $\hat{\beta}^*$ and $\beta^*$are of the same sign:

$$T_{ESC_{aa}} = m^{-1}\, ln\left(\frac{|0.05\beta^*|}{\left|\widehat{\beta^*} - \beta^*\right|}\right). \tag{2.40}$$

Finally, from (2.35) and (2.40):

$$T_{ESC} - T_{ESC_{aa}} = m^{-1}\, ln\left(\frac{\left|\widehat{\beta^*} - \beta^*\right|}{|\beta_0 - \beta^*|}\right). \tag{2.41}$$

Assuming that the model provides a good estimate $\widehat{\beta^*}$ of β^*:

$$0 < \frac{|\widehat{\beta^*} - \beta^*|}{|\beta_0 - \beta^*|} < 1 \tag{2.42}$$

and, consequently,

$$ln\left(\frac{\widehat{\beta^*} \; - \beta^*}{\beta_0 - \beta^*}\right) < 0. \tag{2.43}$$

Since, by definition, $m < 0$, it can be concluded that:

$$T_{ESC} > T_{ESC_{aa}}. \tag{2.44}$$

Note that closer will be $\widehat{\beta^*}$ from β^*, larger will be the gain in time.

2.6 Simulation study: application to MFC

2.6.1 Functional principle of an MFC

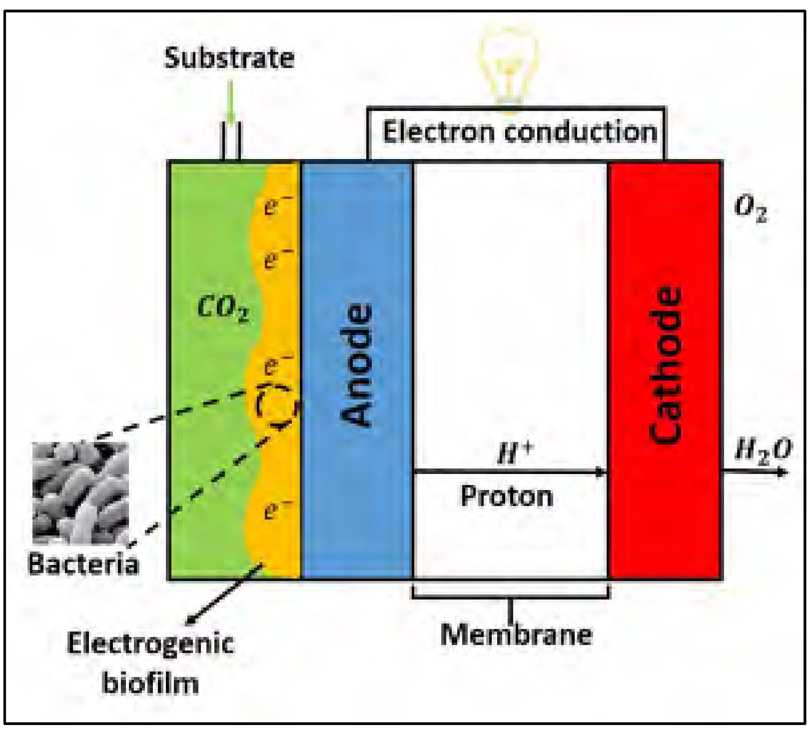

Figure 2.3 Schematic of a microbial fuel cell

A MFC is a bioreactor that uses exoelectrogenic bacteria to produce electrochemical energy (Xia et al., 2018). It consists mainly of an anode in an anaerobic chamber and a cathode exposed to air. In the anaerobic chamber, the bacteria are fed with organic matter (e.g. wastewater, acetate, activated sludge, etc.). During the oxidation-reduction reaction, electrons are released by the bacteria and transferred from the anode to the cathode via an external resistor. The protons migrate to the cathode where they are in contact with oxygen to produce clean water (Figure 2.3).

2.6.2 Specifications of the MFC

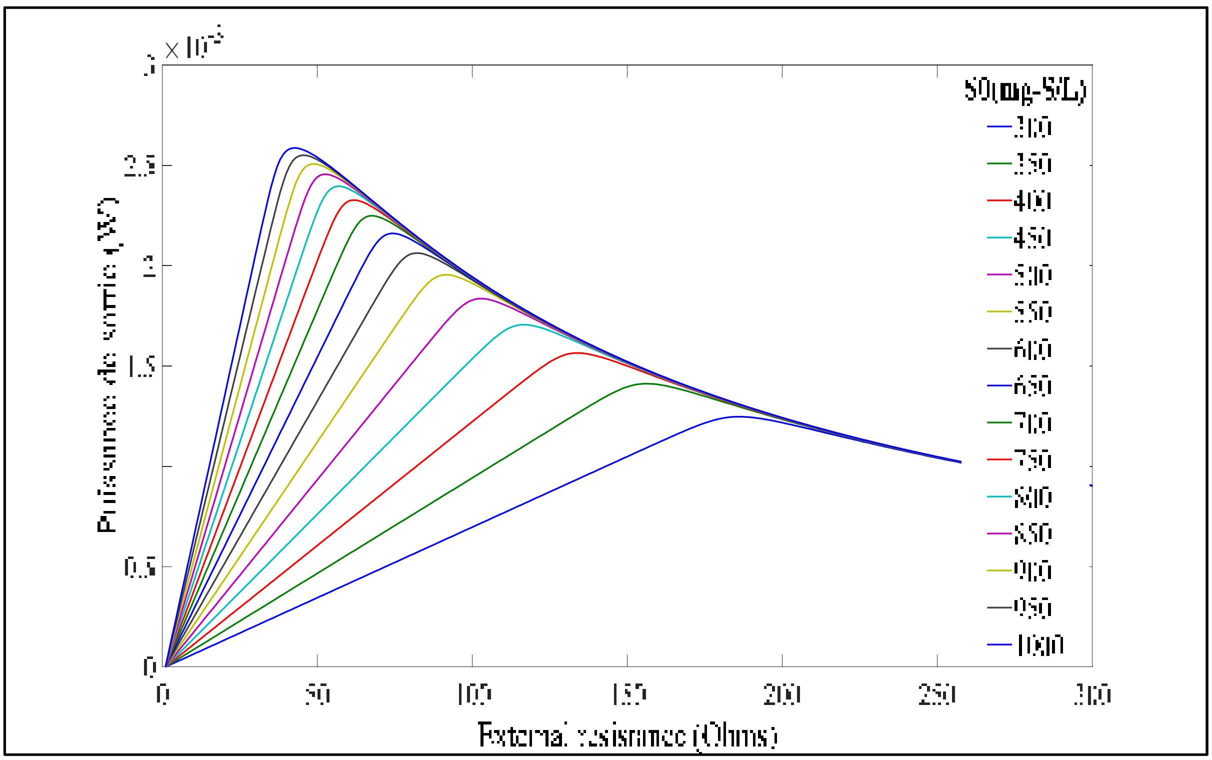

Figure 2.4 Static power curves of the MFC for different concentrations of inlet substrate S_0

In the present study, the MFC behavior has been simulated in Matlab Simulink using the model of (Pinto et al., 2010) Figure 2.4 depicts the output power P_s as a function of the external resistance R_{ex} for different values of the inlet substrate concentration, S_0(considered here as the measurable disturbance d_m) whereas other parameters such as temperature or pH level are kept constant. The external resistor and the concentration were varied respectively from 0 to 300 Ω with a step of 1 Ω and from, 300 and 1000 mg-S / L with a step of 50 mg-S / L.

The static power curves depicted in Figure 2.4 show that, for each inlet substrate concentration S_0 there exist an optimal external load (which corresponds to the internal resistance R_{in} of the MFC) where the maximal power ${P_s}^*$ is delivered. In order to track this optimal power point despite the possible variations of the inlet substrate concentration, a real-time optimization method is needed. It will aim to control the external load R_{ex} so that it matches the unknown MFC's internal resistance, R_{in}.

Although the model presented in (Pinto et al., 2010) gives a simplified and more general presentation of the MFC compared to other models (Kato Marcus, Torres, & Rittmann, 2007; Picioreanu, Katuri, Head, van Loosdrecht, & Scott, 2008; Xia et al., 2018), it is still insufficient to present the MFC under all possible operating conditions. Consequently, the model describing the impact of the external disturbances on the optimal power of the MFC is assumed to be unknown in the context of real-time optimization.

2.6.3 ESC of the MFC

The ESC method is first applied to maximize in real-time the power delivered by a MFC under slow and fast variations of the inlet substrate concentration S_0. In such a context, the optimization problem becomes:

$$\begin{aligned} & Max_{R_{ex}}\, P_s(R_{ex}) \\ s.t. \quad & \dot{x} = f(x, R_{ex}, S_0) = 0 \end{aligned} \quad (2.45)$$

Related to (2.7), P_s is the objective function J, R_{ex} is the control input β and S_0 is the measurable disturbance d_m.

A judicious choice of the ESC parameters is necessary to guarantee a time-scale separation. Thus, the first step aims to determine the time response of the MFC to a change in the external load for different values of S_0. Therefore, for each inlet substrate concentration value, a variation of the external load R_{ex} is made from 0 to 200 Ω with a 10 Ω step in both increasing and decreasing directions to determine the slowest convergence time of the MFC.

Table 2.1 MFC specifications and NN power of generalization test

Sbstrate inlet concentration S_0 (mg-SL^{-1})	**Internal resistance R_{in} (Ω)**	**Optimal Power output P_s^*(mW)**	**Response Time (day)**	**Internal resistance estimated by NN model $\widehat{R_{in}}$(Ω)**
300	188	1.247	0.14	-
350	157	1.412	0.2	159.5
400	134	1.565	0.19	-
450	117	1.706	0.19	117.9
500	103	1.836	0.22	103.8
550	92	1.955	0.22	92.57
600	82	2.063	0.24	-
650	74	2.161	0.17	76.04
700	68	2.249	0.2	69.73
750	62	2.327	0.3	64.20
800	57	2.396	0.25	-
850	53	2.456	0.31	55.19
900	49	2.507	0.26	51.33
950	46	2.55	0.28	47.3
1000	43	2.587	0.33	-

Based on the results shown in Table 2.1, the ESC parameters have been adjusted according to the longest response time of the MFC (T_{MFC}=0.33 day):

- Sinusoidal excitation signal frequency: $F = \frac{1}{5 \times T_{MFC}} = 0.60\ Hz$.

- Cutoff frequencies of the filters: $\omega_l = \omega_h = \frac{2\times\pi}{25\times T_{MFC}}$ =0.76 rad/day.
- Perturbation signal amplitude and the gain of the controller: a = 2 Ω and k = 2.5*10^3 Ω^2 J^{-1} (this choice allows to make a compromise between accuracy and speed of convergence for different inlet substrate concentrations).
- Initial condition of the input: $R_{ex} = R_{ini}$ = 43 Ω.

Table 2.2 Performance evaluation of ESC and ESC_{aa} approaches: power optimization of an MFC

	ESC	**ESC_{aa}**
T_c (days) from $R_{in(S_0=450\,mg-sL^{-1})}$ to $R_{in(S_0=900\,mg-sL^{-1})}$	0.55	192.6
T_c (days) from $R_{in(S_0=900\,mg-sL^{-1})}$ to $R_{in(S_0=450\,mg-sL^{-1})}$	2.99	118
N_p from $R_{in(S_0=450\,mg-sL^{-1})}$ to $R_{in(S_0=900\,mg-sL^{-1})}$	0.33	116.7
N_p from $R_{in(S_0=900\,mg-sL^{-1})}$ to $R_{in(S_0=450\,mg-sL^{-1})}$	1.81	70.7
T_{acc}(%) under $P^*_{s(S_0=450\ mg-sL^{-1})}$	98.9	98.9
T_{acc}(%) under $P^*_{s(S_0=950\ mg-sL^{-1})}$	99.1	99.1
T_{eff} (%)	74.2	98.1

The results are shown in Figure 2.5, Figure 2.6 and Table 2.2. Under a slow variation of the inlet substrate concentration S_0, the ESC method brings the system to converge towards the desired optimum, with a tracking accuracy reaching T_{acc} = 99.06%. However, the convergence time is exorbitant (up to T_c=192.62 days i.e., N_p =116.73). Not surprisingly, as shown in Figure 2.7, Figure 2.8, and Table 2.2, the ESC method is unable to track the optimum under rapid and random variations of S_0, and has a low tracking efficiency (T_{eff} = 74.24%).

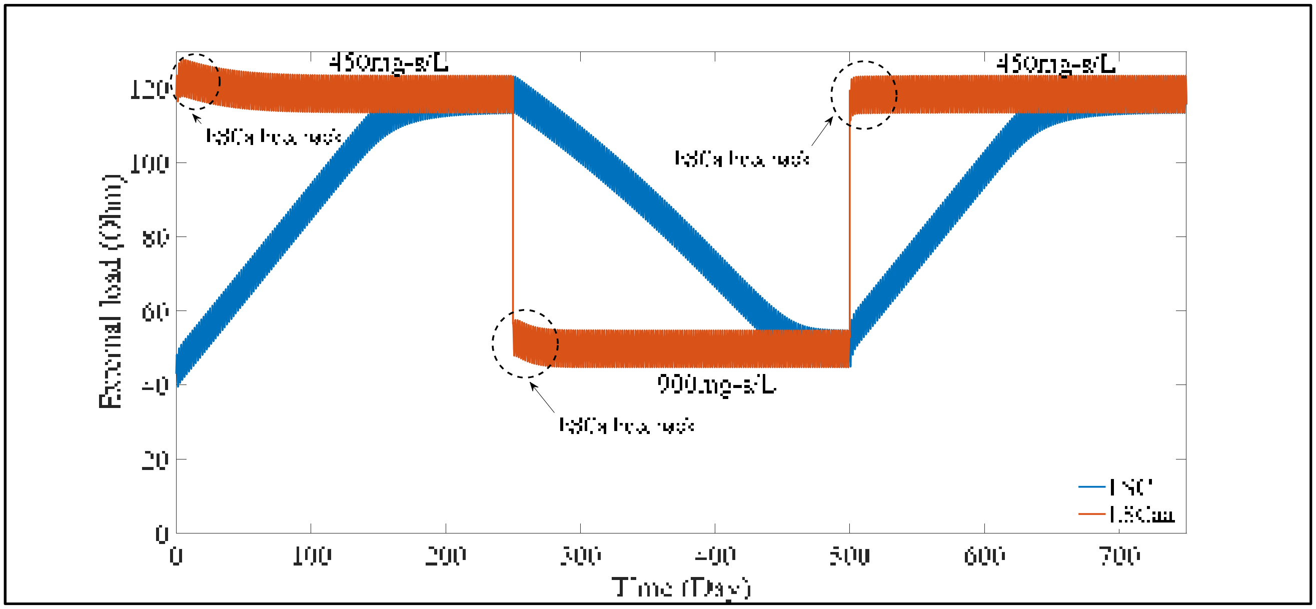

Figure 2.5 Evolution of the external load of the MFC under slow variation of the inlet substrate concentration (S_0) using ESC and ESC$_{aa}$ methods

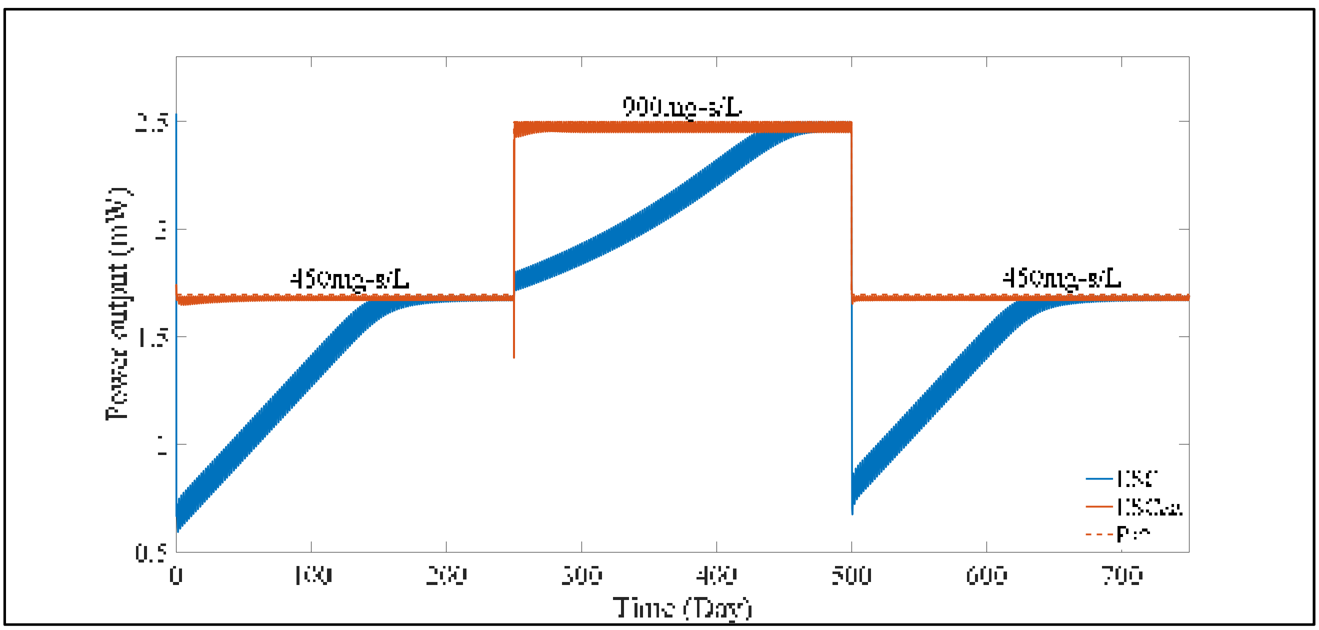

Figure 2.6 Evolution of the MFC power ouput under slow variation of the inlet substrate concentration (S_0) using ESC and ESC$_{aa}$ methods

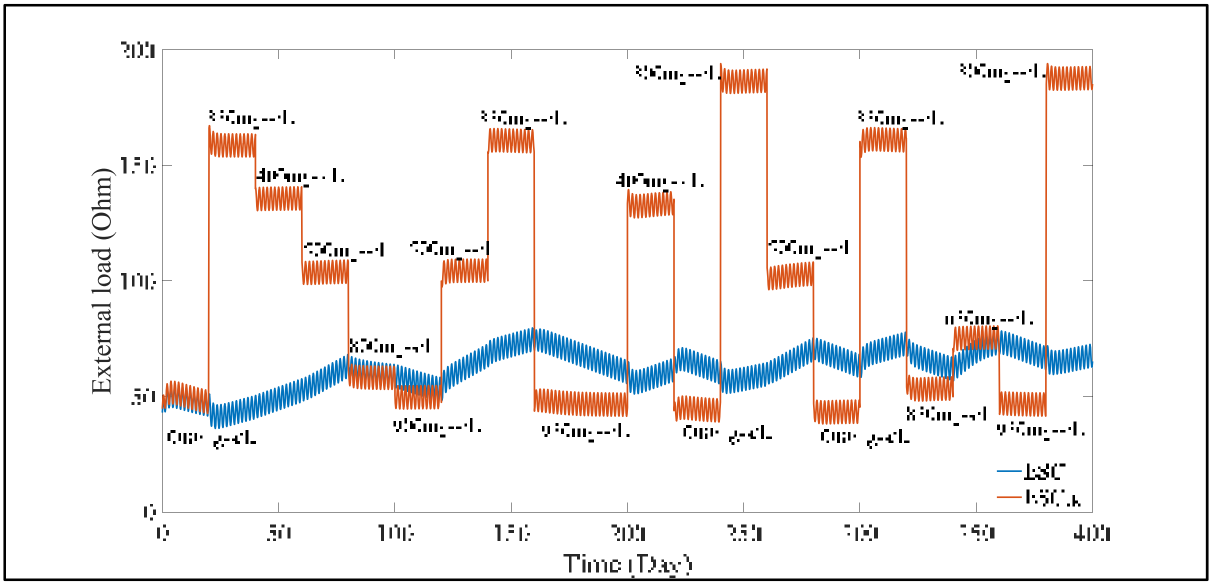

Figure 2.7 Evolution of the external load of the MFC under fast and random variations of the inlet substrate concentration (S_0) using ESC and ESC_{aa} methods.

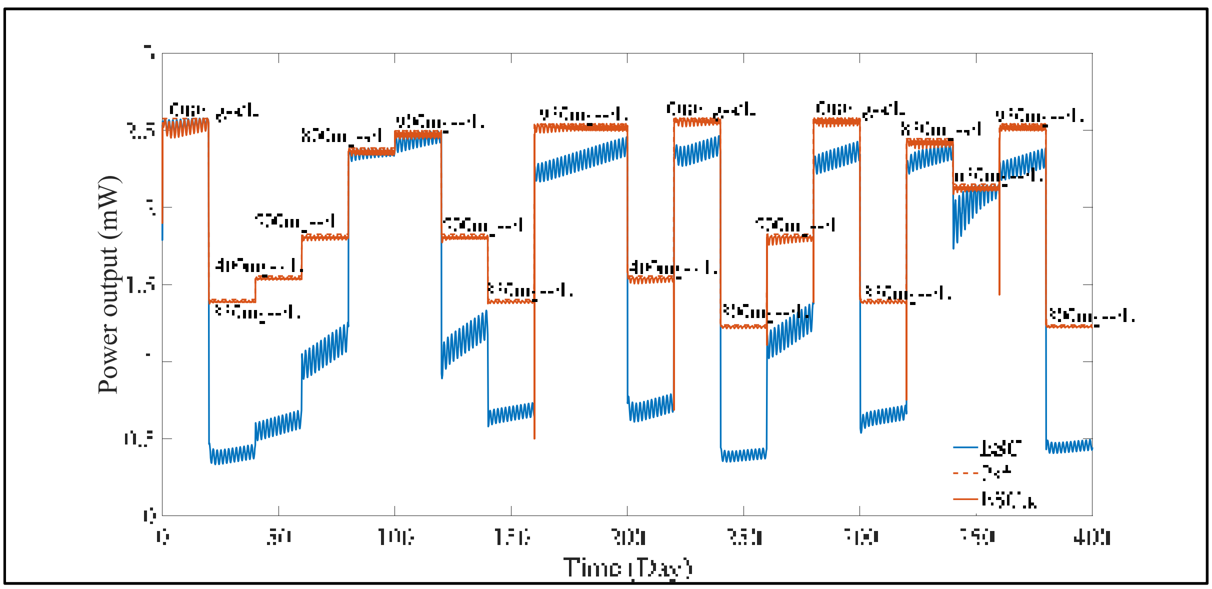

Figure 2.8 Evolution of the MFC power ouput under fast and random variations of the inlet substrate concentration (S0) using ESC and ESC_{aa} methods.

2.6.4 ESC_{aa} of the MFC

The design of the anticipative action requires a model able to describe the effect of external disturbances on the optimal operating point of the system. The relationship between the inlet substrate concentration S_0 and the MFC internal resistance R_{in} is non-linear (Figure 2.4). Therefore, as mentioned previously, this relationship was modeled using a neural network.

Designing a neural network model consists of two steps, i) learning, and ii) testing the power of generalization. The neural network-learning phase was performed using the substrate concentration S_0 as an input and the corresponding internal resistance R_{in} as the desired output data. This learning phase was completed using the values of
corresponding to the following substrate concentration S_0: 300, 400, 600, 800, and 1000 mg-S L-1.

The neural network model (2.26-2.30) is defined considering $\widehat{\beta^*} = \hat{R}_{in}$, the internal resistance of the MFC estimated by the NN model, $c = 10$ (length of the vector χ), $d_m = S_0$ and $bias = 0.5$. For performance comparison purpose, the operating conditions of the MFC and the ESC method parameters used in Section 2.6.3 have been kept the same in the present section.

The neural network generalization power test is performed after the learning phase in order to verify the capacity of the model to estimate the MFC internal resistance for different inlet substrate concentrations S_0. To that end, points from Table 2.1 that were not used during the learning phase are now used. The results of the generalization power test shown in the left column of Table 2.1 confirm that the neural network model gives a good estimate of the internal resistance.

From Figure 2.5, Figure 2.6 and Table 2.2, one can see that under slow variations of the inlet substrate concentration S_0, the ESC_{aa} method makes the system converging with the same good tracking accuracy (T_{acc}) as the ESC loop but, this time, in a shorter time (up to 350 times faster). Moreover, from Figure 2.7, Figure 2.8 and Table 2.2, under rapid disturbances, the ESC_{aa} tracking efficiency reaches $T_{eff} = 98.12\%$ which is much higher than the tracking efficiency reached by the ESC method.

2.7 Experimental study: application to a PV system

2.7.1 Description of the experimental PV setup

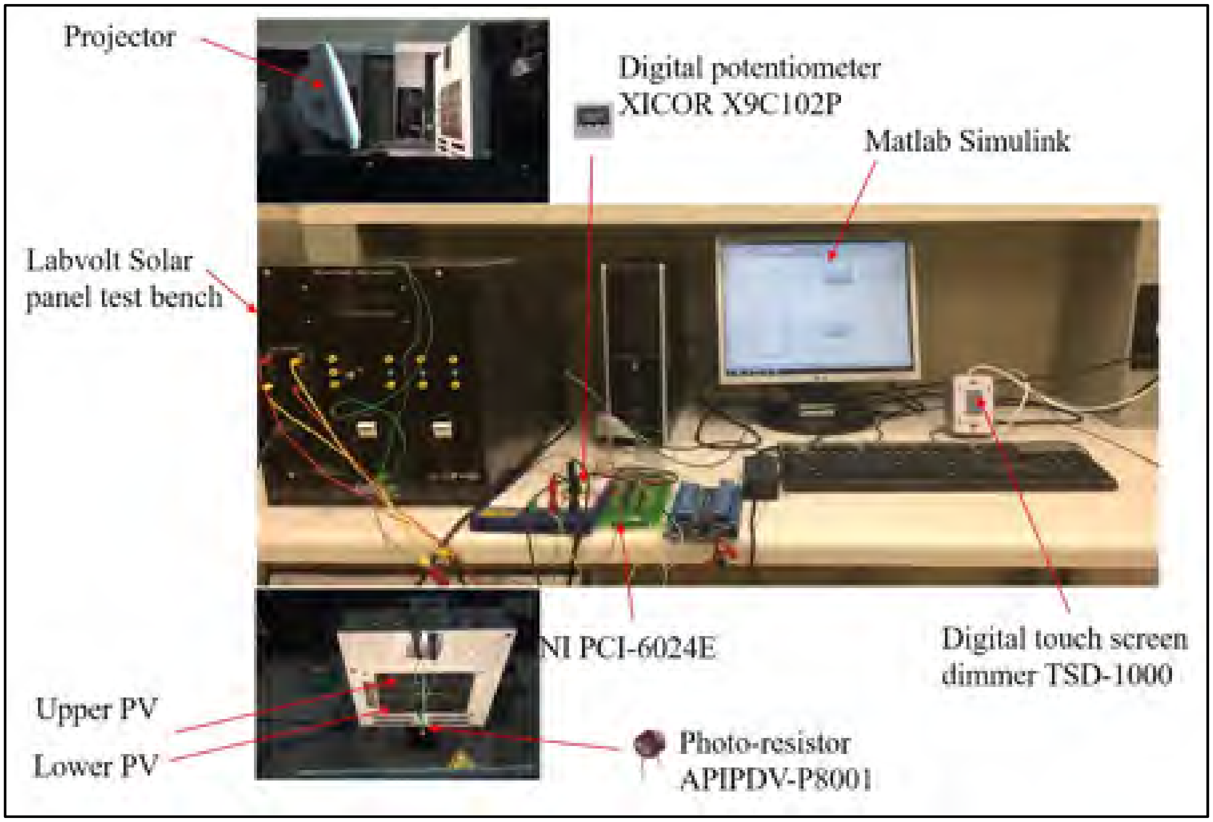

Figure 2.9 Experimental platform

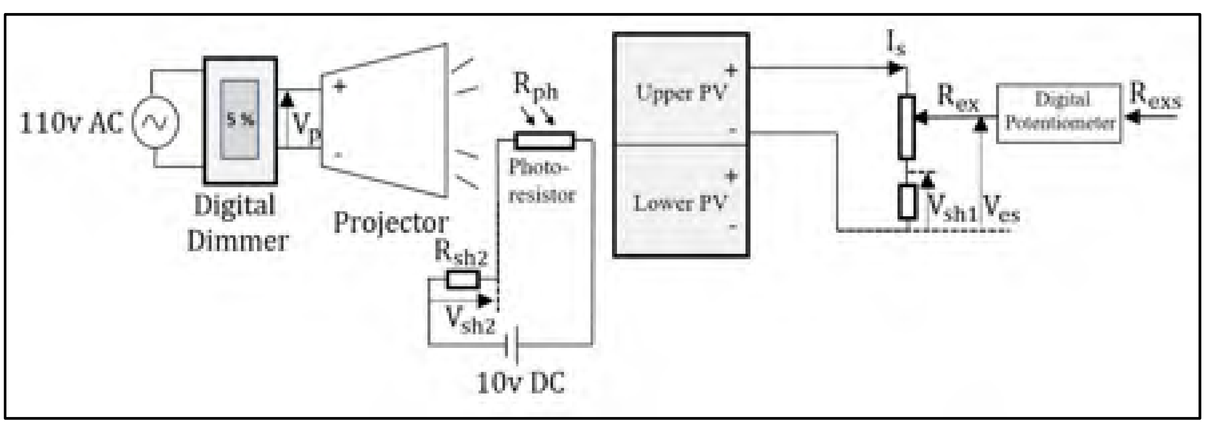

Figure 2.10 Block diagram of the PV experimental platform

In order to compare the performance of ESC and ESC$_{aa}$ approaches, an experimental PV platform was designed (Figure 2.9 and Figure 2.10). A main solar source (Labvolt solar panel test bench, model 8805) constituted by two PV panels, each of them made of 9 monocrystalline silicon cells connected in series was permanently installed in front of a 300 W projector, which was submitted to a variable supply voltage V_p using a digital touch screen dimmer (Uber Haus, TSD-1000). The digital dimmer allows a precise variation of the projector supply voltage from 0 to 100% with a minimal step of 5%. A 1 KΩ digital potentiometer (XICOR X9C102P 1kΩ) was connected to the PV source as an external variable load R_{ex}. The light irradiance is measured using a photocell resistance R_{ph} (API PDV-P8001). An acquisition board (National Instrument, NI-PCI6024E) was used for controlling the digital potentiometer via the reference signal R_{exs}, measuring the external load R_{ex} via the measurements of the output voltage V_{es} and the voltage V_{sh1} at the shunt resistor ($R_{sh1} = 30\ ohm$) and, measuring the photocell resistance (R_{ph}) from the measurement of the voltage V_{sh2} at the shunt resistor $R_{sh2} = 500\ ohm$. The data were sampled using a $0.01\ s$ period and transferred to/from Matlab/Simulink using the PCI-6024E DA block from the Simulink real-time toolbox.

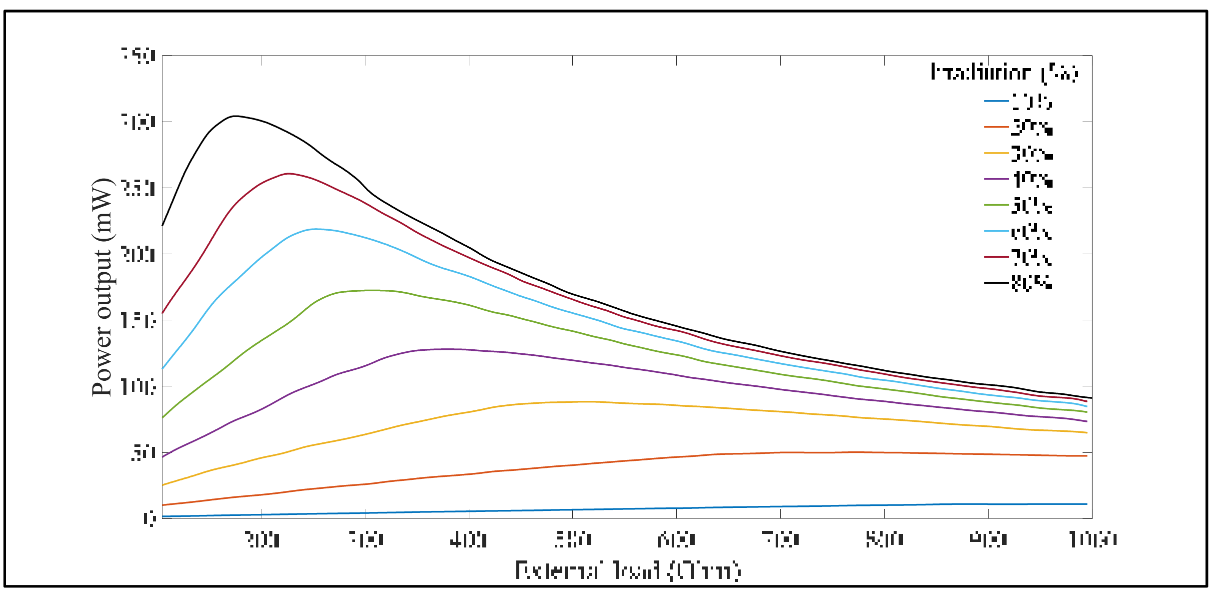

Figure 2.11 Static characteristics of the PV system: output power as a function of the external load for different radiation levels

In order to determine the maximum output power P_s^* and the corresponding internal resistance R_{in} of the PV system for different external disturbances, the radiation was varied by controlling the voltage supplied to the projector using the digital dimmer. The PV static characteristics was obtained by varying the dimmer position from 10% to 90% by steps of 10% and the external digital potentiometer R_{ex} from 100 to 1000 Ω by steps of 10 Ω (Figure 2.11). The optimal values of the power and internal resistance obtained are shown in Table 2.3.

This time, the radiation (G), measured using a photocell resistance (R_{ph}), was chosen to be the measurable external disturbance (d_m). Hence, a lookup table mapping the value of the photocell resistance to the relative dimmer positions was defined (Table 2.3).

Table 2.3 Optimal values of the PV internal resistance, values of the photo-resistor and NN model outputs for different radiation levels, i.e., different dimmer positions

Relative position of the dimmer or G level (%)	**Internal resistance R_{in} for one PV (Ω)**	**Resistance R_{ph} of Photo-resistor (Ω)**	**Internal resistance estimated by NN (Ω)**
90	150	50	--
80	177.3	60	175.2
70	228.5	70	--
60	254.5	80	251.9
50	311	90	305.1
40	396.1	110	--
30	516	140	--
20	774.3	200	771.5
10	978	470	--

Note that usually the duty cycle of a DC-DC converter is usually controlled instead of a potentiometer to perform the power optimization of a PV system. Actually, from a PV system perspective, the duty cycle variation of a DC-DC converter is seen as a variation of the external load. Thus, since the main focus of this paper is on power point tracking techniques, the DC-DC converter was replaced by a digital potentiometer for simplicity purpose.

Considering the PV system presented in Figure 2.10 and according to equation (2.7), the optimization problem to be solved is described by the following equation:

$$\begin{aligned} & Max_{R_{exs}}\, P_s(R_{exs}) \\ s.t. \quad & \dot{x} = f(x, R_{exs}, R_{ph}) = 0 \text{ ,} \end{aligned} \tag{2.46}$$

where the photocell resistance R_{ph} used to measure the radiation G is the measurable disturbance d_m, the PV power output in static mode P_s represents the objective function J, the setpoint of the digital potentiometer R_{exs} is the control input β, and, finally, the state vector (x) includes the current through the potentiometer along with the position and the speed of the digital potentiometer.

2.7.2 ESC of a PV

The performance of the ESC scheme was first evaluated under a slow variation of radiation using the same criteria as for the MFC simulations (T_c , N_p and T_{acc}). This slow disturbance was performed by changing the radiation from 20 % to 80 % and then, from 80% to 50 %. The tracking efficiency T_{eff} was also evaluated using a fast and random variations of radiation.

Once again, the parameters of the ESC scheme were adjusted in order to guarantee a timescale separation between the system, the perturbation signal and the filters. As the digital potentiometer is the slowest element of the whole PV system, with an average response time of $T_P = 0.2$s, the parameters of the ESC loop are chosen with regard to this response time:

- Square wave excitation signal frequency: $F = \frac{1}{2 \times T_P} = 2.5\ Hz$.
- The cutoff frequencies of the filters: $\omega_l = \omega_h = \frac{2 \times \pi}{5 \times T_p} = 10.46\ \text{rad/s}$.

- Perturbation signal amplitude and gain of the controller: $a = 10\ \Omega$, $k = 0.05\ \Omega^2 mW^{-1}$.
- The initial condition of the input: $R_{ini} = R_{in(G=20\%)} = 774.3\ \Omega$.

The choice of using a square wave is justified by two reasons. Firstly, as the minimal step of the digital potentiometer is limited to 10 ohm, the square wave could have smaller amplitude than a sinusoidal signal. Secondly, the use of a square excitation signal in an ESC loop showed a faster convergence to the optimum in comparison with sinusoidal or triangular signals (Ying Tan et al., 2008).

From Figure 2.12, one can see that for each radiation intensity level, the ESC scheme forces the external load to be equal to the internal resistance of the PV module. Consequently, the PV system reaches the maximum power point at each operating condition (Figure 2.13). Even if the ESC method makes the system converge to the desired operating point with a good tracking accuracy (T_{acc}), the time scale separation condition induces a long convergence time (T_c), especially when the change in the internal resistance is large (Table 2.4). Not surprisingly, if the frequency of the disturbance is increased (the radiation level varies randomly within the span 20%-80% at every 20s), the closed-loop system may not have the time to reach the desired optimum. This behavior results in a low tracking efficiency of 68.98 %.

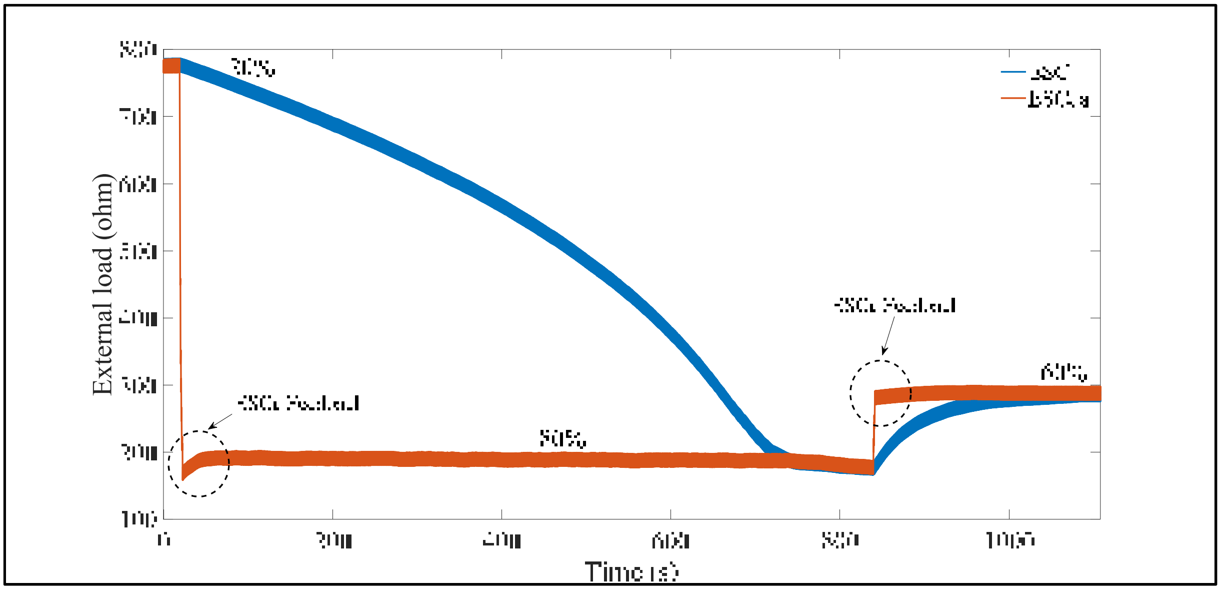

Figure 2.12 Evolution of the external load of the PV system under slow variations of the radiation using ESC and ESC_{aa} methods.

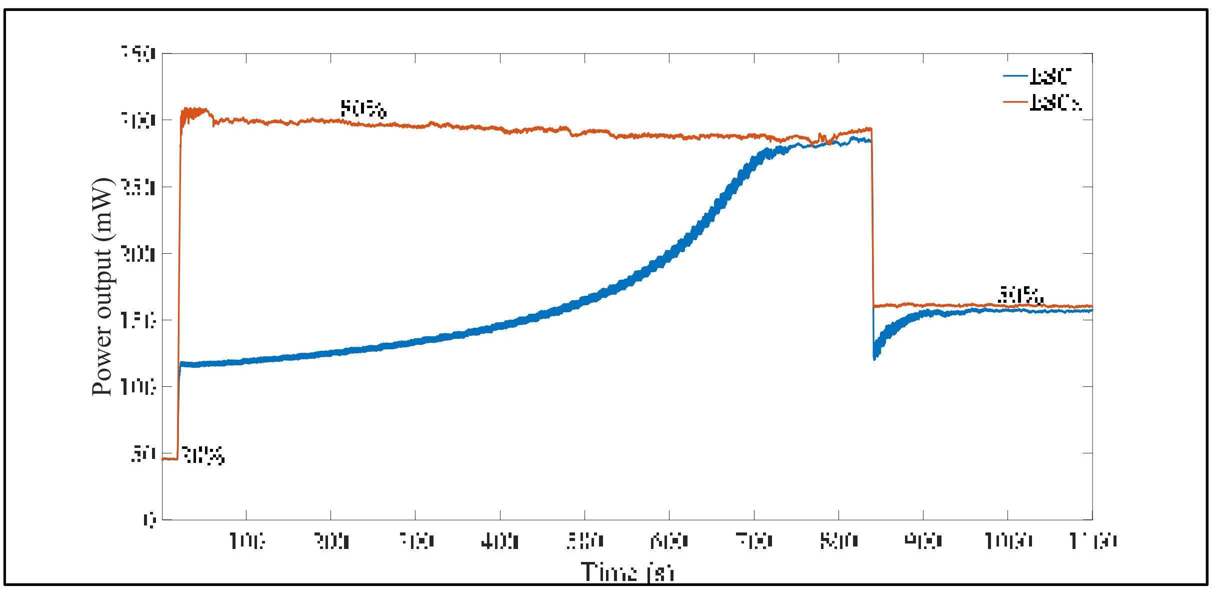

Figure 2.13 Evolution of the power output of the PV system under slow variations of the radiation using ESC and ESC_{aa} methods.

Table 2.4 Performance evaluation of ESC and ESC_{aa} approaches: power optimization of a PV system

	ESC	**ESC_{aa}**
T_c (s) from R_{ini} to $R_{in(G=80\%)}$	708	3.4
T_c (s) from $R_{in(G=80\%)}$ to $R_{in(L=50\%)}$	245	0.9
N_p from R_{ini} to $R_{in(L=80\%)}$	1770	8.48
N_p from $R_{in(G=80\%)}$ to $R_{in(G=50\%)}$	612	2.25
T_{acc} (%) under $P^*_{s(G=80\%)}$	99.2	99.3
T_{acc} (%) under $P^*_{s(G=50\%)}$	99.6	99.6
T_{eff} (%)	67	99.4

2.7.3 ESC_{aa} of PV system

For comparison purpose, the parameters of the ESC_{aa} scheme were set to the same values as for the ESC scheme presented Section 2.7.2.

The neural network-model learning phase was performed using the radiation degree (which is evaluated by measuring R_{ph}) as input and the corresponding internal resistance as the desired output data. Using the values of Table 2.3 corresponding to the following radiation degrees: 90%, 70%, 40%, 30% and 10%.

The neural network model (2.27-2.30) describing the relationship between the internal resistance of the PV source and the radiation measured by the photocell resistance R_{ph} has the same architecture as the one used for the MFC simulation, with $\widehat{\beta^*} = \hat{R}_{in}$ being the internal resistance of the PV system estimated by the NN-model, $d_m = R_{ph}$, $c = 10$ (length of the vector χ) and $bias = 0.5$.

The generalization power test of the neural network model was performed using degrees of radiation differing from those used during the learning phase. Results shown in last column to the right of Table 2.3, confirm that the model was able to estimate the PV internal resistance.

The results presented in Figure 2.12 and Figure 2.13 show that if the neural network anticipative action (offline) is used in ESC (online), the convergence time (T_c) of ESCaa (hybrid) is very fast compared to that obtained with the ESC while guaranteeing the same precision T_{acc} of the latter (Table 2.4). Consequently, the results shown in Figure 2.14, Figure 2.15 and Table 2.4 indicate that the tracking efficiency of the proposed ESCaa method reaches T_{eff} =99.40% under fast and random disturbances. This hybrid method combines the advantages of the offline and online approaches, which are respectively, a rapid convergence and a good precision.

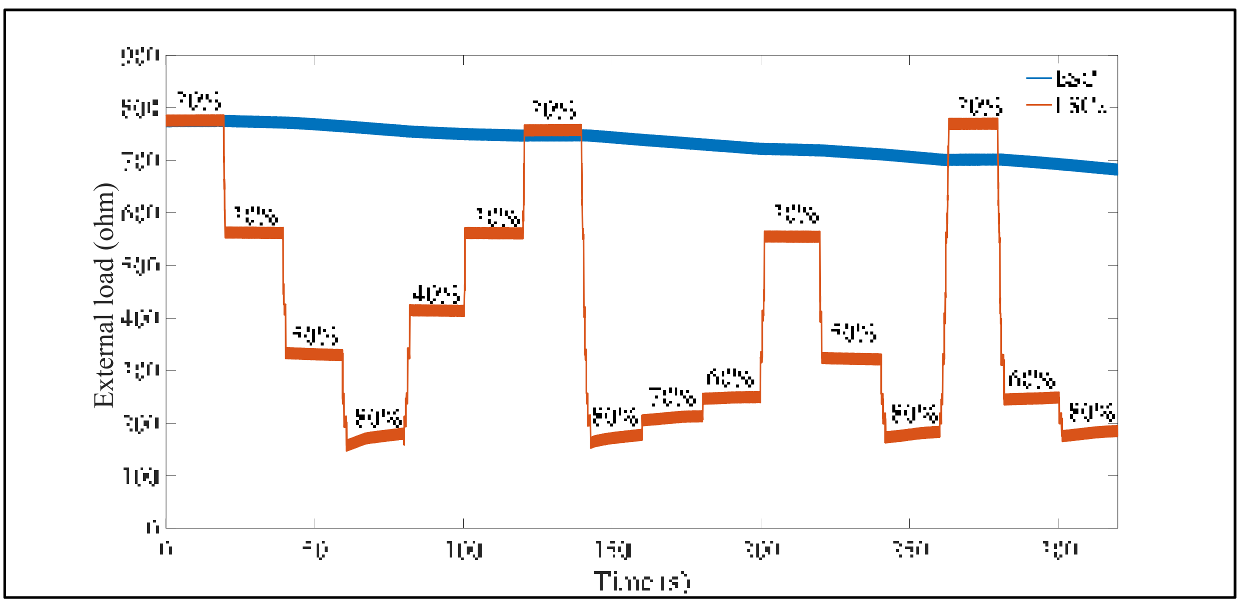

Figure 2.14 Evolution of the external load of the PV system under fast and random variations of the radiation using ESC and ESC_{aa} methods.

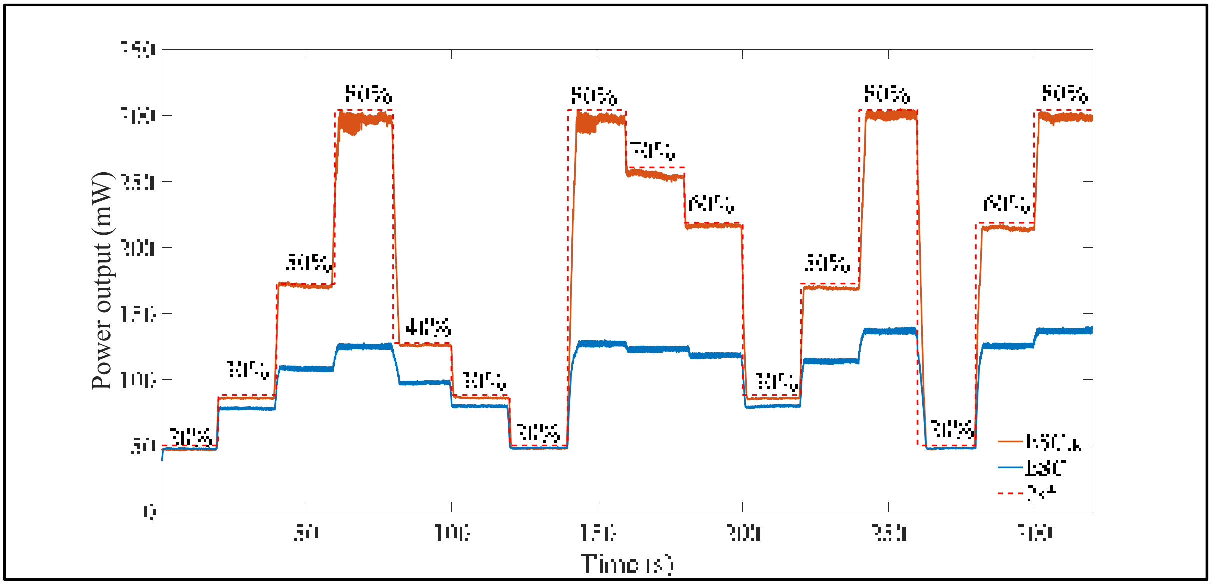

Figure 2.15 Evolution of the power output of the PV system under fast and random variations of the radiation using ESC and ESC_{aa} methods

Note that if a DC-DC converter is to be used instead of the digital potentiometer, the convergence times of the ESC_{aa} and ESC methods will both decrease. However, it should be mentioned that due to the time scale separation conditions, the number of dither periods required to converge to the desired optimum will remain the same for both methods. Consequently, the convergence time factor observed between the two approaches will also remain the same.

2.8 Conclusion

In this study, it has been shown from theoretical comparative analysis, simulation and experimental results that adding a NN model-based anticipative action to the ESC method significantly increases the speed of convergence. This increase in speed, combined with the high accuracy of the ESC loop itself, contribute to a high tracking efficiency. The solar radiation received by a PV system and the concentration of the inlet substrate feeding a MFC were considered as the only measurable disturbances included in the NN model. However, the proposed approach may be extended to include other measurable disturbances in the NN model, such as temperature or humidity, in the case of the PV system, or pH and flow rate of substrate concentration in the case of the MFC. Including these parameters would improve the robustness and accuracy of the NN model. However, it would also contribute to increase the complexity of the whole scheme. Thus, the choice of new parameters to include in the NN model is based on a tradeoff between increased complexity and a possible reduction of the time of convergence.

In the present paper, the learning phase of the NN model was performed offline. Another way of dealing with both measurable and unmeasurable disturbances that may affect the system under control is to update the NN model parameters online, as in (Kohata, Yamauchi, & Kurihara, 2010). This approach is currently under study. Finally, a stability study is possible for NN (T. Zhang & Guay, 2005), and will also be a part of future work.

CHAPITRE 3

EXTREMUM-SEEKING CONTROL WITH ADAPTIVE EXCITATION: APPLICATION TO A PHOTOVOLTAIC SYSTEM

Anouer Kebir [a], Lyne Woodward [b] and Ouassima Akhrif [c]

[a, b, c] Department of Electrical Engineering, École de Technologie Supérieure,
1100 Notre-Dame Ouest, Montréal, Québec, Canada H3C 1K3

Published in IEEE Transactions on Industrial Electronics, March, 2018

Abstract

The objective of this study is to improve the performance of the extremum-seeking control (ESC) technique in terms of time and accuracy of convergence towards the optimum operating point of a dynamic system subject to the effect of external disturbances. More precisely, the idea is to reduce the undesirable effect of time scale separation in ESC on the performance of the closed loop system. The method consists in adaptively controlling the excitation signal amplitude using a neural network (NN) model, which gives a real-time estimate of the optimal operating point based on the measurement of the external disturbances. Stability of the proposed ESC with adaptive excitation, referred to in the following as ESC_a, is demonstrated. The superiority of ESC_a compared to ESC in terms of accuracy and time of convergence to the optimum is demonstrated both theoretically and experimentally, in the case of the optimization of a photovoltaic panel system (PV).

Keywords: Extremum-Seeking Control, Neural Networks, Optimization, Photovoltaic System.

3.1 INTRODUCTION

The increasing complexity of engineering systems has led to numerous optimization challenges. Indeed, analytical solutions to nonlinear optimization problems are difficult or even impossible to obtain. ESC is a real-time optimization approach among others that addresses situations where the model and/or the cost function of the system to be optimized in its static mode are not available to the designer. In this case, the optimization methods are converted into a control problem of the estimated gradient to zero. This gradient is estimated by exciting the system from its input with an excitation signal and correlating this entry with its effect on the output of the system. It requires however the availability of the signals measurements of the input and the output of the system to control. A good review of literature on the ESC can be found in (Ariyur & Krstić, 2003; Y Tan et al., 2010; C. Zhang & Ordóñez, 2011).

For most applications, the dynamics of the system to be optimized are nonlinear. In this case, the main difficulty of the ESC technique (A. Kebir et al., 2015) is the requirement of multiple time scales between the dynamics of the system, the frequency of excitation and the speed of adaptation. The excitation must be an order of magnitude slower than the system dynamics to separate the effect of excitation from the dynamics of the system. Moreover, the adaptation must be slower than the excitation in order to distinguish the effect of excitation from the adaptation one. Unfortunately, these multiple separations of time scales have the effect of slowing down the convergence. In cases where the optimal operating point is moving slowly, ESC will perform correctly but if the system is submitted to frequent external disturbances, the performance achieved will be sub-optimal. In (Ariyur & Krstić, 2003), the issue of the ESC technique convergence time was addressed and the requirement of time scale separation was eliminated. A dynamic compensation scheme was proposed providing a guarantee of stability, a rapid monitoring of changes of the operating point, and a measurement noise rejection. The result was limited however to optimization problems for systems with linear dynamics. Several other approaches were proposed to reduce the effect of time scale separation on the speed of convergence, but these approaches are based on specific conditions such as a priori knowledge of the objective function structure (Banavar, 2003; Guay & Zhang, 2003), a linear time-invariant process (C. Zhang & Ordónez, 2005), a system belonging to a class of well-defined non-linear systems (Adetola, Dehaan, & Guay, 2004) or an unknown linear system (Adetola & Guay, 2006). However, when real applications are considered, ESC must be applied to non-linear systems with unknown dynamics.

External disturbances in many systems are measurable. Assuming that these disturbance measurements are available to the expert, they can be used to improve the performance of ESC (A. Kebir et al., 2015). Indeed, the modeling of the relation between the optimal operating point of the system and the external disturbances allows a real-time estimation of the location of the system optimum for each new measurement of the external disturbances. Based on the estimates provided by this model, it is then possible to adjust the ESC parameters in real time in order to converge more quickly and more precisely towards the desired optimum. The parameters that have a significant effect on the convergence speed and accuracy of ESC include the initial conditions of the manipulated variable and the amplitude of the excitation signal. The sinusoidal signal is generally chosen as an excitation signal in the ESC. In (Ying Tan et al., 2008) a proof that the choice of the shape of the excitation signal has a direct effect on the convergence rate of ESC is demonstrated. The study shows that ESC with a rectangular excitation signal is twice as fast as a sinusoidal signal and four times faster than a triangular signal. In (Marinkov, de Jager, & Steinbuch, 2014) and (A. Kebir et al., 2015), the authors indirectly controlled the initial condition at the ESC integrator, using anticipative action to improve the speed of convergence. In this paper, we perform an adaptive control of the amplitude of the excitation signal. Note that in (Ying Tan, Nešić, Mareels, & Astolfi, 2009), the excitation signal amplitude was also adapted but only to improve the accuracy of ESC in order to converge to a global maximum instead of a local one. Our objective on the other hand is to improve both accuracy and speed of convergence. In this paper, it is assumed that the objective function to be optimized is unimodal. Thus, the proposed approach consists in using the optimum estimation to control in real time the amplitude of the excitation signal in order to precisely and quickly follow the desired optimum operating point. The proposed model linking the external disturbance to the optimal operating point is based on a multilayer neural network structure. The stability of the proposed approach is demonstrated. A comparative study of ESC schemes with and without adaptive excitation in terms of accuracy and time convergence to the optimal operating point is also provided theoretically and experimentally in the case of power optimization of a photovoltaic panel that is subject to a measurable external disturbance represented in this case by radiation of sunlight.

The paper is organized as follows. After an introduction, Section 3.2 defines the optimization problem considered whereas Section 3.3 presents the classical ESC scheme. In Section 3.4 the proposed ESC_a approach is presented and its stability is studied in Section 3.5. A theoretical comparative analysis between ESC and ESC_a is performed in Section 3.6 whereas an experimental evaluation of both methods is provided in Section 3.7. Finally, conclusions of the paper are presented in Section 3.8.

3.2 Optimization problem formulation

Let us consider a dynamic system described by the following equation:

$$\dot{x} = f(x, u, d_m) \tag{3.1}$$

where $d_m \in \mathbb{R}^h$ is the measurable disturbances vector, $x \in \mathbb{R}^n$ is the state vector, $f: \mathbb{R}^n \times \mathbb{R} \times \mathbb{R}^h \to \mathbb{R}^n$ is unknown and $u \in \mathbb{R}$ is the input such that:

$$u = \alpha(x, \beta) \tag{3.2}$$

with α being a smooth control law parameterized by the scalar β in closed loop.

The optimization problem consists in maximizing an objective function J which describes the performance of the system in static mode. Thus the optimization problem is described mathematically as follows:

$$\begin{gathered} Max_\beta \, J(\beta) \\ s.t. \quad \dot{x} = f(x, \beta, d_m) = 0 \end{gathered} \tag{3.3}$$

where $J: \mathbb{R} \to \mathbb{R}$ is unknown but can be evaluated from available measurements.

3.3 Extremum seeking control

ESC is a real-time optimization method that solves the problem defined in (3.3) while assuming that the system dynamics f and the objective function J are unknown. The method consists in exciting the system by periodic signals and observing the output behavior of the system in static mode in order to estimate and control the gradient of the objective function to zero. The ESC structure (see Figure 3.1) is defined as follows:

$$\beta = \hat{\beta} + a\ sin\ (\omega t) \tag{3.4}$$

$$\dot{\hat{\beta}} = k_{ESC}\hat{g} \tag{3.5}$$

$$\dot{\hat{g}} = -\omega_l\hat{g} + \omega_l(J - \eta)a\ sin(\omega t) \tag{3.6}$$

$$\dot{\eta} = -\omega_h\eta + \omega_h J \tag{3.7}$$

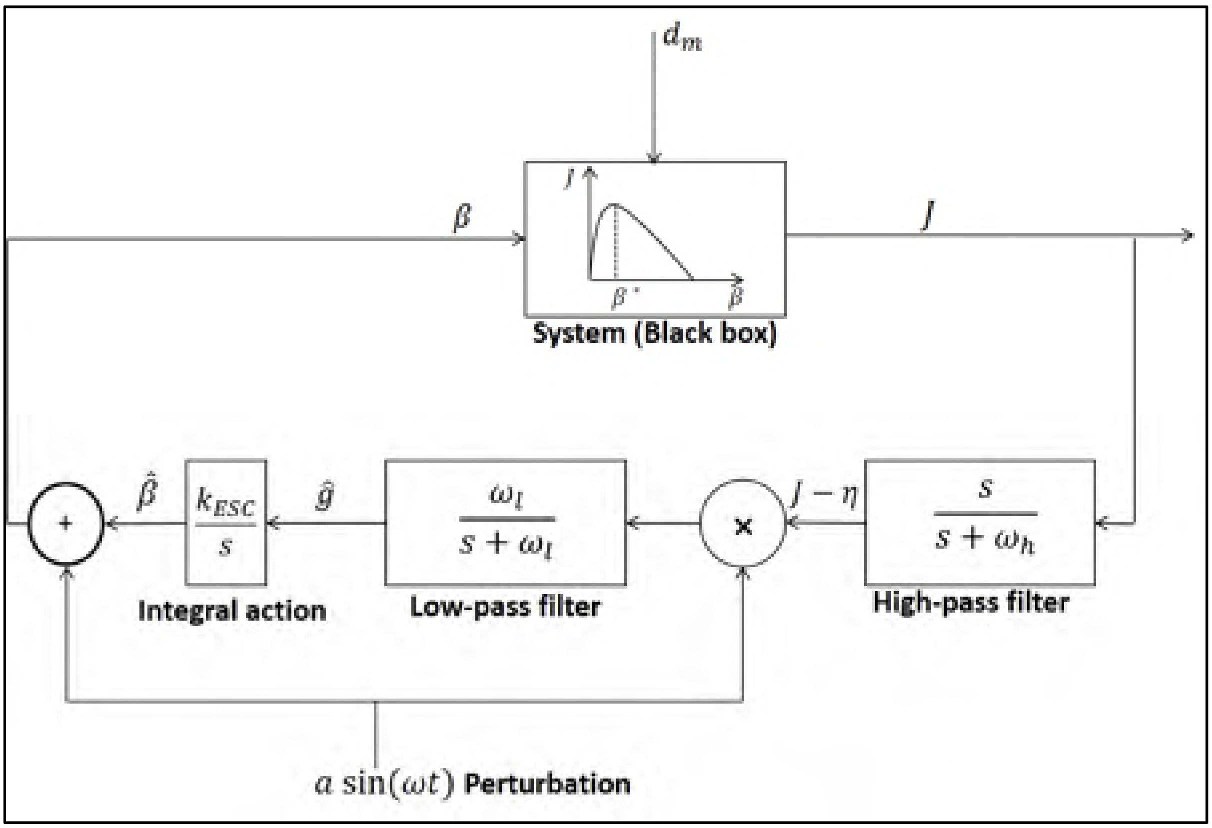

Figure 3.1 Block diagram of ESC scheme

where $a \in [a_{min}\ a_{max}]$ represents the amplitude of the excitation signal which is, in most cases, represented by a sinusoidal signal, ω is the frequency of the excitation signal, a_{min} and a_{max} are small positive constants with $a_{max} = \varepsilon a_{min}$, $\varepsilon \in \mathbb{R}$ and $\varepsilon > 1$, ω_h is the cutoff frequency of the high-pass filter used to eliminate the constant part η of J, ω_l is the cutoff frequency of the low-pass filter used to obtain the average value of the correlation between J and the excitation signal and k_{ESC} is the integral controller gain used to push the estimated gradient $\hat{g}$ to zero.

A judicious choice of ESC parameters is essential to ensure stability and compromise between accuracy and speed of convergence to the optimal operating point. Indeed, if the system is subject to large and rapid external disturbances, these performance criteria will be degraded in the case of optimization of non-linear systems with unknown dynamics as previously shown in a microbial fuel cell application (A. Kebir et al., 2015). Also in (Anouer Kebir et al., 2016), for the same system, the effect of the choice of k_{ESC} and a on ESC performance in terms of accuracy and speed of convergence is shown. Therefore, adapting the ESC parameters, as proposed in this paper, is essential to ensure stability and converge quickly and accurately to the optimal operating point in the presence of external disturbances.

3.4 Proposed approach: ESC_a

3.4.1 ESC_a structure

The amplitude of the ESC excitation signal is among the control parameters which have the most important effect on the precision and convergence time of the optimization method (when the amplitude decreases, the time of convergence towards the optimum increases and the precision increases around the optimum and vice versa). Thus, as in the proposed $\mathrm{ESC_a}$ scheme depicted in Figure 3.2, if an estimate of the optimal operating point position is provided to the ESC loop, the excitation signal amplitude may be adaptively controlled, so that the amplitude becomes smaller when the operating point is near the optimum and larger when it is far from it. As a result, the $\mathrm{ESC_a}$ loop converges both precisely and rapidly to the desired optimal operating point.

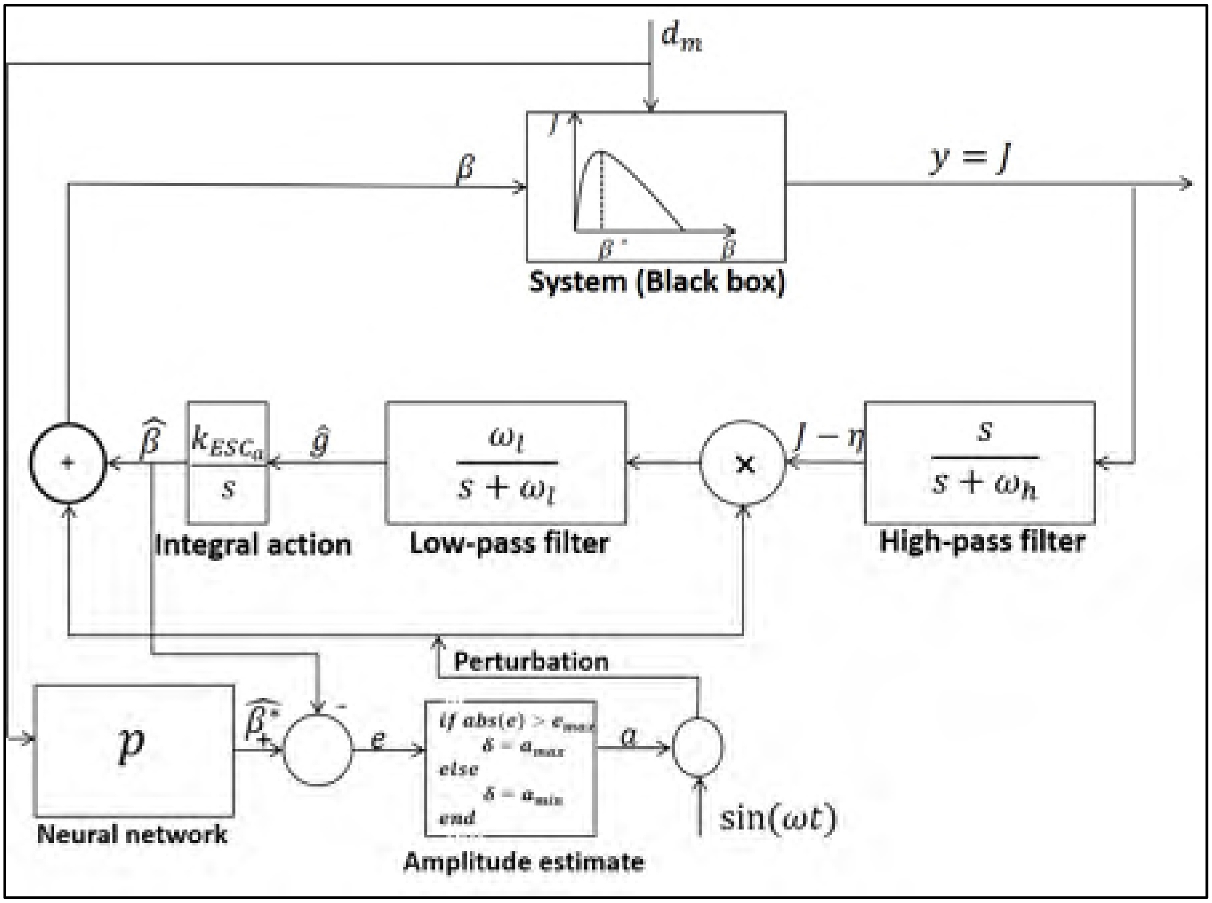

Figure 3.2 Block diagram of the proposed ESC_a

Suppose that there exists a function $p: \mathbb{R}^h \rightarrow \mathbb{R}$ providing an estimate $\widehat{\beta^*}$ of the real optimum β^* using the measurement of the external perturbations vector d_m:

$$\widehat{\beta^*} = p(\, d_m). \tag{3.8}$$

Taking into account the estimate $\widehat{\beta^*}$, one can control the amplitude of the excitation signal according to the error e between $\widehat{\beta^*}$ and $\hat{\beta}$. Hence, the constant amplitude a in the classic ESC will be replaced by variable amplitude δ, whose expression is described by the following equations:

$$\begin{cases} \delta = a_{max} \text{ if } |e| > e_{max} \\ \delta = a_{min} \text{ if } |e| < e_{max} \end{cases} \tag{3.9}$$

with $= \widehat{\beta^*} - \hat{\beta}$, $e_{max} \in \mathbb{R}$ being the maximum estimation error or switching error value prescribed by the expert with $e_{max} \rightarrow 0$ if $\widehat{\beta^*} \rightarrow \beta^*$.

Thus, equations (3.4), (3.5) and (3.6) of the ESC technique scheme are respectively replaced by the following equations:

$$\beta = \hat{\beta} + \delta\, sin(\omega t) \tag{3.10}$$

$$\dot{\hat{\beta}} = k_{ESC_{\mathrm{a}}} \hat{g} \tag{3.11}$$

$$\dot{\hat{g}} = -\omega_l \hat{g} + \omega_l (J - \eta) \delta\, sin(\omega t), \tag{3.12}$$

with $k_{ESC_{\mathrm{a}}}$ is the $\mathrm{ESC_a}$ gain.

3.4.2 Modeling the function *p* using a Neural Network model

Most of the time, as long as real systems are considered, the relation between the optimal operating point β^* and the external perturbation d_m is highly non-linear and very difficult to identify with the laws of physics. In this situation, the Neural Networks modeling method is chosen since it requires only a limited number of input / output data in order to give a good model of the relation between d_m and β^*. Neural Networks approach is very efficient and powerful in the modeling of complex systems (Cotton & Wilamowski, 2011; Haijun, Lucai, Zhaosheng, Houde, & Songhui, 2017; K. Liu & Zhu, 2015) whereas the use of an empirical model having a fixed structure suffers from a lack of flexibility especially in the case where there are several measurable disturbances. Thus, the identification of the model parameters becomes difficult and the optimum estimate becomes imprecise. In (A. Kebir et al., 2015), a comparative study has been carried out between two anticipative ESC schemes using respectively a neural network model and a static linear model in the anticipation loop. The performance of the two approaches was compared through the optimization of the power delivered by a microbial fuel cell for which the measurement of the inlet substrate concentration was considered as the external perturbation. The study showed that the neural network model provides a more accurate estimate than the linear model and brought the system to its optimum with an advance of 20 days on the linear model. In addition, due to its capacity of generalization, the neural network model is able to provide an accurate approximation of the system behavior (R. Zhang & Tao, 2016), starting with only a limited set of experimental data.

In the literature, there are several types of neural networks. The choice of a neural network generally rests on three characteristics: the architecture (multi-layered or not), the learning mode (supervised or unsupervised) and the learning algorithm (quasi-Newton, backpropagation, BFGS, etc.).

Since the input d_m and output β^* measurements are assumed to be available to the expert, the learning mode of the neural network will be supervised and a multi-layered perceptron with a hyperbolic tangent activation function and one hidden layer will be used to identify the function p. Moreover, the backpropagation algorithm (Bishop, 1995) will be used during the learning phase.

Once the learning phase is completed, the model which represents the function p is described by the following equation:

$$p(d_m) = \widehat{\beta^*} = (1 - e^{-m_{NN}*W_2^T*\phi_2})/(1 + e^{-m_{NN}*W_2^T*\phi_2)}, \tag{3.13}$$

where:

$$\phi_2 = \begin{bmatrix} bias \\ \chi \end{bmatrix}, \tag{3.14}$$

χ is the vector of length c with the i^{th} element defined by the activation function of each neuron of the hidden layer, i.e.,

$$\chi(i) = (1 - e^{-m_{NN}\psi(i)})/(1 + e^{-m_{NN}\psi(i)}), \tag{3.15}$$

$$\psi = W_1^T\phi_1, \tag{3.16}$$

$$\phi_1 = \begin{bmatrix} bias \\ d_m \end{bmatrix}, \tag{3.17}$$

and $W_1 \in \mathbb{R}^{bxc}$, $W_2 \in \mathbb{R}^{\lambda xq}$ are respectively the sets of synaptic weights between the neuron input and the hidden layer and between the hidden layer and the output neuron fixed after learning respectively, whereas $m_{NN} \in \mathbb{R}$ is the slope of the hyperbolic tangent activation functions ϕ_1 and ϕ_2 , $b = h + 1$ since the number of input neurons is equal to the number of measurable disturbances, q is the number of output neurons that is equal to 1 since the NN model estimates a single parameter (β^*), $\lambda = c + 1$ with c being the number of neurons in the hidden layer chosen by the expert, *bias* is a constant value chosen by the expert.

3.5 Stability study of $\mathrm{ESC_a}$

In order to lighten the following mathematical analysis of the $\mathrm{ESC_a}$ stability, two small modifications are performed to the scheme shown in Figure 3.2. Firstly, the amplitude of the sinusoidal signal multiplying the output of the high-pass filter is equal to 1. Secondly, the low-pass filter is removed.

Thus,

$$\begin{cases} \dot{\hat{\beta}} = k_{ESC_a} \sin(\omega t) \left(J(\hat{\beta} + \delta \sin(\omega t)) - \eta\right) \\ \dot{\eta} = \omega_h \left(J(\hat{\beta} + \delta \sin(\omega t)) - \eta\right). \end{cases} \tag{3.18}$$

Assuming J admits a local maximum β^*, and β is close to it, using a Taylor series approximation we obtain:

$$J(\beta) \simeq J^* + \frac{J''^*}{2} (\beta - \beta^*)^2 \tag{3.19}$$

with $J^* = J(\beta^*)$ and $J''^* = \left.\frac{\partial^2 J}{\partial \beta^2}\right|_{\beta^*}$.

Thus for $\beta = \hat{\beta} + \delta\, sin(\omega t)$ around β^*:

$$\begin{cases} \dot{\hat{\beta}} = k_{ESC_a} \sin(\omega t) \left(J^* + \frac{J''^*}{2} (\hat{\beta} + \delta \sin(\omega t) - \beta^*)^2 - \eta\right) \\ \dot{\eta} = \omega_h (J^* + \frac{J''^*}{2} (\hat{\beta} + \delta \sin(\omega t) - \beta^*)^2 - \eta). \end{cases} \tag{3.20}$$

From the form of system (3.20) the averaging method is applicable (see, for example, Equations. (8.17)-(8.19) in (Khalil, 1996)). Thus, the average system of (3.20) is described as follows:

$$\begin{cases} \dot{\hat{\beta}}_{av} = -\delta k_{ESC_a} \frac{J^{''*}}{2} (\beta^* - \hat{\beta}_{av}) \\ \dot{\eta}_{av} = \omega_h (J^* + \frac{J^{''*}}{2} ((\beta^* - \hat{\beta}_{av})^2 + \frac{\delta^2}{2}) - \eta_{av}) \end{cases} \tag{3.21}$$

provided that:

$$\delta k_{ESC_a} J^{''*} \ll \omega \text{ and } \omega_h \ll \omega. \tag{3.22}$$

The equilibrium point of the average system (3.21) is:

$$\eta_{av} = J^* + J^{''*} \delta^2 / 4 \tag{3.23}$$

$$\hat{\beta}_{av} = \beta^* \tag{3.24}$$

and the Jacobian matrix A evaluated at this equilibrium point $(\hat{\beta}_{av}, \eta_{av})$ is defined as follows:

$$A = \begin{bmatrix} \delta k_{ESC_a} J^{''*}/2 & 0 \\ 0 & -\omega_h \end{bmatrix} \tag{3.25}$$

with $\delta \in [a_{min}\ a_{max}], a_{min}, a_{max} > 0, k_{ESC_a} > 0, \omega_h > 0$, and $J^{''*} < 0$ by definition. Since the eigenvalues of the Jacobian matrix are:

$$\lambda_1 = \delta k_{ESC_a} \frac{J^{''*}}{2} < 0, \tag{3.26}$$

$$\lambda_2 = -\omega_h < 0, \tag{3.27}$$

the Jacobian matrix at the equilibrium point $(\hat{\beta}_{av}, \eta_{av})$ is Hurwitz. Thus, the average system converges to $\beta^*$and is asymptotically stable. As $\beta = \hat{\beta} + \delta \sin(\omega t)$, then the perturbed system converges on average to β^*.

From (3.9) and (3.25), the average system can be presented in the form of a switching system (DeCarlo, Branicky, Pettersson, & Lennartson, 2000) as,

$$\dot{x}(t) = A_{\sigma(t)} x(t) \tag{3.28}$$

where $\sigma(t): R^* \rightarrow \tau = \{1,2\}$ represents the switching law and $A_{\sigma(t)} \in \{A_1, A_2\}$ with

$$A_1 = \begin{bmatrix} a_{max} k_{ESC_a} J^{''*}/2 & 0 \\ 0 & -\omega_h \end{bmatrix} \tag{3.29}$$

$$\text{and, } A_2 = \begin{bmatrix} a_{min} k_{ESC_a} J^{"*}/2 & 0 \\ 0 & -\omega_h \end{bmatrix}. \tag{3.30}$$

The switching law is described by the following system of equations:

$$\sigma(t) = \begin{cases} 1 \text{ } if \text{ } e = \left|\widehat{\beta}_{av} - \widehat{\beta^*}\right| > e_{max} \\ 2 \text{ } if \text{ } e = \left|\widehat{\beta}_{av} - \widehat{\beta^*}\right| < e_{max} \text{ .} \end{cases} \tag{3. 31}$$

According to (3.29) and (3.30) the two sub systems $\dot{x} = A_1 x$ and $\dot{x} = A_2 x$ are asymptotically stable, but according to (DeCarlo et al., 2000), it is not sufficient to guarantee the stability of the system (3.28) during the switching from A_1 to A_2 or from A_2 to A_1. Hence, we must study the stability of the switching system (3.28).

From (DeCarlo et al., 2000), if the two sub systems are linear and asymptotically stable, we only need to demonstrate the existence of a common Lyapunov function for the two to ensure the stability of the system (3.28).

According to (Shorten & Narendra, 1998), a sufficient condition for the existence of a common Lyapunov function for the linear sub systems $\dot{x} = A_1 x$ and $\dot{x} = A_2 x$ is to have A_1 and A_2 being triangulable simultaneously using a non-singular transformation T.

Theorem (Shorten & Narendra, 1998): If A_i, $(i = 1,2,\ldots\ldots M)$ are real matrices that commute pairwise (i.e $A_i A_j = A_j A_i$ for all i, j) then a matrix T exists such that $T A_i T^{-1}$ are in triangular form. If A_i are stable matrices, a common Lyapunov function $v(x) = x^T P x$ exists for the system $\dot{x} = A_i x$.

Then, according to (3.29) and (3.30):

$$A_1 A_2 = A_2 A_1. \tag{3. 32}$$

Thus, A_1 and A_2 are stable, commute pairwise, and the T matrix exists. Consequently a common Lyapunov function exists and the system (3.28) is therefore asymptotically stable.

3.6 Performance analysis of ESC and ESC$_a$ schemes

3.6.1 Convergence analysis of the ESC scheme

Considering the average model of the closed loop system (Figure 3.1) (Anouer Kebir et al., 2016), the estimated gradient of the performance index $\hat{g}$ can be approximated as follows:

$$\hat{g} \backsimeq \frac{a^2}{2} J'(\hat{\beta}) \tag{3. 33}$$

with $J'(\hat{\beta}) \equiv \frac{\partial J}{\partial \hat{\beta}}$.

Consequently, the time derivative of the input $\dot{\hat{\beta}}$ is described by:

$$\dot{\hat{\beta}} \backsimeq (k_{ESC} a^2/2) J'(\hat{\beta}). \tag{3. 34}$$

Performing a first-order Taylor series expansion of the derivative $J'(\hat{\beta})$ around the optimum β^*:

$$\dot{\hat{\beta}} \backsimeq a^2 k_{ESC} m(\hat{\beta} - \beta^*), \tag{3.5}$$

with $m \equiv \frac{1}{2} \frac{\partial^2 J}{\partial \beta^2}\Big|_{\beta^*} < 0$,

one can provide a linear expression to characterize the evolution of $\hat{\beta}$:

$$\hat{\beta}(t) \backsimeq (\beta_0 - \beta^*) e^{a^2 k_{ESC} m t} + \beta^*. \tag{3.36}$$

Let us define T_{ESC} as the time needed, starting from an initial input β_0 for the ESC loop to approach the optimum β^* within a precision of $\pm 5\%$. Thus,

$$\hat{\beta}(T_{ESC}) \backsimeq (\beta_0 - \beta^*) e^{a^2 m k_{ESC} T_{ESC}} + \beta^* \tag{3.37}$$

$$= \beta^* \pm 0.05\beta^*,$$

$$T_{ESC} \backsimeq \frac{\Gamma}{a \alpha_{max}} \tag{3.38}$$

with $\Gamma = \frac{ln(|\pm 0.05\beta^*|/|(\beta_0 - \beta^*)|)}{m}$ and, $\alpha_{max} = k_{ESC} \times a$ being the maximum combination between k_{ESC} and a chosen by the expert in order to achieve the best performance in terms of precision and time of convergence to the optimum, while respecting the stability conditions:

$$ak_{ESC} \left.\frac{\partial^2 J}{\partial \beta^2}\right|_{\beta^*} \ll \omega \text{ and } \omega_h \ll \omega. \tag{3.39}$$

Moreover, from (3.38) and (3.4) if t ≥ T_{ESC} , the ESC control input β oscillates around the optimum β^* with a maximum error E_{ESC} that can be described as follows:

$$E_{ESC} \simeq a + 0.05|\beta^*|. \tag{3.40}$$

According to (3.33), (3.38) and (3.40), the convergence time depends on k_{ESC} and a whereas the estimated gradient and the maximum error depend only on a. Consequently, it is clear that the amplitude a which is to be chosen by the expert has a large influence on the speed of convergence and the precision. This choice can be summarized in three situations:

-*Situation* 1: the expert wants to reach the maximum of precision around the optimum.

-*Situation* 2: the expert wants to make a compromise between the minimum time of convergence and maximum precision around the optimum.

-*Situation* 3: the expert wants to reach the optimum as quick as possible.

For each of these 3 situations, the choice of the perturbation signal amplitude is done according to Table 3.1. Note that for situation 2, the tuning parameter μ provides some flexibility to the user in the compromise to be done between precision and speed of convergence. In all cases, k_{ESC} is adjusted according to the choice of a such that $k_{ESC} = \alpha_{max}/a$.

Table 3.1 Choice of the excitation amplitude *a* in ESC scheme for 3 different situations

Situation 1	Situation 2	Situation 3
a_{min}	$\frac{(a_{min}+a_{\max})}{\mu}$, $\mu \in R$, $\frac{1+\varepsilon}{\varepsilon} < \mu < 1+\ \varepsilon$	$a_{\max}$

3.6.2 Convergence analysis of the proposed $\mathrm{ESC_a}$

Let us define T_{ESCa} as the time needed for the $\mathrm{ESC_a}$ scheme to converge from β_0 towards the optimum operating point β^* within a precision of $\pm 5\%$:

$$T_{ESC\mathrm{a}} \backsimeq ln(|\pm 0.05\beta^*|/|\beta_0 - \beta^*|)/(\delta^2\ k_{ESC\mathrm{a}}m). \tag{3.41}$$

Considering $\beta_e = \widehat{\beta^*} \pm e_{max}$ as the value of the system input when the switch from $\delta = a_{max}$ to $\delta = a_{min}$ occurs, and $T_{ESC_{NN}}$ the time needed to converge from β_0 to β_e , then,

$$\hat{\beta}\big(T_{ESC_{NN}}\big) \backsimeq (\beta_0 - \beta^*)e^{a_{max}^2 k_{ESC\mathrm{a}} m T_{ESC\,NN}} + \beta^* \tag{3. 42}$$

$$= \beta_e$$

$$\text{and, } T_{ESC_{NN}} \backsimeq ln(|\beta_e - \beta^*|/|\beta_0 - \beta^*|)/(a_{max}^2 k_{ESC_\mathrm{a}} m). \tag{3.43}$$

For t > $T_{ESC_{NN}}$ the input β oscillates around the optimum β^* with a maximum error E_{ESC_a}:

$$E_{\mathrm{ESC_a}} \simeq a_{min} + 0.05|\beta^*|. \tag{3.44}$$

Assuming that the Neural Network model p gives a sufficiently accurate estimate of the optimum such that the expert can choose $e_{max} \in [0\ \ 0.05\beta^*]$, and :

$$\beta^* - 0.05\beta^* \leq \beta_e \leq \beta^* + 0.05\beta^*, \tag{3.45}$$

the time of convergence of $\mathrm{ESC_a}$ can be quantified as follows:

$$T_{ESC_\mathrm{a}} \backsimeq \Gamma/(a_{max}\alpha_{max}). \tag{3.46}$$

A performance comparison of ESC and $\mathrm{ESC_a}$ for the three situations described in Section 3.6.1 is provided in Table 3.2.

Table 3.2 Performance comparison of ESC and ESC_a
in the three situations

Situation 1	**Situation 2**	**Situation 3**
$\begin{cases} T_{ESC} \gg T_{ESC_a} \\ E_{ESC} = E_{ESC_a} \end{cases}$	$T_{ESC} > T_{ESC_a}$ $E_{ESC} > E_{ESC_a}$	$T_{ESC} = T_{ESC_a}$ $E_{ESC} \gg E_{ESC_a}$

It can be seen that in the aforementioned situations, ESC_a converges either more quickly, more precisely or both to the optimum than ESC.

Note that the variation of the excitation signal from a_{min} to a_{max} could be performed as a continuous variation if desired. Doing this, however, the convergence time of the ESC_a scheme to the optimum is expected to be longer than the one obtained when an instantaneous variation of the excitation signal amplitude is used as it is the case in the present paper. Moreover, the stability study will be different from that proposed in section V. The system would become time variant and the stability could not be based on a switching system as it is the case right now. Instead, a Lyapunov-based approach should be followed to demonstrate stability ((Khalil, 2002)).

3.7 Experimental study: application to PV system

Several techniques in the literature have been applied specifically for PV integrated systems: Hybrid MPPT (Moradi & Reisi, 2011), open circuit voltage (Enslin, Wolf, Snyman, & Swiegers, 1997), short circuit current (Noguchi, Togashi, & Nakamoto, 2002), predictive control approaches (Qi, Liu, Chen, & Christofides, 2011; Rahbar, Xu, & Zhang, 2015), etc. These techniques rely on the PV model for optimization. The non-model based conventional ESC has also already been used to optimize the PV system. In (Reisi et al., 2013), a comparative study was carried out between the methods used for the optimization of a PV system model. The study shows that the ESC scheme is more robust and efficient than other online optimization methods such as Perturbation and observation method (P&O) with fixed perturbation size (Salas, Olias, Lazaro, & Barrado, 2005) or variable perturbation size (Yu, Jung, Choi, & Kim, 2004).

The proposed approach ESC_a aims at developing a real time optimization technique that simultaneously insures good precision and speed of convergence towards the optimum operating point of a dynamic system subject to external disturbances. The approach is not intended specifically for a PV application, but can be applied to several other types of systems where the model is difficult to describe from physics laws. It has already been applied in simulations to a microbial fuel cell (MFC) model which is characterized by slower and much more complex dynamics than the one for PV systems. In (Anouer Kebir et al., 2016), the ESC_a allowed the MFC system to converge towards the optimum with high accuracy and to gain days in terms of convergence time compared to the conventional ESC.

In the present study, the PV system was chosen to highlight the proposed approach and validate it experimentally because of its speed and practicality compared to MFC. The time of convergence towards the optimum of an MFC system is in terms of days while the time convergence of PV system is in term of seconds. Also, it is more accessible in the laboratory than an MFC. So, the comparative study between ESC and ESC_a will be established in the case of optimization of the power produced by a photovoltaic system. The optimal power produced by a PV is very sensitive to external disturbances, mainly sunlight radiations and temperature. According to (Marinkov et al., 2014), in real operating conditions, the influence of a temperature disturbance on the PV optimal power is negligible compared to the radiation disturbance. Hence, only the radiation is considered here as a measurable disturbance.

3.7.1 Description of the experimental PV setup

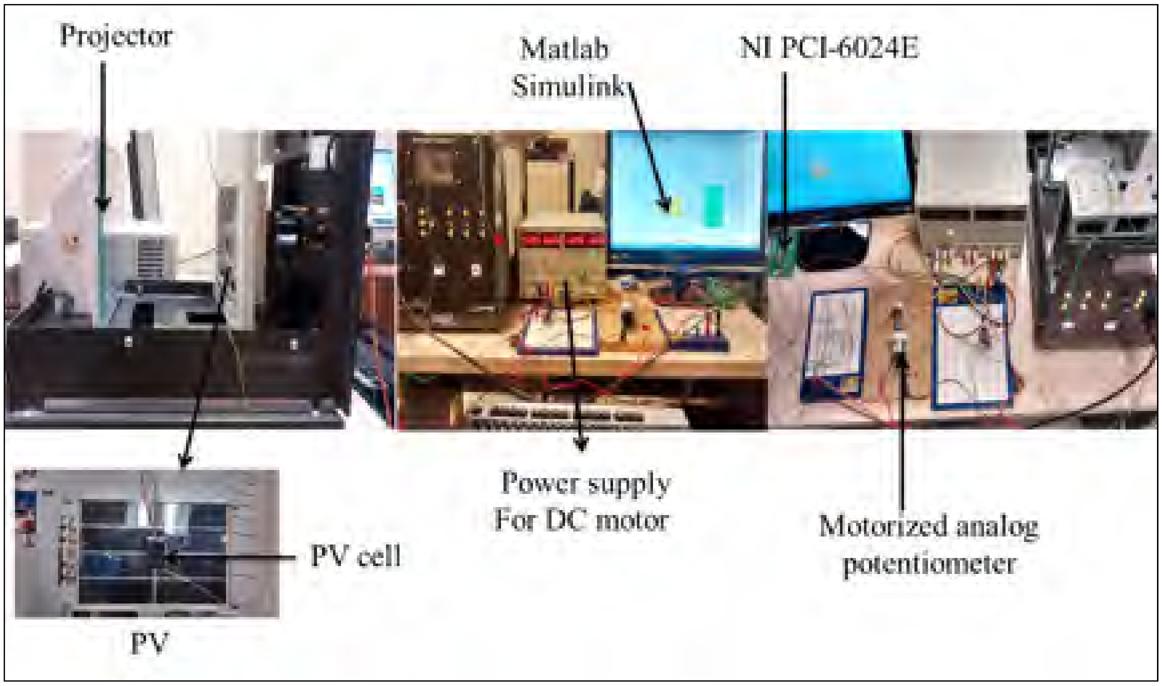

Figure 3.3 Experimental platform

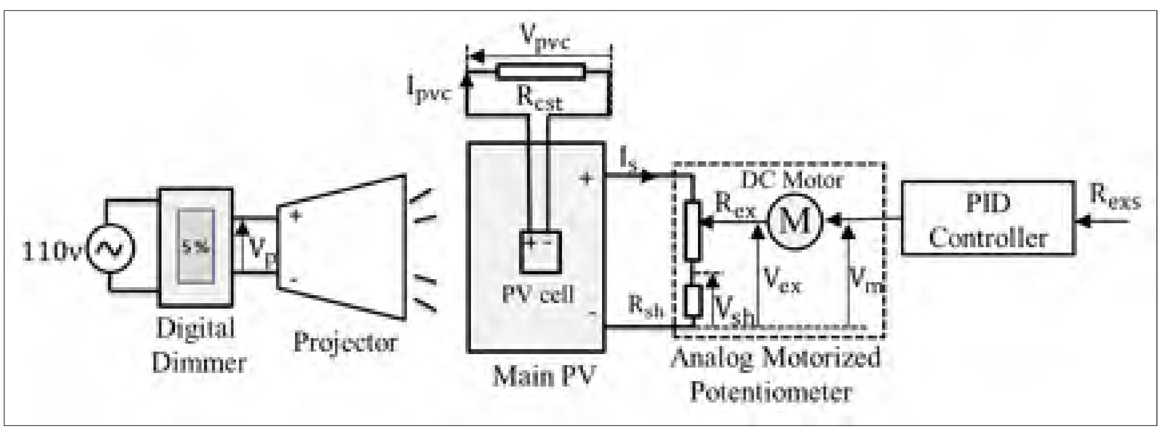

Figure 3.4 Block diagram of the experimental platform

As shown in Figure 3.3 and Figure 3.4, the experimental setup consists of:

- A PV module (Labvolt solar panel test bench, model 8805) permanently fixed in front of a 300 W projector acting as a light source;

- A digital touch screen dimmer (Uber Haus, TSD-1000) which allows to control the radiation emitted by the projector by adjusting its supply voltage (V_p) from 5% to 100% with a step of 5%;
- A small photovoltaic cell (Solarbotics SCC2433B-MSE) which feeds a constant load (270 ohm) to evaluate the radiation disturbance based on the measurement of its output voltage;
- An analog motorized potentiometer constituted by a DC geared motor (Hsiang Neng DC Micro Motor Manufacturing Corporation, HN-GH35GMB) mechanically linked to an analog 1K potentiometer (Precision Electronics Corporation RV4NAYSD102A), playing the role of a variable external load (R_{ex}) at the output of the main PV module;
- An acquisition board (National Instrument NI PCI-6024E) which allows the measurement of the voltage at the PV module (V_{ex}), at the small photovoltaic cell (V_{pvc}) and at the shunt resistor $R_{sh} = 30$ ohm (V_{sh}) used to compute the power;
- A Matlab Simulink software for the implementation of the ESC and $\mathrm{ESC_a}$ schemes (sampling time: T_s = 0.01s).

A PID controller is used to adjust the DC geared motor supply voltage (V_m) in order to control the load value R_{ex} to the load setpoint (R_{exs}). The PID controller parameters have been adjusted following the analog motorized potentiometer model identification. This identification was performed using the Ident function in Matlab. The controller parameters have been chosen with the help of the auto-tune function provided with the PID Controller block from Simulink.

The PID controller form is parallel, the filter coefficient is 0.7611 and the proportional, integration and derivative gains were set respectively to $0.023\, V/\Omega$, $0.00213\, V/(\Omega s)$ and $0.0152\, V\mathrm{s}/\Omega$.

Considering the PV system described above, the optimization problem defined in (3.6) becomes:

$$\begin{aligned} &Max_{R_{exs}}\, P_s(R_{exs}) \\ s.t.\quad &\dot{x} = f(x, R_{exs}, G) = 0 \end{aligned} \tag{3.47}$$

where the radiation G is the measurable disturbance d_m, the PV power output in static mode, P_s, represents the objective function J, the state vector x includes the armature current, the supply voltage, the position and the speed of the DC motor and, β is the setpoint of the PID loop (R_{exs}).

In order to observe the effect of radiation on the PV optimal power (P_s^*), a variation in R_{ex} from 100 to 1000 ohm was performed with a step of 50 ohm for each level of radiation going from 100% to 10% with a step of 10%.

From Figure 3.5 it can be seen that for each level of radiation, the optimal power P_s^* changes, and, not surprisingly, the PV generates its maximum power when the external load R_{ex} is equal to its internal load (R_{in}) (Table 3.3). Thus, the motorized potentiometer will be controlled in order to match the internal load of the PV at each level of radiation.

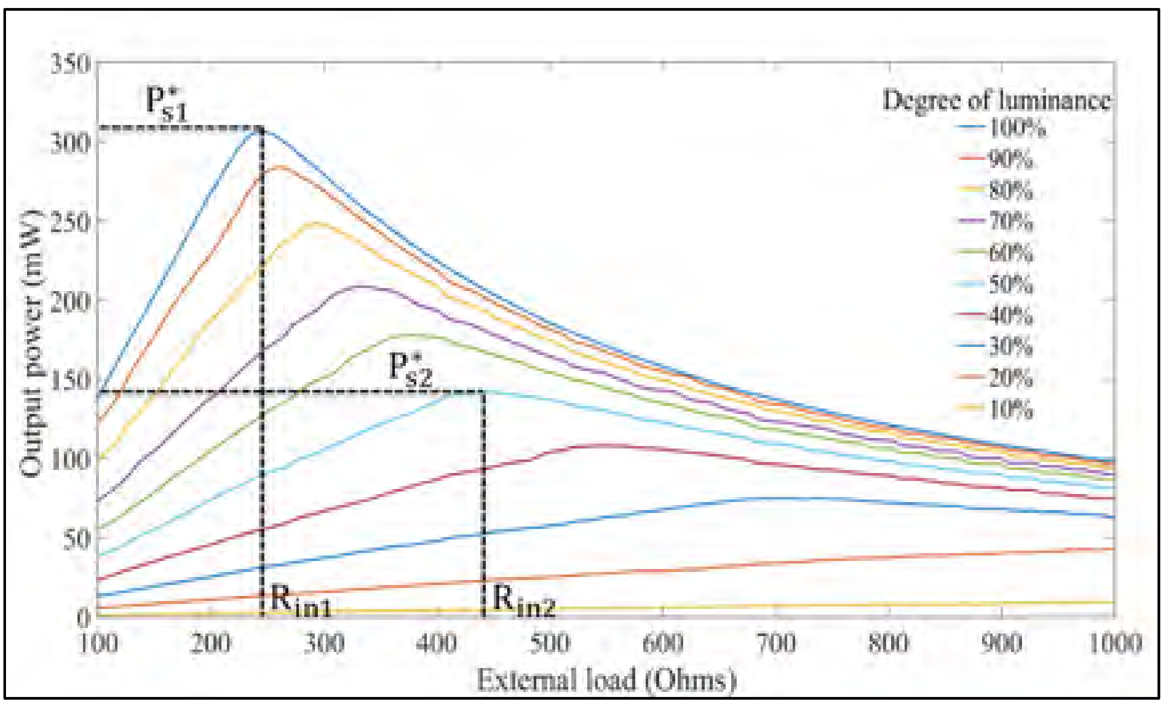

Figure 3.5 Static characteristics of PV output power as a function of the external load for different radiation or luminance levels %

Table 3.3 Optimal values of PV internal resistance and output power of the small PV cell and NN model outputs for different luminance levels, i.e. different dimmer positions

Relative position of the dimmer	**Internal resistance R_{in} of PV (Ω)**	**Power of the PV cell P_{pvc} (mW)**	**Internal resistance estimated by NN (Ω)**
100%	244	30.8	--
90%	230	26	235
80%	260	18.9	274
70%	300	13.2	--
60%	335	9.9	340
50%	447	6	--
40%	550	3.8	522
30%	695	1.7	--
20%	910	0.4	927
10%	990	0.18	--

As the external load is normally imposed to the PV system, a DC-DC converter is usually used to perform impedance matching. Indeed, the duty cycle variation of a DC-DC converter has a direct effect on the impedance seen by the PV source in the case where a fixed load is connected to the output of the DC-DC converter. However, since the focus of our paper is more on the design of a new optimization method (applicable to other types of systems needing to be optimized in real-time), the experimental setup has been kept simple.

The efficiency of both approaches (ESC and $\mathrm{ESC_a}$) will be evaluated using the following efficiency factors used in many papers related to the optimization of renewable energy sources (Bizon, 2016; Khan & Xiao, 2016; Wang, Li, & Ruan, 2016): time of convergence (T_c), tracking efficiency (T_{eff}) and tracking accuracy in steady-state (T_{acc}). Note that the time of convergence will be evaluated both in terms of seconds and in terms of number of dither periods (N_p) in order to relate the performance to the optimization method rather than to the system itself. Hence, if a DC-DC converter is used, the performance remains the same in terms of number of periods whereas the time of convergence (in seconds) is shorter than the one obtained with an analog potentiometer due to the faster dynamics of the system itself.

3.7.2 Performance of ESC and ESC_a under the radiation disturbance effect

In order to evaluate the ESC and ESC_a performance under the effect of the radiation, a variation of radiation will be performed at specific times by operating the digital dimmer from 100% to 50%. As shown in Figure 3.5, these two levels of radiation correspond to two different optimal operating points: $R_{in1} = 244.4\ ohm, P_{s1}^{*} = 306{,}3\ mW$ for 100% of radiation and $R_{in2} = 447.9\ ohm\ , P_{s2}^{*} = 141.9\ mW$ for 50% of radiation. In such a situation, the role of the two optimization methods is to converge to the internal load of the PV system for each level of radiation by controlling the R_{ex} with the PID controller.

As shown in Section 3.5, the first step to implement the ESC_a technique is to model the effect of the external disturbance on the optimal operating point of the system. According to Table 3.3 the relation between the radiations generated by the projector and the PV internal resistance is a nonlinear relation. Therefore, as mentioned in Section 3.5, the proposed approach is to use a neural network model.

Table 3.4 Performance evaluation of ESC and ESC_a approaches

	ESC			**ESC_a**		
	Situation 1	**Situation 2**	**Situation 3**	**Situation 1**	**Situation 2**	**Situation 3**
T_c (s) from R_{ini} to R_{in1}	337	85.8	43.4	46.1	43.7	43.7
T_c (s) from R_{in1} to R_{in2}	214	54.4	24.5	25.6	31.3	31.3
N_p from R_{ini} to R_{in1}	84.2	21. 4	10.8	11.5	10.9	10.9
N_p from R_{in1} to R_{in2}	53.6	13.6	6.12	6.4	7.82	7.82
T_{acc} (%) under P_{s1}^{*}	97.2	93.1	82.6	99	99.4	99.4
T_{acc} (%) under P_{s2}^{*}	98.9	96.6	92.5	99.7	99.4	99
T_{eff} (%)	78	86.2	84.7	97.5	93.7	93.7

The performance of NN model in terms of estimation accuracy depends directly on the richness of information contained in the dataset used during the training phase (Esram & Chapman, 2007). For systems such as PV, the rich data collection describing the relation between the optimal operating points and external disturbance (temperature, irradiation, etc.) can be performed by plotting the static power curves as a function of the control input (duty cycle, external load, etc.). This method indirectly gives a general idea of the effect of external perturbation on the PV internal load. In such a condition, after the learning phase, the NN model offers very good accuracy in estimating the optimal control input of the system (Di Piazza & Pucci, 2016; Reisi et al., 2013).

The NN modeling is performed in two stages. The first step consists in training the NN model using the level of radiation (evaluated by measuring the output power of the small photovoltaic cell P_{pvc}) as an input and the corresponding internal resistance as the desired output (Table 3.3). The second step is the test of NN generalization power.

In this study, the learning database is defined by the measurements shown in Table 3.3 which correspond to the following degrees of radiation: 100%, 70%, 50%, 30% and 10%. Once the learning phase is completed, the neural network model that describes the relation between R_{in} and P_{pvc} is represented by equations (3.13) to (3.17) where $d_m = P_{pvc}$, $\widehat{\beta^*} = \widehat{R_{in}}$, $h = 1$, $c = 10$ and $bias = 0.5$. The power of generalization test was performed to verify the model ability to estimate the PV internal resistance at degrees of radiations which differ from those used during the learning phase (results shown in Table 3.3, column 4).

Note that the internal resistances estimated by NN for 100%, 70%, 50%, 30% and 10% degrees of irradiation have not been included in the fourth column of Table 3.3 since as these points were used during the learning phase of the NN model, the corresponding estimation error is negligible.

Before the implementation of ESC or $\mathrm{ESC_a}$, the control parameters are adjusted to respect the time scale separation condition between the system, the excitation signal and the filters. The entire system includes the motorized potentiometer, the PID controller and the PV panel itself. Compared to other components of the whole system, the PID controller is the slowest element, with an average response time of $T_{PID} = 1\,s$. Hence, the parameters of the two methods are selected according to the response time of the PID regulator.

Consequently, the ESC and ESC_a are designed as follows: the perturbation signal is a sinusoidal wave with frequency $F = 1/(4T_{PID}) = 0.25\,Hz$; the cutoff frequencies of the high pass and low pass filters are set to $\omega_l = \omega_h = 2F\pi/5 = 0.314$ Hz and, the initial external load (at the integrator) is fixed to $R_{ini} = 500$ ohm.

In order to ensure the stability of the ESC and ESC_a loops, the combinations $a \times k_{ESC}$ and $\delta \times k_{ESC_a}$ should be chosen such as to respect the conditions (3.39) with $\beta^* = R_{ex}^*$. In the present case, the stability conditions (3.39) are met by choosing $a \times k_{ESC}$ and $\delta \times k_{ESC_a}$ to be less or equal to $\alpha_{max} = 0.5$. Note that this value of α_{max} was found by trial and error in order to ensure the stability of the closed-loop system.

As in the theoretical study, ESC scheme will be tested in the three situations described in Table 3.1 with $a_{min} = 25$ohm, $a_{max} = 100$ohm and $\mu = 2.5$. In the case of ESC_a the amplitude of the excitation signal δ will be switched from the same values a_{max} to a_{min} according to (3.9) with $e_{max} = 50$ ohm $\gg Max\left(R_{in}(z) - \hat{R}_{in}(z)\right)$, $z\{1,2,\dots,N_g\}$ and N_g being the total number of points used for the generalization test (shown in Table 3.3).

Since the system to be controlled remains the same, the values of high-pass and low-pass filters parameters and of the frequency of the excitation signal are identical for both ESC and ESC_a methods. Consequently, the gains k_{ESC} in ESC and k_{ESC_a} in ESC_a will be chosen based on the value of α_{max} in order to guarantee the maximum speed of convergence towards the optimum while respecting the stability condition (3.39). Thus, in order to guarantee the fastest possible convergence to the optimum for all values of a (Table 3.1), $k_{ESC} = \alpha_{max}/a$ in each situation. In the case of ESC_a, since the amplitude of the excitation signal δ is variable, the gain $k_{ESC_a} = \alpha_{max}/a_{max}$ in all three situations in order to guarantee the maximum convergence speed towards the optimal operating point while respecting the stability condition (3.39) even when δ varies from a_{max} to a_{min}.

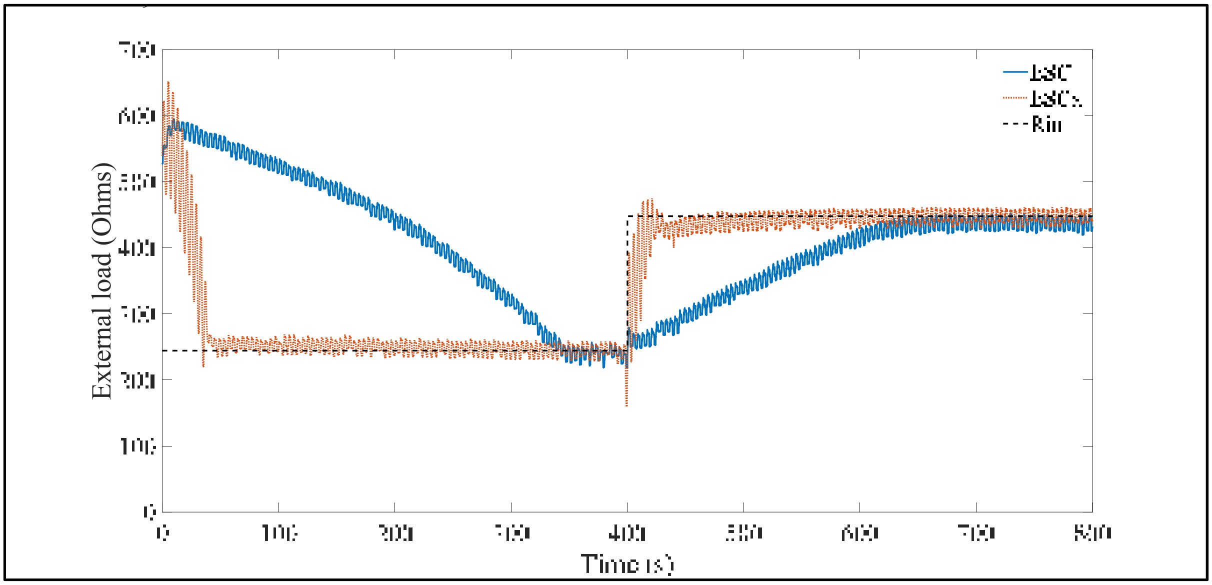

(a)

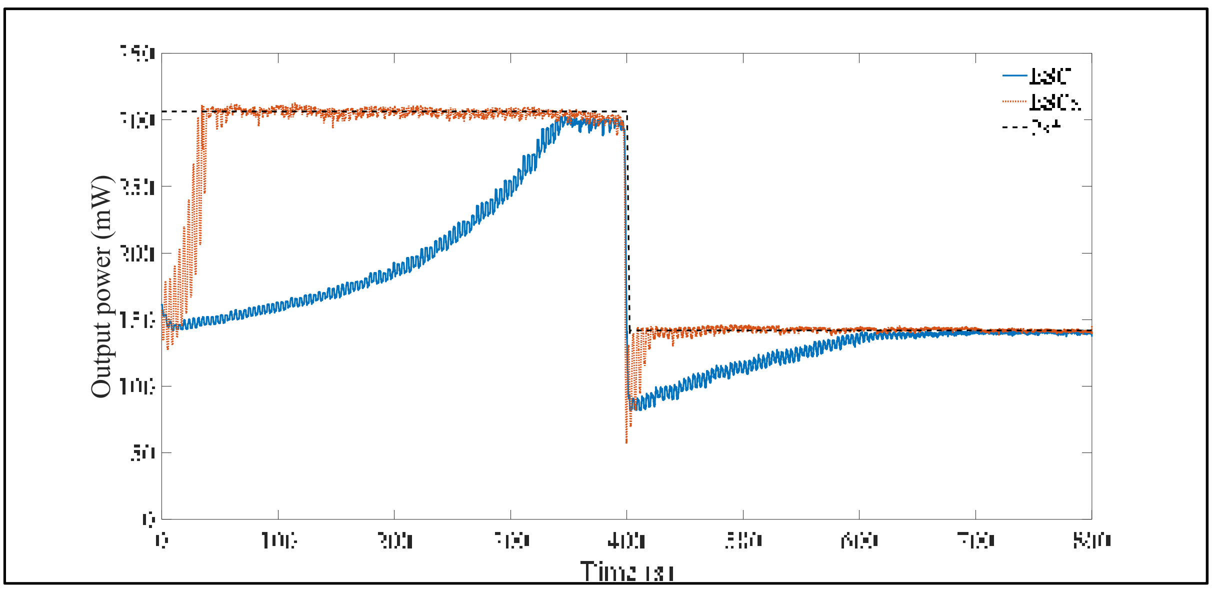

(b)

Figure 3.6 Evolution of the system under ESC_a and ESC in situation 1 for a disturbance of radiation level going from 100% to 50% at T= 400 s: (a) external load and (b) external power

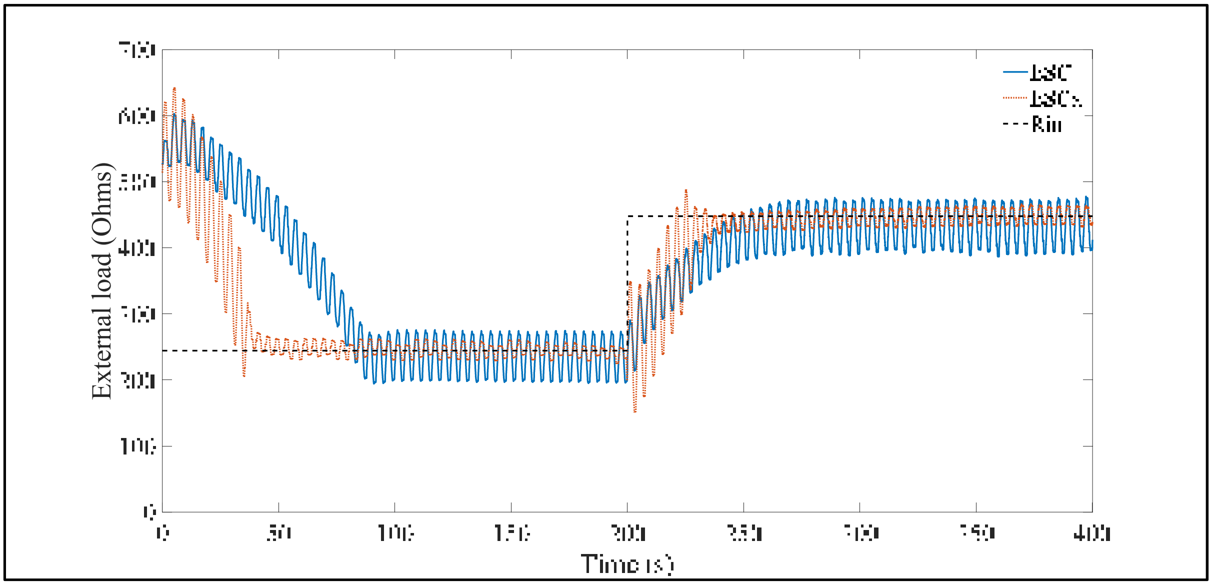

(a)

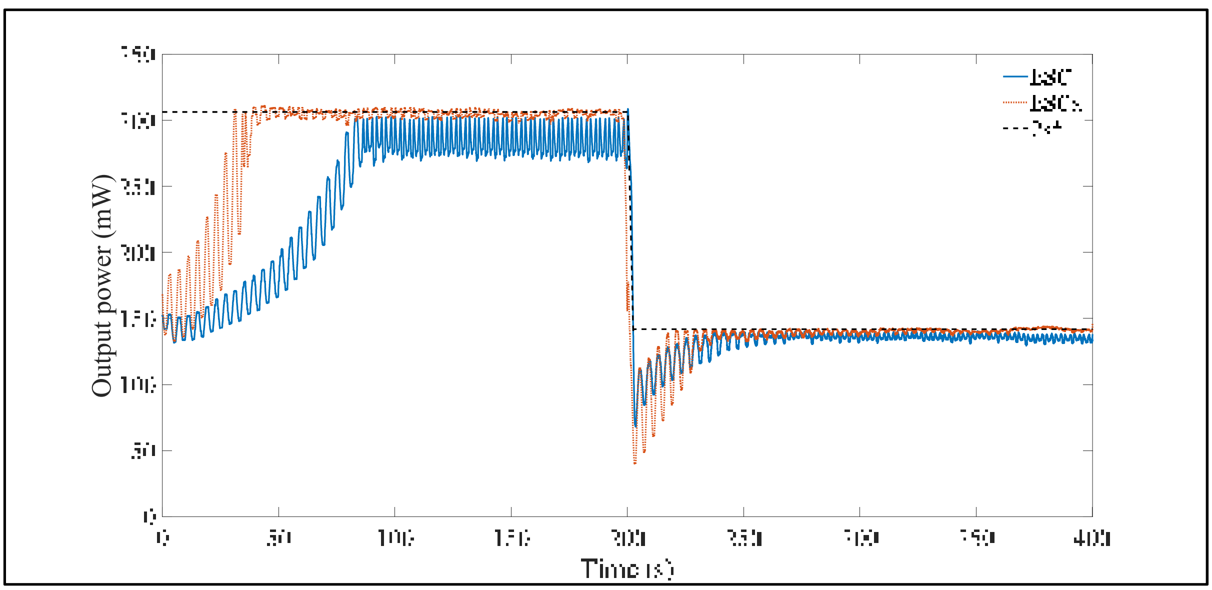

(b)

Figure 3.7 Evolution of the system under ESC_a and ESC in situation 2 for a disturbance of radiation level going from 100% to 50% at T= 200 s: (a) external load and (b) external power

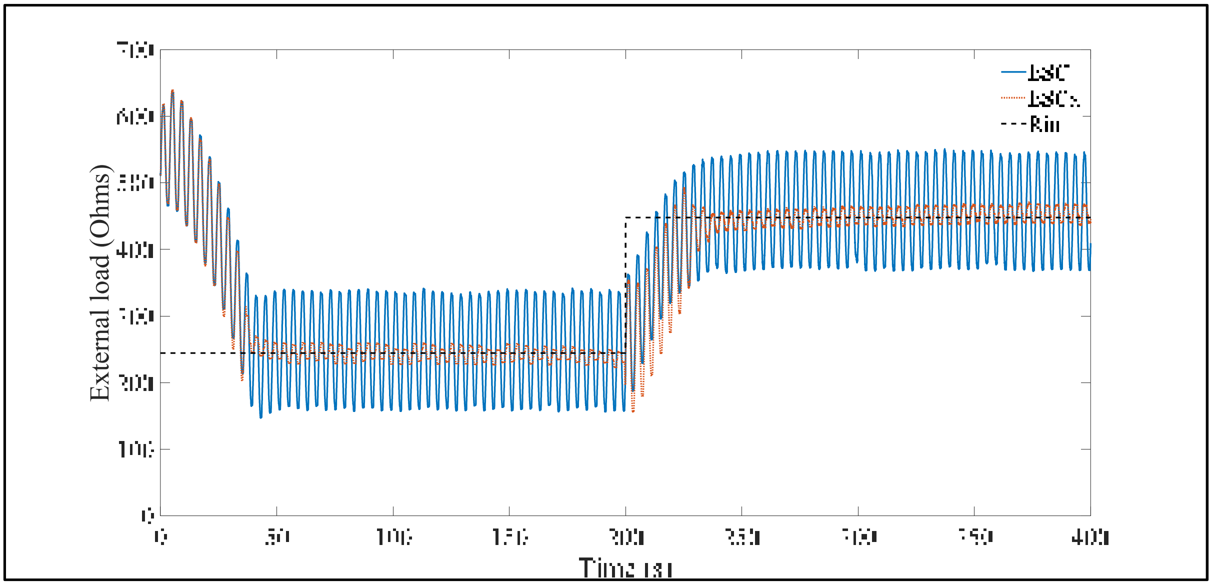

(a)

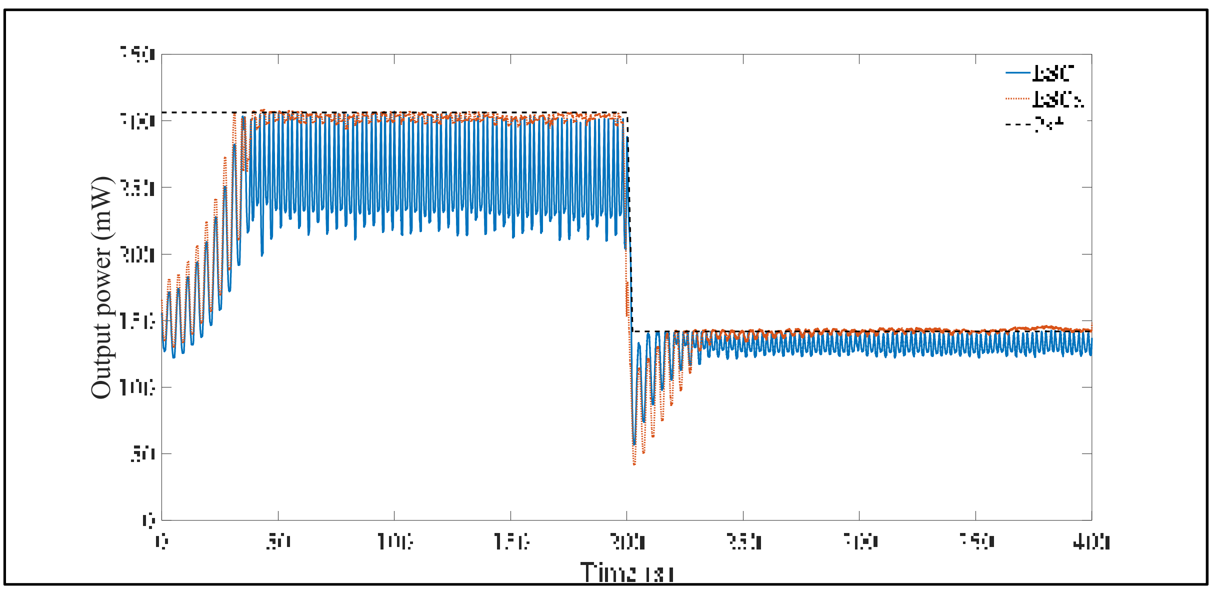

(b)

Figure 3.8 Evolution of the system under ESC_a and ESC in situation 3 for a disturbance of radiation level from 100% to 50% at T= 200s: (a) evolution of the external load and (b) external power

Figure 3.6, Figure 3.7, Figure 3.8 and Table 3.4 give a complete comparison between ESC_a and ESC performance in the three situations. In situation 1, ESC_a method converges nearly with the same tracking accuracy in steady state as the classical ESC one while it converges up to 8.4 times faster (when a 50% radiation disturbance occurs). In Situation 2, $\mathrm{ESC_a}$ approach converges more quickly and accurately than classic ESC loop. Finally, in Situation 3, the $\mathrm{ESC_a}$ methods converges nearly within the same time toward the optimum (with a small delay however because e_{max} is slightly superior to $0.05\beta^* = 0.05R_{in}$) than the conventional ESC loop, but it provides a higher precision around the optimum.

Looking at equations (3.38) and (3.7), one can see that the choice of the amplitude, the initial point of operation and the curvature around the optimum will influence the time of convergence of both methods. Moreover, from these two equations, the theoretical time ratio $T_{ESC}/T_{ESC_a} \approx a_{max}/a$ is equal to 4, 2 and 1 for situations 1, 2 and 3 respectively. In practice, from Table 3.4, the experimental convergence time ratios can be computed to be respectively equal to 7.3, 2 and 1 (when moving from R_{ini} to R_{ini_1}) and to 8.4, 1.7 and 1 (when moving from R_{ini_1} to R_{ini_2}). Hence, for situations 2 and 3, the experimental results are near the theoretical one whereas for situation 1, results differ. This can be explained by the fact that since the theoretical development provided in Section 3.6 is based on a first order Taylor series expansion, it is valid around the optimum. However, in the experimental study, the system was started far away from its optimum. Since in situation 1, the convergence of the ESC method was slower, the system remains far from the optimum for a long period of time and it may be the reason why the experimental convergence time ratio differs from the theoretical one.

Note that in order to let the ESC method find enough time to converge to the desired optimum, the radiation disturbance was performed at 400 s in situation 1 (Figure 6) rather than at 200s as in situations 2 (Figure 3.7) and 3 (Figure 3.8). Thus, since the parameters of $\mathrm{ESC_a}$ are identical in all three situations, the results shown for situations 2 and 3 were obtained from the same experiment whereas another experiment was required for situation 1. As a result, the values of the performance criteria for the $\mathrm{ESC_a}$ method slightly differs in situation 1 from the one obtained in situations 2 and 3.

When applied to a renewable energy source like PV, the precision and convergence time towards the optimum of the two optimization methods have a significant effect on the system performance in terms of energy production. Results depicted in Figure 3.6 and Table 3.4 show that in the first situation, the ESC scheme converges precisely towards the desired optimal operating point in steady state (good tracking accuracy) by bringing the external load around a value near to the internal resistance of the PV. However, the ESC technique takes a long time (large number of periods) to converge to the desired optimum if the initial external resistance is far from the PV internal resistance or if there is a significant variation of radiation. This slow convergence causes a decrease of the tracking efficiency which results in a loss of power. This can lead to a problem of inaccuracy if the disturbance frequency is high. In Situation 2, we can see from Figure 3.7 and Table 3.4 that if the designer makes a compromise between speed of convergence and accuracy by increasing the amplitude of the excitation signal from 25 to 50 ohm and adjusting the gain consequently (from 0.02 to 0.01), the convergence time decreases compared to Situation 1, but the precision around the optimum decreases as well. This choice of parameter values leads to an increase of the tracking efficiency but can cause a loss of power if the curvature of the static curve around the optimum is very stiff as it is the case when the radiation level is 100%. Finally, in Situation 3 (Figure 3.8 and Table 3.4) if the expert favors speed over accuracy, the ESC loop converges very quickly to the desired optimum operating point, but the large oscillations around the internal resistance of the PV system generate a loss of power even when the curvature of the power static curve around the optimum is small as it is the case when the radiation level is 50%. Hence, the tracking efficiency is inferior to the one observed in Situation 2.

Most of the time, the expert designing an ESC scheme chooses Situation 2 in order to make a compromise between the time of convergence and the precision and obtain the best tracking efficiency. However, according to these results, it is not possible to ensure the best time of convergence and the best precision simultaneously. Hence the ESC_a parameter (excitation amplitude) is controlled in an adaptive manner in order to guarantee fast convergence and precision at the same time. Then, from Figure 3.6, Figure 3.7, Figure 3.8 and Table 3.4 with

ESC_a the maximum tracking efficiency is guaranteed, therefore the PV system produces more power compared to ESC in three situations if the PV system is subject to radiation disturbance.

3.8 Conclusion

In this study, a modification of the classic ESC scheme was proposed in order to adapt the excitation signal amplitude using the power of neural network estimation. Theoretical and experimental results show that this approach is stable and significantly reduces the undesirable effects of the time-scale separation condition on the performance of the closed loop system while increasing the tracking efficiency. This method can contribute to achieve higher power performance for PVs or other renewable energy sources like microbial fuel cells, wind generators or any system which must be optimized subject to measurable external disturbances. The neural network learning in this study is offline. Thus, if a non-measurable disturbance occurs, the accuracy of NN estimation may decrease. The objective of our next research is to replace the offline NN-learning phase by an online NN adaptation in ESC_a, in order to increase the precision of NN estimation by providing a better adaptation of the NN model parameters under unmeasurable disturbances.

CHAPITRE 4

EXTREMUM-SEEKING CONTROL WITH ADAPTIVE NEURAL-NETWORK-BASED ANTICIPATIVE ACTION TO MAXIMIZE THE POWER OF A PHOTOVOLTAIC SYSTEM

Anouer Kebir [a], Ouassima Akhrif [b] and Lyne Woodward [c]

[a, b, c] Department of Electrical Engineering, École de Technologie Supérieure, 1100 Notre-Dame Ouest, Montréal, Québec, Canada H3C 1K3

Submitted to IEEE Transactions on Industrial Electronics, July, 2018

Abstract

In the present study, a modification to the extremum seeking control (ESC) method is proposed to improve both its precision and convergence speed when used to drive a black box system submitted to measurable and unmeasurable disturbances towards its optimum. The approach consists mainly in superposing a neural network (NN) model with online update capabilities to the ESC scheme in order to model in real time the impact of the external disturbances on the optimal operating point of the system. Thus, the NN adaptive model can provide in real time an estimate of the optimal point of operation of the system to the ESC scheme so that the latter may use it as a starting point and converge faster toward the desired optimum. The stability of the proposed approach is demonstrated. The performance of the method is validated experimentally through the optimization of the power produced by photovoltaic panels submitted to measurable and unmeasurable disturbances, namely luminance variations and PV system failure.

Keywords: Extremum-seeking control, Neural networks, Optimization, Photovoltaic system.

4.1 INTRODUCTION

Many engineering systems such as chemical processes or renewable energy systems exhibit complex dynamics and strong nonlinearities. Moreover, these systems often face the need for real-time optimization where a static performance index is optimized despite the system dynamics. For this type of systems, the use of a model-based optimization technique to find the static optimal operating point is very difficult or downright impossible. Furthermore, accuracy and reliability cannot be guaranteed if changes occur on the system and no adaptation of the model parameters is performed. In such a context, the use of a non-model-based optimization method is preferable. Extremum seeking control is part of this class of methods since it does not require a priori knowledge of the system dynamics. Instead, available measurements of the system output are used to bring the system around its optimal operating point. The general principle of the ESC method consists simply in estimating the gradient of the static performance index with the use of a periodic signal in order to control it to zero to meet the necessary conditions of optimality. Since the first proof of local stability established in 2000, the community was attracted by the robustness of this optimization method and thus, several applications and schematics of the ESC method have been proposed. An overview of the history of the ESC approach is presented in (Ariyur & Krstić, 2003; Y Tan et al., 2010; C. Zhang & Ordóñez, 2011).

In order to optimize a non-linear system in its static mode, the ESC scheme requires a multiple time scale separation condition guaranteed by a judicious choice of the control parameters. The condition includes that the parameters are adjusted such that the excitation signal is slower than the system response time and that the adaptation is slower than the excitation signal in order to distinguish the effect of the adaptation, the excitation and the system dynamics on the output measurements. However, if this condition is met, it causes a slow convergence towards the desired optimum, which can be tedious (days or months) in the case of the optimization of slow chemical systems such as, for example, microbial fuel cells (Anouer Kebir et al., 2016). Moreover, even in the case where fast systems are considered, rapid variations of external disturbances causing large changes in system’s optimal operating point may make the ESC loop unable to bring back the system to the desired operating point in a reasonable time frame. Thus, several approaches have been proposed in order to reduce the undesirable effect of the time scale separation condition on the convergence speed of the ESC scheme. In (Ariyur & Krstić, 2003), this undesirable effect was eliminated by the development of a scheme able to compensate the system dynamics while guaranteeing stability as well as rapid convergence towards the desired optimum. However, this compensation is only possible for systems with linear dynamics, which is rarely the case with real systems. Other approaches require precise conditions such as: the system belongs to a well-defined class of nonlinear systems (Adetola et al., 2004), the structure of the objective function is known a priori (Banavar, 2003; Guay & Zhang, 2003), the system is assumed to be unknown but linear (Adetola & Guay, 2006), or must include many identical subsystems (Khong, NešIć, Tan, et al., 2013). Thus, all these approaches are applicable to a restricted set of systems.

In all types of systems, the optimal operating point variation is caused by measurable and/or unmeasurable disturbances. Thus, if there exists a function able to provide an optimal operating point estimate from the measurable disturbances and able to adapt to manage the effect of unmeasurable disturbances on this estimate, an anticipative action can then be added to the ESC scheme. In [4], the anticipative action is used to rapidly push the system towards an estimate of the optimal operating point. However, no online adaptation is performed on the parameters of the model used in the anticipative action. As a result, when unmeasurable disturbances occur, an error in the estimation of the optimal operating point will cause a slow convergence.

This paper proposes a new ESC-based real-time optimization scheme (ESC_{ad}) which relies on an anticipative action based on an adaptive multilayer NN model. The online update of the NN model parameters allows the estimation of the optimal operating point from the measured disturbance even in presence of unmeasurable disturbances. The results obtained from the application of the proposed scheme to a PV system show its ability to converge quickly and precisely towards the desired optimum.

The paper is organized as follows. Following the introduction, Section 4.2 defines the optimization problem and Section 4.3 explains the extremum seeking control method. In Section 4.4 the proposed $\mathrm{ESC_{ad}}$ approach is presented whereas its stability is studied in Section 4.5. An experimental study is carried out in Section 4.6 to evaluate the performance in terms of speed of convergence of the $\mathrm{ESC_{ad}}$ scheme. Results are compared to those obtained from the application of the ESC scheme to the maximization of the output power of a photovoltaic system subject to measurable and unmeasurable disturbances. Finally, conclusions of the paper are presented in Section 4.7.

4.2 Optimization problem formulation

Let us consider a system submitted to the effect of measurable ($d_m \in \mathbb{R}^h$) and unmeasurable ($d_u \in \mathbb{R}^\rho$) external disturbances described by the following equations:

$$\dot{x} = f(x, u, d_m, d_u) \tag{4.1}$$

$$y = h(x) \tag{4.2}$$

where $x \in \mathbb{R}^n$ is the state vector, $f: \mathbb{R}^n \times \mathbb{R} \times \mathbb{R}^h \times \mathbb{R}^\rho \to \mathbb{R}^n$ is unknown, $y \in \mathbb{R}$ and $u \in \mathbb{R}$ are respectively the output and the input of the system.

Let us consider:

$$u = \alpha(x, \beta) \tag{4.3}$$

With α being a smooth control law, parameterized by the scalarβin closed loop.

Then from (4.1) and (4.3) the dynamics of the closed-loop system is:

$$\dot{x} = f(x, \beta, d_m, d_u). \tag{4.4}$$

The optimization problem consists in maximizing the output of the system, y, in steady-state. Let us define an objective function J which quantifies the performance of the system in its static regime. Thus the optimization problem is mathematically described by the following equation:

$$\left.\begin{array}{c} \max\limits_{\beta} y \\ s.t. \quad \dot{x} = f(x, \beta, d_m, d_u) = 0 \end{array}\right\} i.e., \qquad \max\limits_{\beta} J \tag{4.5}$$

where $J: \mathbb{R} \to \mathbb{R}$ is unknown but can be evaluated from available measurements.

The following assumptions hold:

Assumption 1: For each $\beta \in \mathbb{R}$, the equilibrium $x = l(\beta, d_m, d_u)$ of the system (4.1- 4.3) for which the constraint in (4.5) is active, is globally asymptotically stable, uniformly in β. Consequently, $J \equiv h \circ l(\beta, d_m, d_u)$.

Assumption 2: For each disturbance d_m and/or d_u there exists a unique β^* maximizing J and, the following equations hold:

$$J'(\beta^*) = 0 \qquad\qquad J''(\beta^*) < 0 \tag{4.6}$$

$$J'(\beta^* + \varrho)\varrho < 0 \; \forall \; \varrho \neq 0. \tag{4.7}$$

with $\varrho \in \mathbb{R}$

4.3 The extremum seeking control scheme

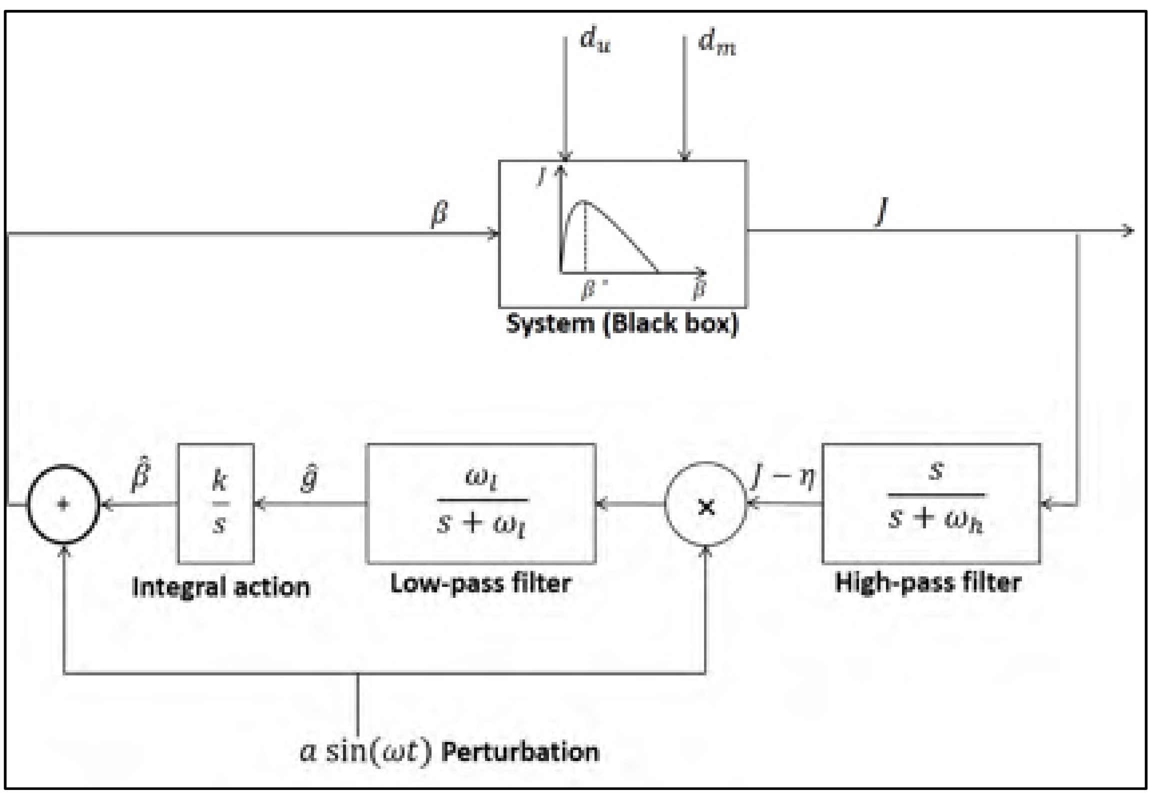

Figure 4.1 The ESC structure

The objective of the ESC scheme is to solve the optimization problem presented in (4.5) by controlling the inputβusing the measurement of the objective function J. In order to achieve this objective, according to (Anouer Kebir et al., 2016) and as shown in Figure 4.1, the ESC approach is constituted by a high-pass filter with a cut-off frequency ω_h to eliminate the constant part η of the objective function J, a sinusoidal excitation signal with amplitude a, a low-pass filter with a cut-off frequency ω_l used to obtain the mean value of the correlation between the excitation signal and the output of the high-pass filter, and, finally, an integrator with a gain k to control the estimated gradient $\hat{g}$ to zero. Thus, the ESC control law is described by the following equations:

$$\beta = \hat{\beta} + asin(\omega t) \tag{4.8}$$

$$\dot{\hat{\beta}} = k\hat{g} \tag{4.9}$$

$$\dot{\hat{g}} = -\omega_l \hat{g} + \omega_l (y - \eta) a \, sin(\omega t) \tag{4.10}$$

$$\dot{\eta} = -\omega_h \eta + \omega_h y \tag{4.11}$$

where$a \in \mathbb{R}^+$is sufficiently small and$k \in \mathbb{R}^+$.

4.4 Proposed ESC_{ad} approach

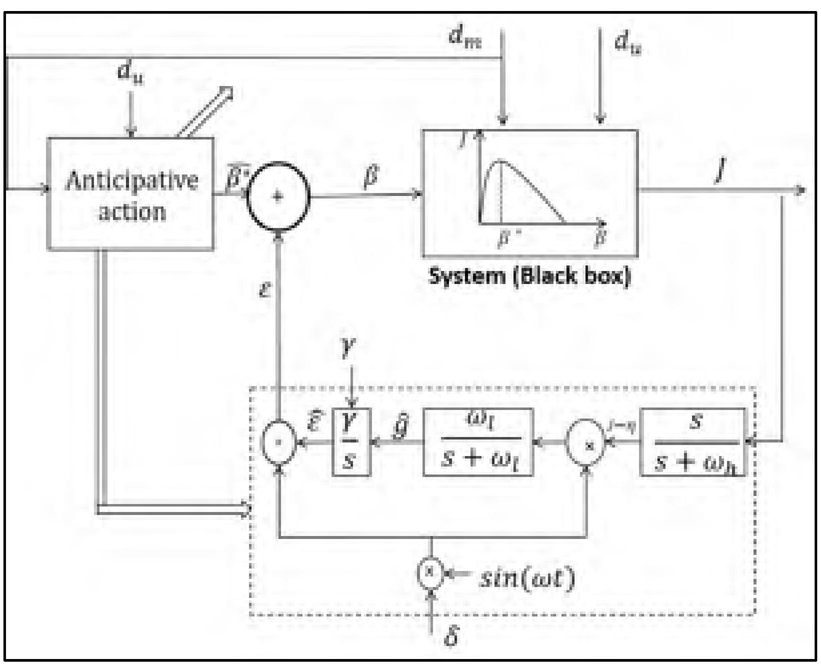

Figure 4.2 The ESC_{ad} structure

In order to improve the speed of convergence of the ESC loop, it is proposed to add an online adaptive anticipative action to rapidly bring the system close to its optimal point of operation (β^*) by means of an estimate of the latter ($\widehat{\beta^*}$)whenever a disturbance affecting the optimal point of operation occurs. Thus, the ESC_{ad} scheme is mainly constituted by two units: the ESC feedback loop and the anticipative action (Figure 4.2).

4.4.1 ESC Feedback Loop

The main role of the ESC feedback loop is to compensate the error,ε between the input, β and the estimated optimal operating point provided by the anticipative action unit, $\widehat{\beta^*}$ in order to converge to the real optimum, β^*. Hence, from an ESC loop point of view the optimization problem becomes:

$$\begin{aligned} &\max_{\varepsilon} y \\ s.t. \quad &\dot{x} = f(x, \varepsilon, d_m, d_u) = 0 \end{aligned} \tag{4.12}$$

with $\varepsilon = \beta - \widehat{\beta^*}$. The convergence will be achieved when $\varepsilon = \varepsilon^* = \beta^* - \widehat{\beta^*}$.

The ESC feedback loop control law is described by the following equations:

$$\varepsilon = \hat{\varepsilon} + \delta sin(\omega t) \tag{4.13}$$

$$\dot{\hat{\varepsilon}} = \gamma \widehat{g_\varepsilon} \tag{4.14}$$

$$\dot{\hat{g}}_\varepsilon = -\omega_l \widehat{g_\varepsilon} + \omega_l (y - \eta) \delta \, sin(\omega t) \tag{4.15}$$

$$\dot{\eta} = -\omega_h \eta + \omega_h y \tag{4.16}$$

with $\delta \in \{0, a\}$and $\gamma \in \{0, k\}$. The amplitude of the excitation δ and the gain γ are set to zero whenever measurable disturbances occur in which case the NN model is the one providing the estimate of the optimal condition to be reached by the system. Otherwise they are respectively set to a and k. The selection of all other parameters in the ESC feedback loop is carried out in order to guarantee a multiple time scale separation (Anouer Kebir et al., 2018), i.e. according to the following equations:

$$ak \left. \frac{\partial^2 J}{\partial \varepsilon^2} \right|_{\varepsilon^*} \ll \omega, \tag{4.17}$$

$$\omega_h = \omega_l \ll \omega. \tag{4.18}$$

4.4.2 Anticipative action unit

The anticipative action unit anticipates the effect of the disturbances on the optimal point of operation β^* by providing an estimateof the optimum, $\widehat{\beta^*}$ as a set point to the system. The anticipation of the effect of d_m and/or $d_u$on β^* is performed by real-time modeling of the function that connects $\beta^*$to d_m. The online modeling is carried out whenever a new optimum is detected following a disturbance d_m and/or d_u (by means of the follow-up of the gradient evolution $\hat{g}_\varepsilon$). Moreover, the anticipative action unit disables the ESC feedback loop (by forcing δ = γ = 0) in order to push the system directly to $\widehat{\beta^*}$. Once the estimate is reached, the anticipative action unit will enable the ESC loop (by setting $\delta = a$ and $\gamma = k$) in order to let the system reach the real optimum β^*. This results in a rapid convergence towards the optimum whenever a disturbance occurs.

The anticipative action unit is made of 4 units (Figure 4.3) respectively performing the following tasks: convergence detection, database update, online update of the neural-network model and switching between ESC feedback loop and the anticipative action.

The functionality of each of these blocks will now be defined.

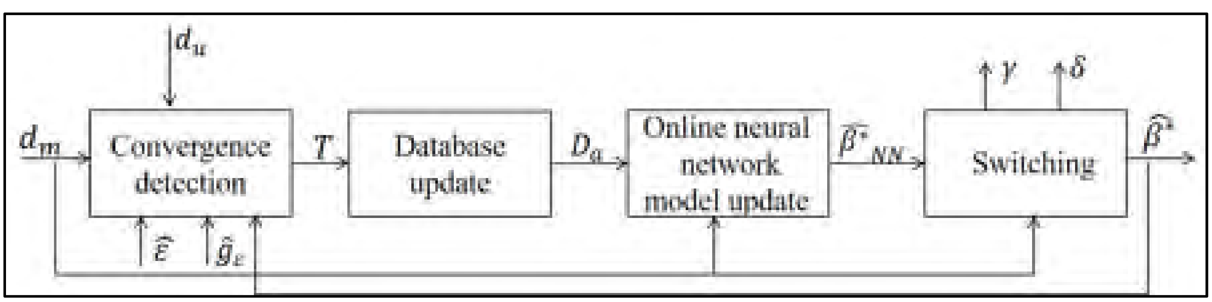

Figure 4.3 Anticipative action unit

4.4.3 Convergence detection unit

The database used to train the NN model is updated once the convergence of the system to the optimum is detected i.e., when $\hat{g}_\varepsilon$ is sufficiently small. At this moment, the value of the optimal control input and the corresponding measurable disturbance are stored in the database, D_a. The following conditions are used to detect the convergence even in the presence of measurement noise:

$$\widehat{g_\varepsilon}_{av} \equiv \left|\frac{1}{\Delta_g}\int_{t-\Delta_g}^{t} \widehat{g_\varepsilon}\, d\tau\right| \leq |\vartheta_g| \tag{4.19}$$

with Δ_g and ϑ_g being respectively the delay defining the rolling horizon on which the average of the gradient $\widehat{g_\varepsilon}_{av}$ is computed and the tolerance within which the system is considered to have converged. These values are chosen by the expert. When (4.19) becomes true, the vector $T = [d_m^T \beta_e]$ is added to the database, with $\in \mathbb{R}^{1\times q}$, $q = h + 1$, $\beta_e = \widehat{\beta^*} + \varepsilon_e$, $(1-\mu)\varepsilon^* \leq \varepsilon_e \leq (1+\mu)\varepsilon^*$ and μ being the relative tolerance on ε^*.

The choice of the tolerance ϑ_g depends on the desired precision but also, on the amplitude of the perturbation and the curvature of the static performance index function. Knowing that, $\widehat{g_\varepsilon} \backsimeq \frac{a^2}{2} J'(\hat{\varepsilon})$ with $J'(\hat{\varepsilon}) \equiv \frac{\partial J}{\partial \hat{\varepsilon}}$ (Krstić & Wang, 2000) and performing a first-order Taylor series expansion of the derivative $J'(\hat{\varepsilon})$ around the optimum ε^*, the tolerance can be approximated by the following equation:

$$\vartheta_g \backsimeq \frac{a^2}{2}(\pm\mu\varepsilon^*)J''(\varepsilon^*). \tag{4.20}$$

Note that the choice of Δ_g directly affects the time needed to detect the convergence as well as the accuracy of the average gradient: the larger is Δ_g, the more accurate is the average gradient and slower is the convergence detection and vice versa. The expert must then make a compromise between the speed and the accuracy of the convergence detection when tuning Δ_g.

4.4.4 Database update unit

The accuracy of the NN model depends directly on the wealth of information collected and so, on a frequent update of the database, D_a used for its training. Prior to enabling the control loop, the database is initialized using the data obtained from a priori knowledge about the system.

Note that the maximal number of lines (N_D) that may contain the database is fixed according to the desired resolution. Once the controller has been enabled, whenever (4.19) becomes true, the database is updated as follows:

Step 1: Search for a line of the database having the same disturbance values as the one freshly detected i.e., first element of T;

Step 2: If a line having the same disturbance values is found, update the values of this line with the ones of T and go to step 4. Otherwise go to step 3;

Step 3: Add T as a new line to the database

Step 4: Go back to step 1 whenever a new update is neede

4.4.5 Online Neural Network model update

A multi-layer neural network model was used to model the nonlinear function that describes the effect of the disturbances on the optimal operating point owing to its ability to provide a good precision even for complex systems (Cotton & Wilamowski, 2011; Lin, Wang, Teng, Dai, & Li, 2017; K. Liu & Zhu, 2015). The input and the hidden layers contain respectively h and c neurons. In the scalar case where only one parameteris estimated by the NN model, as in the case study that will be presented in section 4.6, the output layer is made of a unique neuron. Note that the dimension of the input layer matches the one of the NN model input, d_m. Finally, the activation function ρ is a hyperbolic tangent function and the bias is chosen by the expert.

The output neuron of the NN model is activated by the following equation:

$$\widehat{\beta^*}_{\mathrm{NN}} = \rho_2 = \frac{1-e^{-m_{NN}*W_2^T*\phi_2}}{1+e^{-m_{NN}*W_2^T*\phi_2}}, \tag{4.21}$$

where:

$$\phi_2 = \begin{bmatrix} bias \\ \rho_1 \end{bmatrix}, \tag{4.22}$$

ρ_1 is the vector of length c with the i^{th} element defined by the activation function of each neuron of the hidden layer, i.e.,

$$\rho_1(i) = \frac{1-e^{-m_{NN}\mathrm{H}_1(\mathrm{i})}}{1+e^{-m_{NN}\mathrm{H}_1(\mathrm{i})}}, \tag{4.23}$$

$$H_1 = W_1^T * \phi_1 , \tag{4.24}$$

$$\phi_1 = \begin{bmatrix} bias \\ d_m \end{bmatrix}, \tag{4.25}$$

$m_{NN} \in \mathbb{R}$ is the slope of the hyperbolic tangent activation function and $W_1 \in \mathbb{R}^{b \times c}$ and $W_2 \in \mathbb{R}^{\lambda \times p}$ are respectively the sets of synaptic weights between the neuron input and the hidden layer and between the hidden layer and the output neuron with $b = h + 1$ and $\lambda = c + 1$.
An online supervised learning is required to account for measurable and unmeasurable disturbances in the estimation of the optimal operating point. This learning phase consists in updating the NN model parameters, i.e. updating the synaptic weights W_1 and W_2 whenever a change occurs in the database. Once the learning phase is achieved, new synaptic weights are sent to the NN model.

The gradient retro propagation algorithm is used to train the NN model. Thus, the synaptic weights are adjusted according to their effect on the error between the values of β_e included in the database and the ones modeled by the NN. The synaptic weights are updated using the steepest descent algorithm:

$$W_{1_{new}} = W_1 - \mu \sum_{k=1}^{N_D} \frac{\partial E}{\partial W_1}(k), \tag{4.26}$$

$$W_{2_{new}} = W_2 - \mu \sum_{k=1}^{N_D} \frac{\partial E}{\partial W_2}(k), \tag{4.27}$$

with μ being the learning rate fixed by the expert, N_D, the number of lines in the database (D_a) and E, the quadratic error computed for line k of the database, $E(k) = \frac{1}{2}\left(\beta_e(k) - \widehat{\beta^*}_{NN}(k)\right)^2$.
Note that from (4.21-4.27), it can be shown that the derivatives $\frac{\partial E}{\partial W_2}(k)$ and $\frac{\partial E}{\partial W_1}(k)$ can be retro propagated from the output layer up to the input one:

$$\frac{\partial E}{\partial W_2}(k) = \left(\beta_e - \widehat{\beta^*}\right) \frac{\mathrm{m_{NN}} e^{-m_{NN}*\mathrm{H}_2}}{(1 + e^{-m_{NN}*H_2})^2} \phi_2 \tag{4.28}$$

and, for each neuron i of the hidden layer,

$$\frac{\partial E_i}{\partial W_{1_i}}(k) = W_{2_{i+1}} \frac{\partial E}{\partial W_2}(k) \frac{\mathrm{m_{NN}} e^{-m_{NN}*\mathrm{H}_{1i}}}{\left(1+e^{-m_{NN}*H_{1i}}\right)^2} \phi_1. \tag{4.29}$$

Hence, the learning algorithm can be summarized as follows:

Step 0: Set $k = 1$;

Step 1: Considering the values d_m and β_e of line k, compute the output of (4.21-4.25);

Step 2: Compute the synaptic weights using (4.26-4.29);

Step 3: If the last line of the database is reached ($k = N_D$), go to step 4. Otherwise, increase the iteration index k and go back to step 1;

Step 4: Compute the average error per line of the database:

$$E_{av} = \frac{\sum_{k=1}^{N_D} E(k)}{N_D} \tag{4.30}$$

Step 5: If the average error is greater than the error tolerance E_{max} set by the expert, go back to step 0. Otherwise, update the synaptic weights of the NN model unit as follows:

$$\begin{aligned} W_1 &= W_{1_{new}} \\ W_2 &= W_{2_{new}} \end{aligned} \tag{4.31}$$

and wait for the next disturbance detection to run the learning algorithm again.

4.4.6 The switching unit

Whenever a disturbance d_m occurs, the ESC loop is disabled, i.e., $\varepsilon = 0$ and the system input is solely driven by the estimate provided by the NN model, $\beta = \widehat{\beta^*} = \widehat{\beta^*}_{NN}$. However, when the measurable disturbance d_m is constant, the last estimate of $\widehat{\beta^*}$ is kept constant and the ESC feedback loop is active. In order to determine if the measurable disturbance is constant or not, a rolling average $d_{m_{av}}$ of the measurable disturbance is performed over a period Δ_d:

$$d_{m_{av}}(\mathrm{t}) = \frac{1}{\Delta_d}\int_{t-\Delta_d}^{t} d_m \, d\tau. \tag{4.32}$$

Considering $t = t_0 \in \mathbb{R}$ to be the moment when d_m becomes constant, the input of the system, β is controlled as follows by the switching unit:

$$\left.\begin{aligned} \beta(t) &= \widehat{\beta^*} + \mathcal{E}(t) \\ \widehat{\beta^*} &= \widehat{\beta^*}_{NN}(t_0) \end{aligned}\right\} \text{if } \left|d_{m(t)} - d_{m_{av}}\right| \leq |\vartheta_d| \tag{4.33}$$

$$\left.\begin{array}{c}\beta(t) = \widehat{\beta^*}(t) = \widehat{\beta^*}_{NN}(t) \\ \mathcal{E}(t) = 0\end{array}\right\} \text{if } \left|d_{m(t)} - d_{m_{av}}\right| > |\vartheta_d| \tag{4.34}$$

where, $\widehat{\beta^*}_{NN}(t) \in [\beta_{min}\ \ \beta_{max}]$ and $\beta_{min}, \beta_{max}, \vartheta_d \in \mathbb{R}$. The values of $\beta_{min}, \beta_{max}, \vartheta_d$ and Δ_d are set by the expert.

4.5 Stability study of ESC$_{ad}$

The stability of the proposed scheme will be analyzed according to the two operation modes defined by (4.33-4.34). When (4.34) applies, the system dynamics becomes:

$$\dot{x} = f(x, \widehat{\beta^*}_{NN}(t), d_m, d_u) \tag{4.35}$$

and, due to Assumption 1, its equilibrium is globally asymptotically stable.

When (4.33) applies, the system is described as follows:

$$\dot{x} = f(x, \widehat{\beta^*}_{NN}(t_0) + \hat{\varepsilon}(t) + \delta sin(\omega t), d_m, d_u) \tag{4.36}$$

$$\dot{\hat{\varepsilon}} = \gamma\, \widehat{g_\varepsilon} \tag{4.37}$$

$$\dot{\hat{g}}_\varepsilon = -\omega_l \widehat{g_\varepsilon} + \omega_l (y - \eta)\delta\ sin(\omega t) \tag{4.38}$$

$$\dot{\eta} = -\omega_h \eta + \omega_h y. \tag{4.39}$$

Defining $\tilde{x} = x - x^*$, $\tilde{\varepsilon} = \hat{\varepsilon} - \varepsilon^*$, $\widetilde{g_\varepsilon} = \widehat{g_\varepsilon}$, $\tilde{\eta} = \eta - J^*$, $\zeta = \omega t$, $\gamma = \omega\tau K$, $\omega_l = \omega\tau\omega_{\mathrm{L}}$, $\omega_h = \omega\tau\omega_H$, with τ, ω_H, ω_{L}, $K \in \mathbb{R}^+$and, ω and τ being small parameters, the system becomes:

$$\omega\frac{d\tilde{x}}{d\zeta} = f\left(\tilde{x} + x^*, \widehat{\beta^*}_{NN}(t_0) + \tilde{\varepsilon} + \varepsilon^* + asin(\zeta), d_m, d_u\right) \tag{4.40}$$

$$\frac{d\tilde{\varepsilon}}{d\zeta} = \tau K \widetilde{g_\varepsilon} \tag{4.41}$$

$$\frac{d\widetilde{g_\varepsilon}}{d\zeta} = -\tau\omega_L(\widetilde{g_\varepsilon} - (y - \tilde{\eta} - J^*)a\ sin(\zeta) \tag{4.42}$$

$$\frac{d\tilde{\eta}}{d\zeta} = -\tau\omega_H(\tilde{\eta} + J^* + y). \tag{4.43}$$

Since, when (4.33) applies, d_m and $\widehat{\beta^*}_{NN}(t_0)$ are constant, and considering d_u constant (or slowly varying), the singular perturbation theory applies as in (Ying Tan et al., 2006).

Thus, according to Theorem 4 in (Ying Tan et al., 2006), the closed-loop system (4.40-4.43) with parameters $\epsilon = [a^2, \tau, \omega]^T$ is semi-practically asymptotically stable, uniformly in a^2.

Consequently, it is possible to adjust the set of parameters ϵ so that the system can be controlled arbitrarily close to the extremum $J^*$from an arbitrarily large set Δ of initial conditions, i.e., $\left\| \begin{matrix} \tilde{x}(t_0) \\ \tilde{\varepsilon}(t_0) \end{matrix} \right\| < \Delta$.

As, by definition, $\tilde{\varepsilon}(t_0) = \hat{\varepsilon}(t_0)$-$\beta^* + \widehat{\beta^*}_{NN}(t_0)$, and considering that $\tilde{\varepsilon}(t_0) = 0$, this condition becomes:

$$\left\| \begin{matrix} \tilde{x}(t_0) \\ \widehat{\beta^*}_{NN}(t_0) - \beta^* \end{matrix} \right\| < \Delta \tag{4.44}$$

and the following theorem can be established.

<u>Theorem:</u>

As long as $\beta_{min} \leq \widehat{\beta^*}_{NN} \leq \beta_{max}$, $\beta_{min} \leq \beta^* \leq \beta_{max}$ and, $\left\| \begin{matrix} \tilde{x}(t_0) \\ \beta_{max} - \beta_{min} \end{matrix} \right\| < \Delta$, there exist parameters $\epsilon = [a^2, \tau, \omega]^T$making the ESCad scheme semi-practically asymptotically stable, uniformly in a^2.

Note: The ESC and ESCad loops have the same parameters vector ϵ, thus the ESCad method has the same Δ and the same convergence domain of the ESC.

4.6 Experimental study: application to a PV system

In order to compare the performance of the ESC and ESCad schemes, there were both applied to a PV system. Among the external disturbances affecting the optimal power that can be extracted from this type of system, there are mainly the luminance and the temperature. According to (Marinkov et al., 2014), in the usual climatic conditions, the impact of the temperature on the optimal operating point of the PV system is insignificant compared to the disturbance of luminance. Thus, in the present study, the luminance has been considered as the measurable disturbance.

Among the non-measurable disturbances affecting the PV system, there are mainly the aging and the damaging of PV system components. These unmeasurable disturbances can change slowly (aging) or radically (damaging) the operation of the PV system and, consequently, the optimum operating point itself. As the average lifespan of a PV system is 25 years, the aging factor is very difficult to emulate. Thus, in the present study, the components damage of the PV system has been chosen as the unmeasurable disturbance and was emulated by disconnecting one of the two panels of the PV system.

4.6.1 Description of the experimental setup

The experimental setup shown in Figure 4.4 and in Figure 4.5 consists of the following components:

- A PV module (Labvolt solar panel test bench, model 8805) constituted by two PVs, permanently fixed in front of a 300 W projector acting as a light source;

A digital touch screen dimmer (Uber Haus, TSD-1000) which allows to control the luminance emitted by the projector by adjusting its supply voltage (V_p) from 5% to 100% with a step of 5%;

- A digital potentiometer (XICOR X9C102P 1kΩ) playing the role of a variable external load (R_{ex}) at the output of the main PV module;
- A relay (SONGLE Relay Module) for automatically controlling the opening and closing of the parallel connection between the upper and lower PV panels;
- A photocell (API PDV-P8001) used as a sensor to measure the level of luminance through the evaluation of the photocell resistance R_{ph};
- An acquisition board (National Instrument NI PCI-6024E) for controlling the digital potentiometer via the reference signal R_{exs}, measuring the external load R_{ex} via the measurement of the output voltage V_{es} and the voltage V_{sh1} at the shunt resistor R_{sh1} = 30 ohm, controlling the opening and closing of relays from the voltage V_R and evaluating the

photocell resistance (R_{ph}) from the measurement of the voltage V_{sh2} at the shunt resistor R_{sh2} = 500 ohm;

- The Matlab/Simulink software to implement ESC and ESC$_{ad}$ schemes using a sampling period $T = 0.01\ s$.

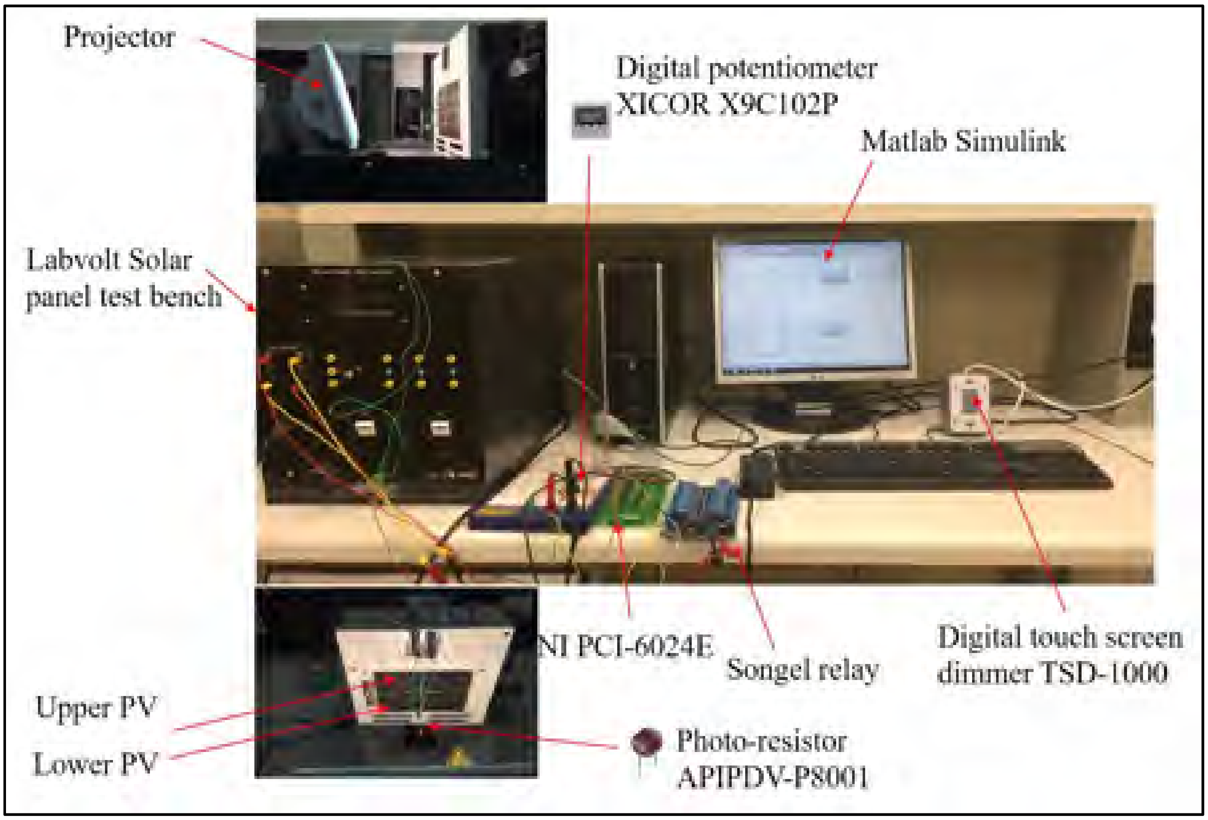

Figure 4.4 PV platform used for experimental validation.

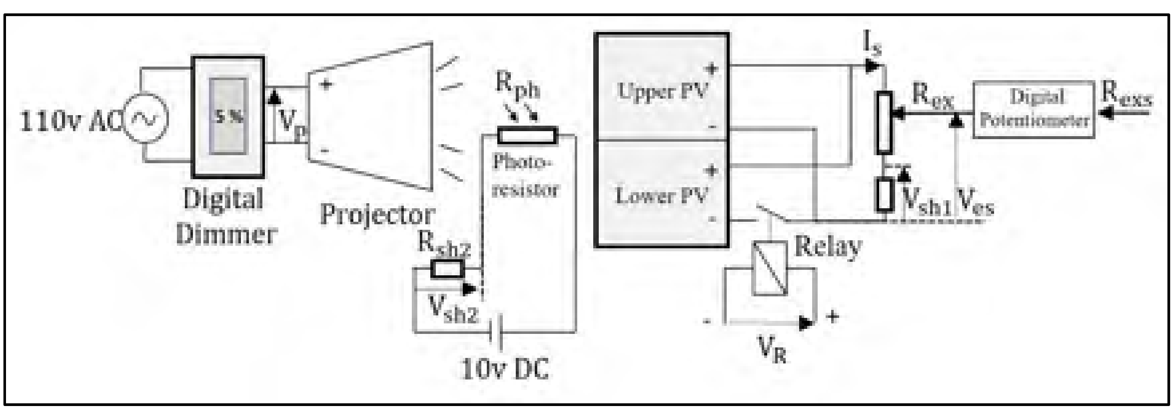

Figure 4.5 Block diagram of the experimental platform

4.6.2 Static characteristics of the PV system

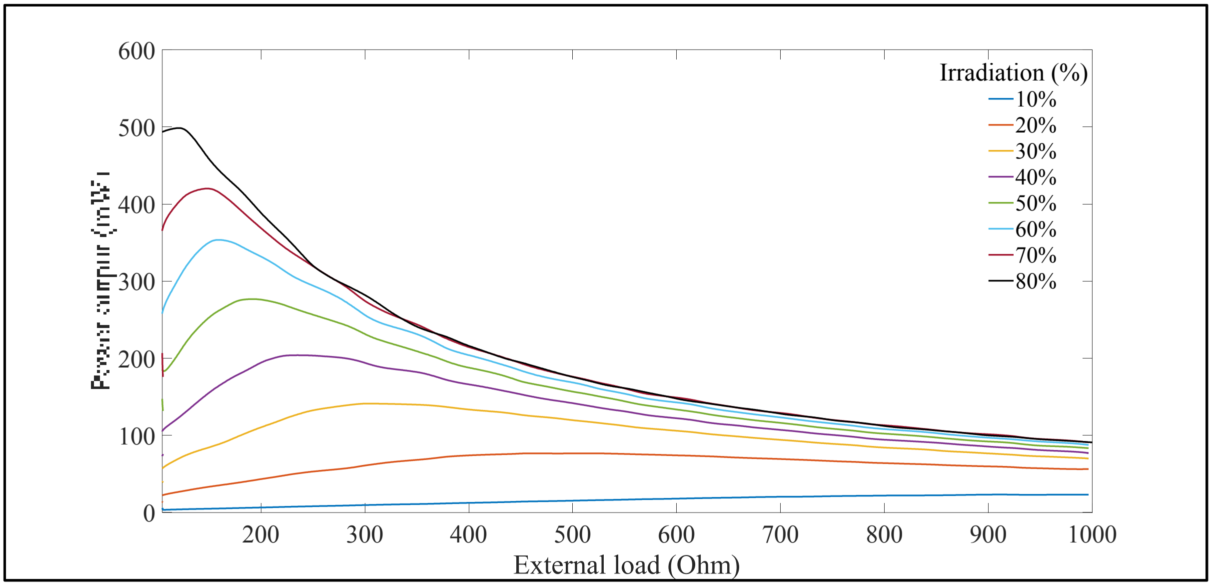

Figure 4.6 Static characteristics of the PV system using 2 PV panels in parallel: output power as a function of the external load for different luminance levels

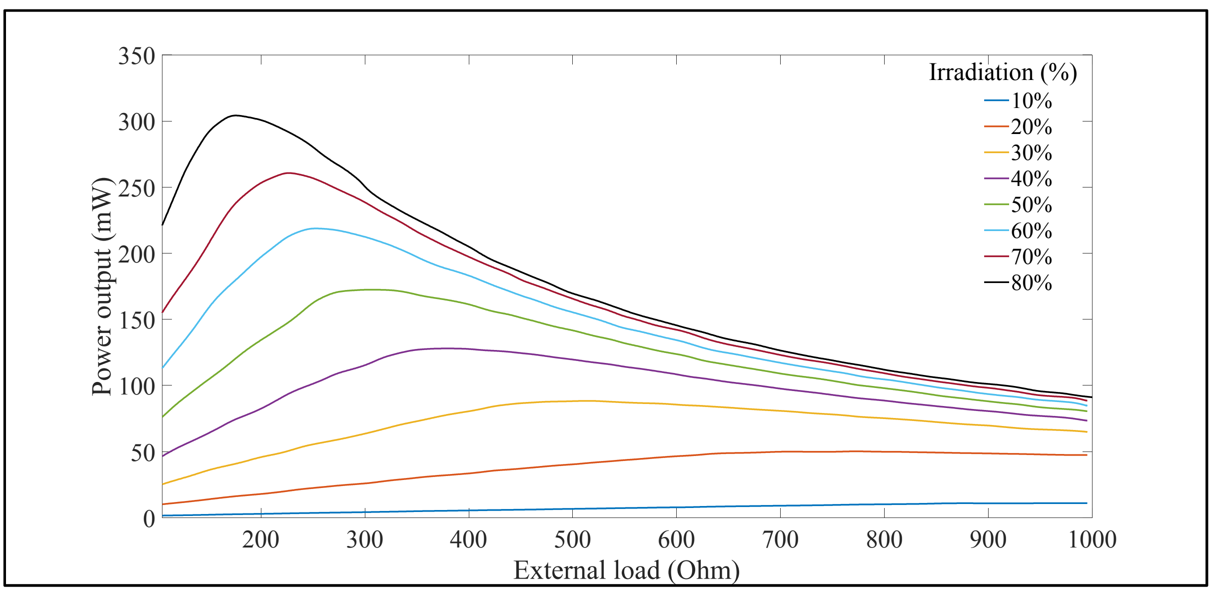

Figure 4.7 Static characteristics of the PV system using only 1 PV panel: output power as a function of the external load for different luminance levels

Before implementing ESC and ESC_{ad} schemes, the static characteristics of the PV system were plotted. They depict the output power as a function of the external load for different levels of luminance when 2 PVs are used in parallel (Figure 4.6) and when only 1 PV panel is used (Figure 4.7).

Not surprisingly, from these curves, it can be seen that the maximum power produced by the PV module and the optimal external load vary as a function of the luminance level and the number of PV panels used. It is well known that the maximum power of a PV source is reached whenever its external load equals its internal resistance. In real PV systems, this external load includes a DC-DC converter which has its duty cycle controlled by the maximum power point tracking algorithm. Since the main objective of the present experimental study was to evaluate and compare the performance of ESC and ESC_{ad} approaches (rather than the energy conversion itself), a digital potentiometer was directly connected to the PV panels and controlled instead of using a DC-DC converter. Therefore, the optimization problem becomes:

$$\max_{R_{exs}} P_s \qquad s.t. \quad \dot{x} = f(x, R_{exs}, L, V_R) = 0 \tag{4.45}$$

where the luminance level, L is the measurable disturbance (d_m), the voltage supply to the relay,V_R is the unmeasurable disturbance (d_u), the static PV power output, P_s is the objective function (J), the state vector (x) includes the current through the potentiometer, the position and the speed of the digital potentiometer. Finally, the desired set point of the digital potentiometer R_{exs} is the control input β.The optimal operating point to be tracked by the optimization methods is $\beta^* = R_{exs}^* = R_{in}$ with R_{in} being the internal resistance of the PV system.

4.6.3 Parameters setting of ESC and ESC_{ad} methods

4.6.3.1 Parameters of the ESC loop

The parameters of the ESC method have been chosen in order to make a compromise between the speed of convergence towards the optimum and the precision of the solution obtained while respecting the conditions guaranteeing the time scale separation and the stability as described by (4.17-4.18). The time response of the PV system has been evaluated to be $T_r = 0.2$s.

Table 4.1 Optimal values of the PV system for different luminance levels and corresponding photo-resistor values

Luminance level L (%)	**Internal resistance R_{in}(ohm)**		**Photoresistor R_{ph} (ohm)**
	2 PV panels	**1 PV panel**	
80%	121.4	177.3	60
70%	147.3	228.5	70
60%	158.8	254.5	80
50%	173.9	311.0	90
40%	241.1	396.1	110
30%	290.2	516.0	140
20%	513.0	774.3	200
10%	916.3	978.0	470

Consequently, the control parameters have been set as follows:

- the excitation signal period:$T = 2 \times T_r = 0.4s$;
- theamplitude of the excitation signal:$a = 10\ ohm$;
- thecut-off frequency of the two filters:$\omega_l = \omega_h = \frac{2\pi}{3Tr} = 10.46\ rad / s$;
- thegain: $k = 0.05\ ohm^2/mW$;
- theinitial external load: $R_{ini} = 140\ ohm$.

In(Ying Tan et al., 2008), a comparative study was performed between sinusoidal, square and triangular excitation signals in terms of convergence speed. In has been shown that using a square signal makes the ESC scheme converge faster than using a sinusoidal signal and triangular one. Based on these results, a square wave was chosen as the excitation signal in the present paper.

4.6.3.2 Parameters of the ESC_{ad} loop

In order to make a fair comparative study between the two schemes, the parameters of the ESC loop described by (4.13-4.16) in the ESC_{ad} scheme were adjusted to the same values as the ones of the ESC loop described by (4.8-4.11). For each unit composing the anticipative action, the parameters were adjusted as follows:

- Convergence detection unit:
  - detection tolerance: $\vartheta_g = 50\, W/\Omega\,;$
  - delay: $\Delta_\mathrm{g} = 20$ s;
  - relative tolerance on ε^*: $\mu = 0.05$;
- Database update unit:
  - number of lines in the database: $N_D = 100$
  - resolution: $r = 10\ \Omega$ (since the total range of the potentiometer is 1000 Ω);
  - initial database D_{ai}: values of R_{ph} and R_{in} corresponding to luminance levels of 80%, 40%, 20% and 10% in Table 4.1;
- Online NN-model update unit:
  - number of neurons in the input layer: $h = 1$;
  - number of neurons in the hidden layer: $c = 10$;
  - slope of the activation functions: $m_{NN} = 0.5$;
  - bias of the activation functions: $bias = 0.5$;
- Switching unit :
  - delay: $\Delta_d = 0.1s$.

4.6.4 Experimental results

Different tests were performed on the experimental platform in order to evaluate and compare the performance of ESC and ESC_{ad} approaches under measurable and unmeasurable disturbances. Their performance was quantified using the following criteria: the time, T_c (and the corresponding number of periods of the excitation signal, N_p) required to converge to the optimum and the tracking efficiency (Anouer Kebir et al., 2018).

4.6.4.1 Performance of ESC and ESC_{ad} schemes under measurable disturbance (luminance variation)

The comparison between ESC and ESC_{ad} methods was firstly performed with the two main PV panels connected in parallel and under a slow variation of the luminance level, L. The changes of the luminance levels were made in order to guarantee the convergence of both methods towards the optimum each time.

Table 4.2 Performance of ESC and ESC_{ad} schemes under slow variation of luminance using 2 PV panels

	Criteria	From L = 80% to L = 50%	From L = 50% to L=30%
ESC	T_c(s)	16	117
	N_p	41	292
ESC_{ad}	T_c(s)	2	1
	N_p	5	3

The system was first submitted to luminance levels (L=50%, L=30%) different from those included in the initial database D_{ai} used to train initially the NN model. From the results shown in Figure 4.8, Figure 4.9 and Table 4.2, it can be seen that when the luminance level L is changed from 80% to 50%, the ESC_{ad} loop converges 8.6 times faster than the ESC loop. This is due to the generalization power of the NN model which makes the anticipative action unit of the ESC_{ad} scheme able to provide a good estimate of the internal resistance $\widehat{R}_{in}$ of the PV system. Once the convergence was detected, the new pair of points L = 50% (d_m) and the corresponding R_{in} (β_e) were added to the database in order to improve the NN model. A change of luminance from 50% to 30% leads to an accurate estimate of $\hat{R}_{in}$ by the anticipative action unit which makes the ESC_{ad} loop converge 115.9 times faster than the ESC loop (Table 4.2).

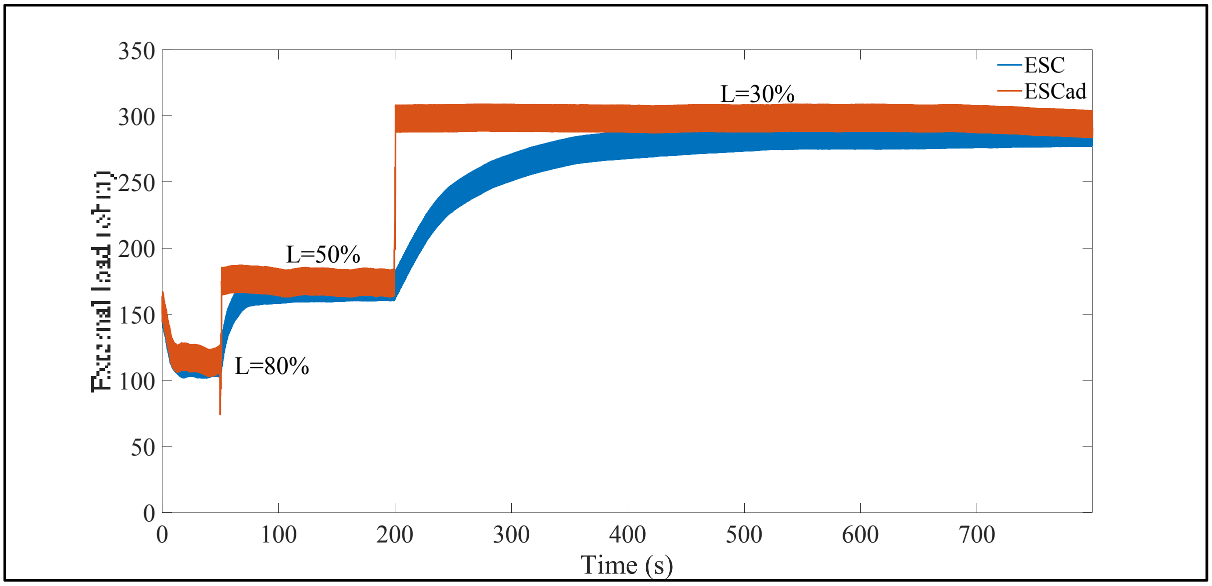

Figure 4.8 Evolution of the external load using ESC and ESC_{ad} schemes under slow variation of luminance

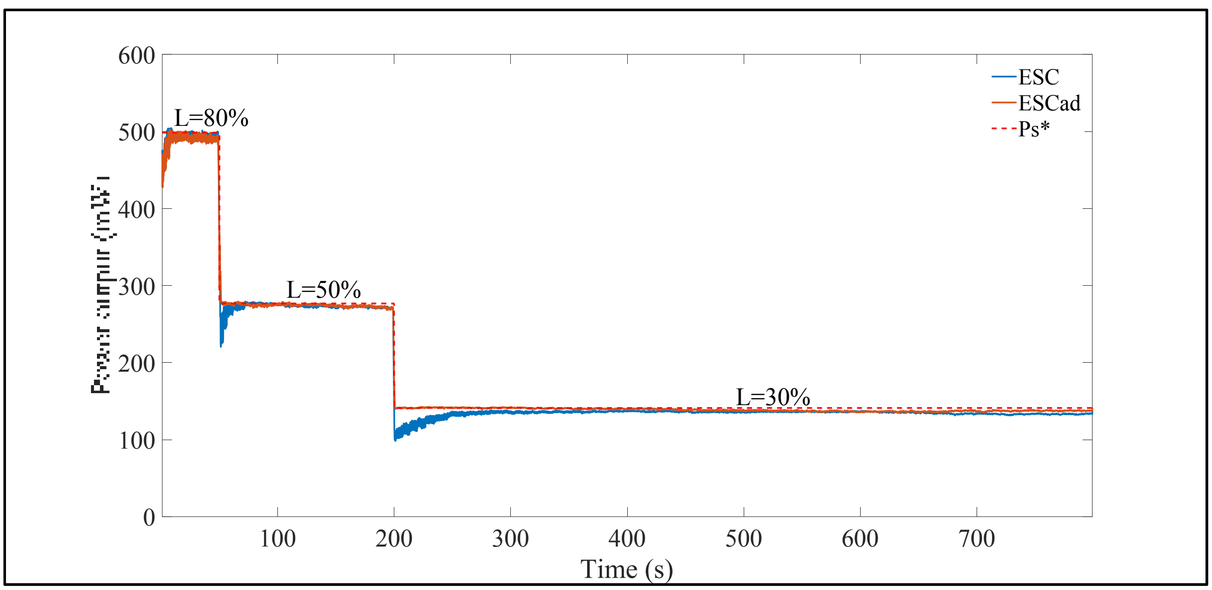

Figure 4.9 Evolution of the PV power output using ESC and ESC_{ad} schemes under slow variation of luminance

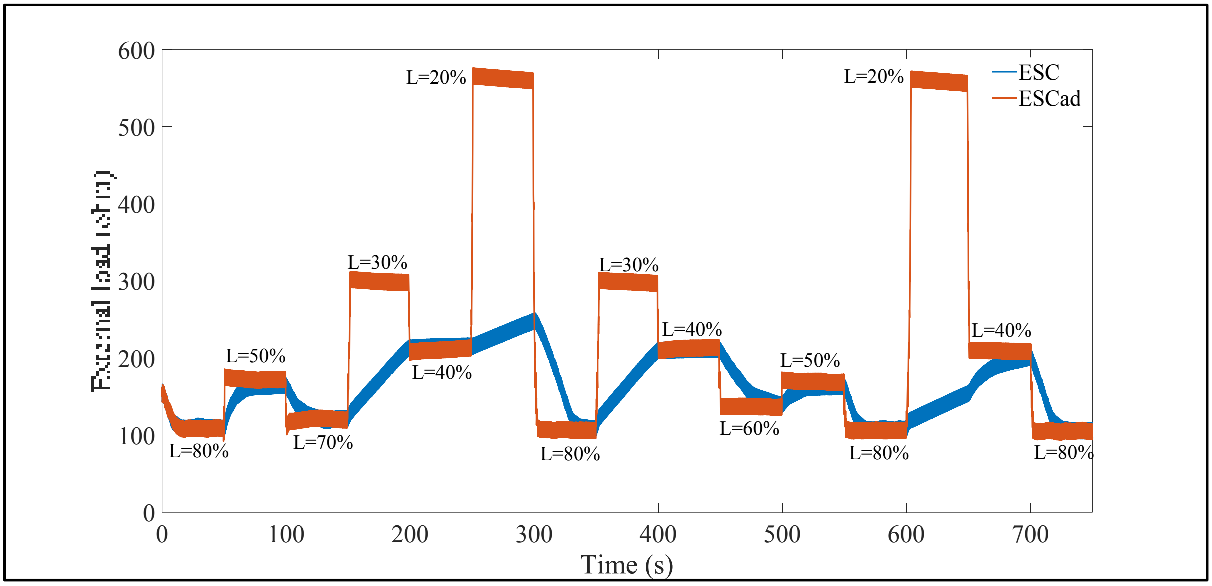

Figure 4.10 Evolution of the external load using ESC and ESC$_{ad}$ schemes under rapid variation of luminance

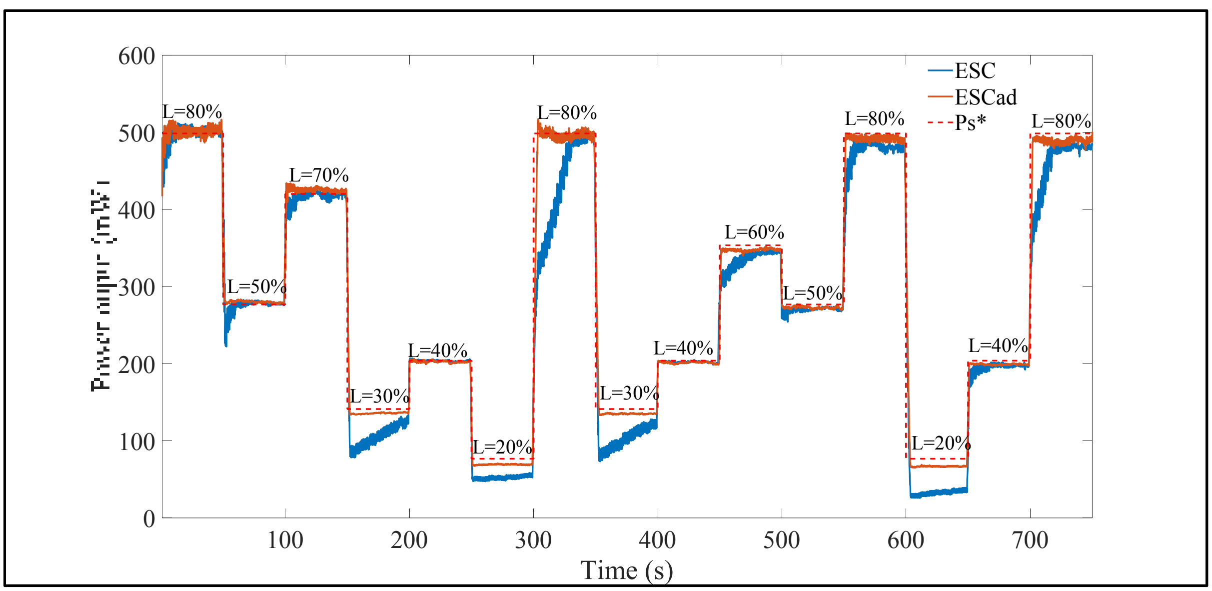

Figure 4.11 Evolution of the PV power output using ESC and ESC$_{ad}$ schemes under rapid variation of luminance.

The tracking efficiency was then evaluated for both approaches by submitting the PV system to faster luminance variations. From the results shown in Figure 4.10 and Figure 4.11, the ESC$_{ad}$ scheme showed a tracking efficiency of 98.6% to follow the desired optimum despite the rapid and large variations of luminance level. On the other hand, the ESC loop could not follow as efficiently the desired optimum especially for large variations of luminance with a tracking efficiency evaluated at 89.2 %.

4.6.4.2 Performance of ESC and ESC_{ad} schemes under unmeasurable disturbance (PV system failure)

The performance of the two approaches was then evaluated under both measurable and unmeasurable disturbances. The unmeasurable disturbance was generated by setting the voltage V_R which supplies the relay coil to zero in order to disconnect one of the two PV panels.

For 0 < t < 220s, the two panels were connected and the luminance varied from 80% to 40% and from 40% to 80%. From Figure 4.12, Figure 4.13 and Table 4.3 it can be seen that in this case, the ESC_{ad} method converged up to 22 times faster than the ESC method. Once again, the NN model had a sufficient knowledge about the PV system (including 2 PV panels) to lead to such a performance. At t = 220s, one of the two panels was disconnected to emulate a system failure whereas the luminance level was kept to 80%. From Table 4.1, it can be seen that this unmeasurable disturbance makes the internal resistance of the system change from 121.4 ohm to 177.3 ohm. In this case, the convergence time of both approaches is nearly the same (Table 4.3). Afterwards, the luminance level was changed from 80% to 40% leading to a faster convergence of the ESC_{ad} loop to the desired optimum compared to the ESC loop. However, this time the ESC_{ad} method takes more time to reach this new optimal point (at 40 % of luminance) than the time it takes before the unmeasurable disturbance occurs for the same level of luminance (Table 4.3). This lower performance can be explained by the fact that the NN model has not acquired enough information in its database D_a about the new system (consisting of only one PV panel). Thus, it provides a less accurate estimate of the PV system internal resistance. At t = 600 s, the luminance level was set back to 80%. As shown in Figure 4.13, this time, the ESC_{ad} method converges more rapidly towards the desired optimum since the NN model has learned from the information received at each measurable disturbance that occurred for t >220s (when only 1 PV panel is connected). Finally, at t = 750 s, the luminance was changed from 80% to 60%. This time, the NN model leads to a very precise estimate of the optimal resistance and makes the ESC_{ad} method converge quickly towards this point (Table 4.3).

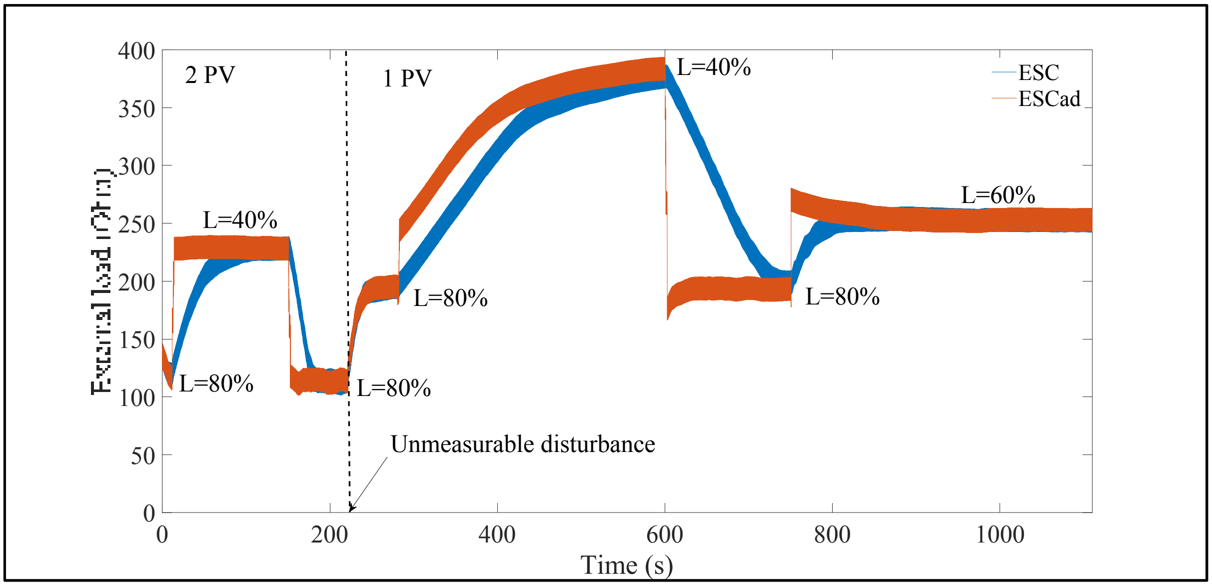

Figure 4.12 Evolution of the external load using ESC and ESC_{ad} schemes under unmeasurable disturbance and slow variation of luminance

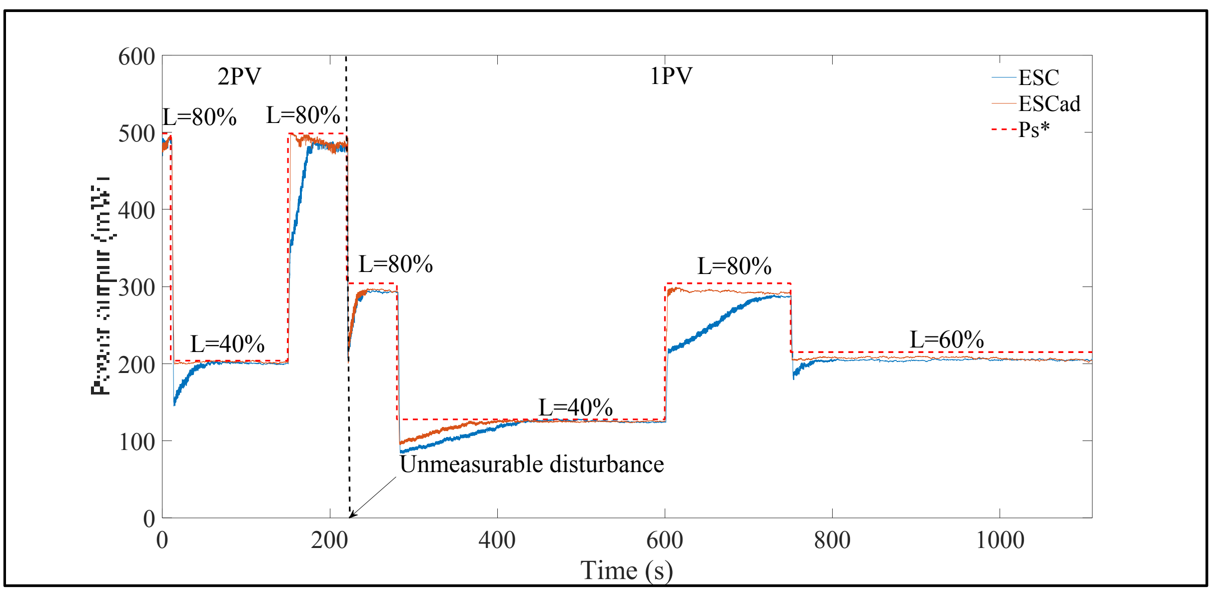

Figure 4.13 Evolution of the PV power output using ESC and ESC_{ad} schemes under unmeasurable disturbance and slow variation of luminance

Table 4.3 Performance of ESC and ESC_{ad} schemes under unmeasurable disturbance and slow variation of luminance

		2 PV panels		**From 2 to 1 PV panel**	**1 PV panel**		
		From L = 80% to L = 40%	**From L = 40% to L = 80%**	**L =80%**	**From L = 80% to L = 40%**	**From L = 40% to L = 80%**	**From L = 80% to L= 60%**
ESC	T_c(s)	104	24	27	320	118	22
	N_p	260	59	68	801	296	54
ESC_{ad}	T_c(s)	6	3	26	246	2.8	1
	N_p	12	7.0	66	614	7.0	2

The performance of both approaches under unmeasurable and high-frequency measurable disturbances was also evaluated (see Figure 4.14 and Figure 4.15). This time, the tracking efficiency of the ESC_{ad} and ESC approaches were respectively evaluated to be 96.1% and 81.0%.

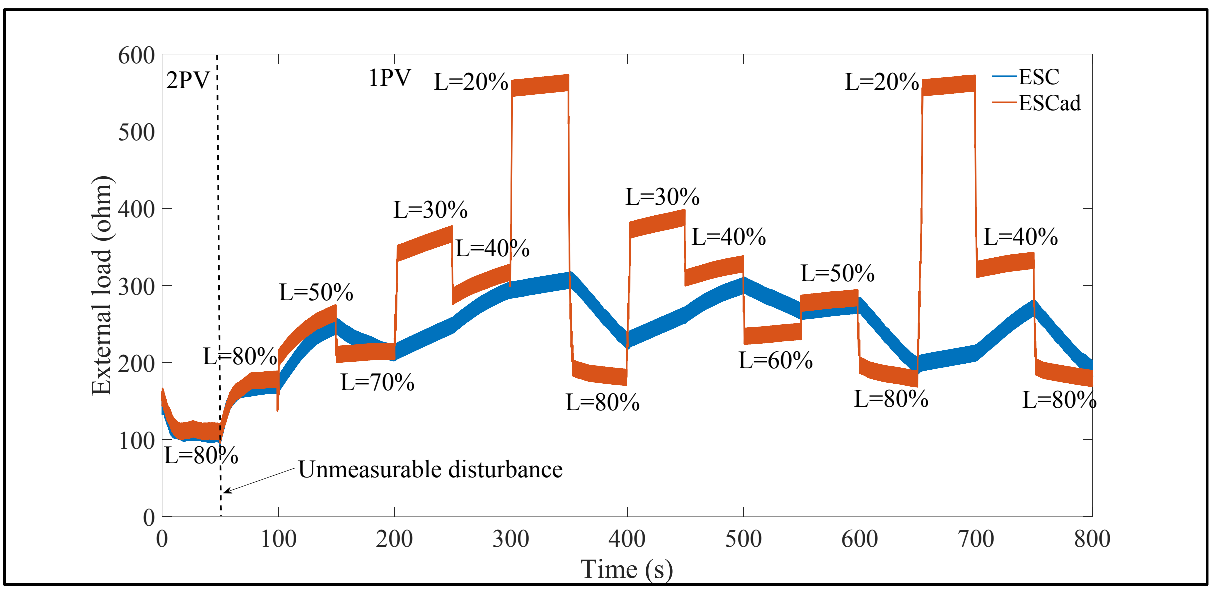

Figure 4.14 Evolution of external load using ESC and ESC_{ad} schemes under unmeasurable disturbance and rapid variation of luminance

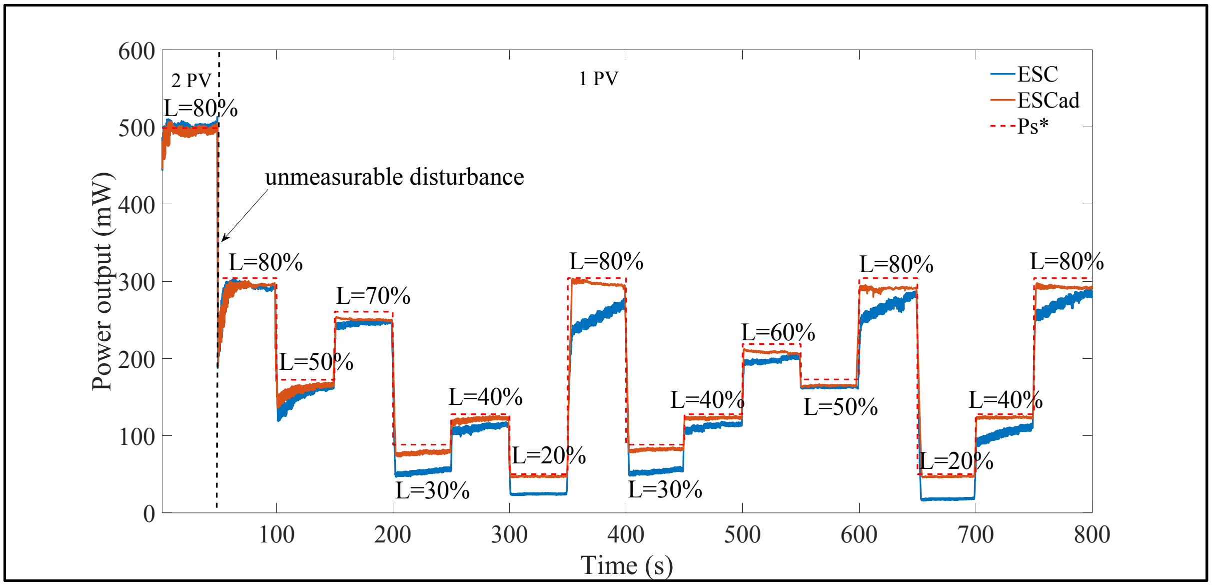

Figure 4.15 Evolution of the PV power output using ESC and ESC_{ad} schemes under unmeasurable disturbance and rapid variation of luminance

Note that if a DC-DC converter had been used, the convergence time T_c of the two optimization methods would have been reduced (Table 4.2 and Table 4.3). However, the number of periods N_p would have been the same since the frequency of the excitation signal is adjusted according to the system dynamics.

4.7 Conclusion

In this study, an adaptive neural-network model was used to add an anticipative action to the ESC approach in order to improve its performance to optimize in real-time a black box system under measurable and unmeasurable disturbances. The stability of the proposed approach is established and the performance improvement of the proposed ESC_{ad} method is confirmed through an experimental case study based on the real-time optimization of the power output of a PV system. Results obtained showed that the ESC_{ad} scheme is more efficient to track the power optimum under measurable and unmeasurable disturbances namely, luminance variation and PV system failure.

The $\mathrm{ESC_{ad}}$ scheme can be applied to other renewable energy sources and other complex or slow systems such as chemical systems or other types of renewable energy systems. Thus, in a near future, we would like to apply the proposed approach to a set of microbial fuel cells which are characterized by non-linear, complex and slow dynamics.

CONCLUSION

Dans le cadre de cette thèse, l'ESC est choisie comme méthode d'optimisation en temps réel afin d'optimiser un système dont la dynamique est inconnue et dont le point d'opération optimal varie en raison de perturbations externes. Dans cette thèse, on a d'abord montré qu'en raison de sa vitesse de convergence lente, l'ESC peut amener le système à converger vers un point de fonctionnement sous-optimal lorsque que des perturbations externes causant une variation importante et rapide du point d'opération optimal surviennent. Ce problème a été identifié pour deux types de systèmes différents, l'un ayant une dynamique plus lente (MFC) que l'autre (PV). Pour résoudre ce problème, trois nouvelles méthodes de commande extrémale sont proposées. Le principe général des trois méthodes consiste à intégrer une action anticipative à base d'un réseau de neurones multicouche dans la structure de l'ESC afin de prédire l'impact des perturbations externes sur le point de fonctionnement optimal du système et d'adapter en temps réel les paramètres de commande de l'ESC en fonction de cette prédiction. Ceci permet de ramener le système rapidement et précisément vers son point de fonctionnement réel.

L'amélioration de la performance de l'ESC avec les méthodes proposées a été démontrée théoriquement dans le cas de l'optimisation d'un système quelconque, en simulation dans le cas de l'optimisation d'une MFC et, expérimentalement, dans le cas de l'optimisation d'un système PV. La stabilité a également été établie. Les approches proposées peuvent être appliquées à une multitude d'autres systèmes puisque celles-ci ont la particularité de considérer le système comme une boîte noire.

Les deux premières méthodes visent l'adaptation des paramètres de l'ESC afin d'améliorer ses performances lorsque le système est soumis à des perturbations externes mesurables. La première méthode contrôle la condition initiale dans la commande extrémale avec l'utilisation de l'estimation de l'action anticipative comme un point de départ pour converger vers l'optimum réel à chaque fois que le système est soumis à l'effet de perturbations mesurables. Cette méthode diminue significativement l'effort requis par la boucle de commande extrémale pour amener le système à converger vers l'optimum, ce qui réduit significativement le temps de convergence et augmente l'efficacité de suivi de la méthode. Celle-ci augmente de 24% dans la situation où la MFC est soumise à une perturbation mesurable rapide, soit une variation de la concentration du substrat d'alimentation, S_0. L'efficacité de suivi augmente de 30% dans le cas de l'optimisation d'un système PV soumis à l'effet d'une variation rapide d'irradiance, G. La seconde méthode utilise l'estimation du point de fonctionnement optimal fournie par le modèle de réseau de neurones pour contrôler l'amplitude du signal d'excitation en fonction de l'impact de la perturbation mesurable sur l'erreur entre l'entrée du système et son optimum. Cette solution donne la possibilité de converger avec la vitesse maximale permise par l'ESC qui garantit la stabilité avec la meilleure précision possible autour de l'optimum. Il en résulte une augmentation de l'efficacité de suivi de l'optimum allant jusqu'à 20% pour un système PV soumis à l'effet d'une perturbation mesurable rapide, soit une variation d'irradiance, G.

Dans la troisième méthode, une action anticipative à base d'un réseau de neurones adaptif est intégrée afin d'ajuster les paramètres de commande de l'ESC lorsque le système est soumis à l'effet d'une perturbation, qu'elle soit mesurable ou non. Cette méthode est inspirée principalement de l'idée de la première méthode, mais une toute nouvelle structure est proposée afin de permettre l'adaptation en temps réel du modèle par réseau de neurones. Ainsi, une estimation de l'optimum du système est rendue possible malgré la présence de perturbations mesurables et non-mesurables. Par conséquent, la boucle d'ESC commence la recherche de l'optimum réel au voisinage de ce dernier quelque soit le type de perturbations externes. Cette fois, l'efficacité de suivi de l'optimum augmente jusqu'à 15 % pour le système PV en comparaison avec la méthode de perturbation.

RECOMMANDATIONS

Récemment, dans les laboratoires du GREPCI, des MFCs ont été construites afin de produire de l'électricité à partir d'un substrat d'alimentation solide. Ce type de piles a la capacité de générer de l'électricité à partir de la dégradation de matière organique qui se trouve dans les déchets alimentaires, dans les boues activées ou dans une autre matière organique solide. Les méthodes développées dans cette étude afin d'améliorer la performance de l'ESC sont validées en simulation lorsqu'on a un système lent à optimiser comme la MFC. Ainsi, un des objectifs dans nos recherches futures est de valider expérimentalement la performance des approches proposées en termes de vitesse de convergence et de précision et d'exploiter ces méthodes afin de maximiser la puissance produite par une MFC.

Pour ce qui est de l'approche proposée qui consiste à utiliser l'action anticipative pour contrôler l'amplitude du signal d'excitation, une amélioration possible serait de faire l'apprentissage du modèle par réseau de neurones en ligne. Ceci permettrait de converger rapidement et précisément vers l'optimum désiré, et ce, même en présence de perturbations non mesurables. Toutefois, dans une telle situation, le seuil de tolérance ne pourra être fixé à une valeur universelle pour chaque perturbation non-mesurable. Il faudra donc trouver une façon d'adapter ce paramètre également. Finalement, pour cette nouvelle approche, il faudra établir la preuve de stabilité.

Les approches proposées ont été appliquées à un système monovariable (SISO) constitué par une entrée de commande et une sortie, soumis à des perturbations externes. D'après (Dong et al., 2018; Ghaffari, Krstić, & Seshagiri, 2014), l'ESC peut également être utilisé afin d'optimiser un système multi variable (MIMO) constituée par plus d'une entrée de commande et par plus d'une sortie. Ainsi, une autre amélioration possible aux approches proposées vise leur adaptation aux systèmes MIMO soumis à des perturbations externes. Ceci permettrait par exemple l'application de ces méthodes à l'optimisation de systèmes constitués par plusieurs sources d'énergie renouvelable telles que des éoliennes, des panneaux photovoltaïques ou tout autre système MIMO soumis à des perturbations externes comme l'irradiance, la vitesse du vent et d'autres perturbations.

Dans certaines situations, la fonction de performance du système à optimiser peut être constituée de plusieurs optima, un optimum global et des optima locaux. Dans ce genre de problème d'optimisation, le rôle de la méthode d'optimisation en temps réel est d'éviter de converger vers l'un des optima locaux et d'assurer la convergence vers un optimum global. Dans un tel contexte, l'ESC, de par sa structure même, ne peut garantir qu'une convergence vers un optimum local (qui n'est pas nécessairement l'optimum global). La stabilité et l'amélioration de la performance de l'ESC en termes de temps de convergence et de précision avec les approches proposées ne sont prouvées que lorsque la fonction objectif du système est constituée d'un seul optimum. Ainsi, il faut étudier la capacité des méthodes proposées à converger vers un optimum global si la fonction objectif est constituée par plusieurs optima.

BIBLIOGRAPHIE

Adetola, V., Dehaan, D., & Guay, M. (2004). Adaptive extremum-seeking receding horizon control of nonlinear systems. Dans *American Control Conference, 2004. Proceedings of the 2004* (Vol. 4, pp. 2937-2942). IEEE.

Adetola, V., & Guay, M. (2006). Adaptive output feedback extremum seeking receding horizon control of linear systems. *Journal of Process Control, 16*(5), 521-533.

Ahmed, J., & Salam, Z. (2015). An improved perturb and observe (P&O) maximum power point tracking (MPPT) algorithm for higher efficiency. *Applied Energy, 150*, 97-108.

Ariyur, K. B., & Krstic, M. (2003). *Real-time optimization by extremum-seeking control*. New Jersey: John Wiley & Sons.

Åström, K. J., & Wittenmark, B. (2013). *Adaptive control* (2e éd.). Mineola, N.Y.: Dover Publications.

Azar, F. E., Perrier, M., & Srinivasan, B. (2011). A global optimization method based on multi-unit extremum-seeking for scalar nonlinear systems. *Computers & chemical engineering, 35*(3), 456-463.

Bahr, K. D., Jokiel, P. L., & Rodgers, K. u. S. (2016). Influence of solar irradiance on underwater temperature recorded by temperature loggers on coral reefs. *Limnology and Oceanography: Methods, 14*(5), 338-342.

Banavar, R. (2002). Extremum seeking loops with assumed functions: estimation and control. Dans *American Control Conference, 2002. Proceedings of the 2002* (Vol. 4, pp. 3159-3164). IEEE.

Banavar, R. (2003). Extremum seeking loops with quadratic functions: estimation and control. *International Journal of Control, 76*(14), 1475-1482.

Bhatnagar, P., & Nema, R. (2013). Maximum power point tracking control techniques: State-of-the-art in photovoltaic applications. *Renewable and Sustainable Energy Reviews, 23*, 224-241.

Bishop, C. M. (1995). *Neural networks for pattern recognition*. Oxford: Clarendon Press.

Bizon, N. (2013). Energy harvesting from the PV hybrid power source. *Energy, 52*, 297-307.

Bizon, N. (2016). Global Extremum Seeking Control of the power generated by a Photovoltaic Array under Partially Shaded Conditions. *Energy Conversion and Management, 109*, 71-85.

Bo, E., & Larsson, S. (2005). On a Parameter Adaptive Extremum Controller. Dans *Proceedings of the 44th IEEE Conference on Decision and Control* (pp. 4809-4814). IEEE.

Bonvin, D. (2017). *Real-Time Optimization*. Basel, Switzerland: MDPI.

Brunton, S. L., Rowley, C. W., Kulkarni, S. R., & Clarkson, C. (2010). Maximum power point tracking for photovoltaic optimization using ripple-based extremum seeking control. *IEEE transactions on power electronics, 25*(10), 2531-2540.

Burns, D. J., Laughman, C. R., & Guay, M. (2016). Proportional-integral extremum seeking for vapor compression systems. Dans *American Control Conference (ACC),* (pp. 2352-2357).

Burns, D. J., Weiss, W. K., & Guay, M. (2015). Realtime setpoint optimization with time-varying extremum seeking for vapor compression systems. Dans Dans *American Control Conference (ACC)* (pp. 974-979).

Chichka, D. F., Speyer, J. L., Fanti, C., & Park, C. G. (2006). Peak-seeking control for drag reduction in formation flight. *Journal of guidance, control, and dynamics, 29*(5), 1221-1230.

Chioua, M. (2008). *Synthèse d'algorithmes d'optimisation en-ligne par commande extrémale* (Thèse de doctorat, École polytechnique de Montréal, Montreal).

Clarke, D., & Godfrey, K. (1966). Simultaneous estimation of first and second derivatives of a cost function. *Electronics Letters, 2*(9), 338-339.

Cotton, N. J., & Wilamowski, B. M. (2011). Compensation of nonlinearities using neural networks implemented on inexpensive microcontrollers. *IEEE Transactions on Industrial Electronics, 58*(3), 733-740.

DeCarlo, R. A., Branicky, M. S., Pettersson, S., & Lennartson, B. (2000). Perspectives and results on the stability and stabilizability of hybrid systems. *Proceedings of the IEEE, 88*(7), 1069-1082.

Di Piazza, M. C., & Pucci, M. (2016). Induction-Machines-Based Wind Generators With Neural Maximum Power Point Tracking and Minimum Losses Techniques. *IEEE Transactions on Industrial Electronics, 63*(2), 944-955.

Dicks, A. L., & Rand, D. A. (2018). *Fuel cell systems explained*. John Wiley & Sons.

Dong, L., Li, Y., Salsbury, T. I., House, J. M., & Wu, Z. (2018). Multi-variable extremum seeking control for a multi-functional variable refrigerant flow system. *Science and Technology for the Built Environment, 24*(4), 382-395.

Draper, C. S., & Li, Y. T. (1951). *Principles of optimalizing control systems and an application to the internal combustion engine*. American Society of Mechanical Engineers.

Dürr, H.-B., Krstić, M., Scheinker, A., & Ebenbauer, C. (2015). Singularly perturbed Lie bracket approximation. *IEEE Transactions on Automatic Control, 60*(12), 3287-3292.

Dürr, H.-B., Stanković, M. S., Ebenbauer, C., & Johansson, K. H. (2013). Lie bracket approximation of extremum seeking systems. *Automatica, 49*(6), 1538-1552.

Ebrahimi-Moghadam, A., Mohseni-Gharyehsafa, B., & Farzaneh-Gord, M. (2018). Using artificial neural network and quadratic algorithm for minimizing entropy generation of Al 2 O 3-EG/W nanofluid flow inside parabolic trough solar collector. *Renewable energy, 129*, 473-485.

Eltawil, M. A., & Zhao, Z. (2013). MPPT techniques for photovoltaic applications. *Renewable and Sustainable Energy Reviews, 25*, 793-813.

Jean-Louis, B., Miguel Arias, C., Adnan, Z. A., & Arthouros, Z. (2016). We Got Power: Because We Save Energy, Use Renewables and Save Energy. *Distributed Generation & Alternative Energy Journal, 31*(1), 5-6.

Enslin, J. H., Wolf, M. S., Snyman, D. B., & Swiegers, W. (1997). Integrated photovoltaic maximum power point tracking converter. *IEEE Transactions on Industrial Electronics, 44*(6), 769-773.

Esmaeil-Zadeh-Azar, F. (2010). *An efficient global optimization method based on multi-unit extremum seeking* (Thèse de doctorat, École Polytechnique de Montréal, Montreal).

Esram, T., & Chapman, P. L. (2007). Comparison of photovoltaic array maximum power point tracking techniques. *IEEE Transactions on energy conversion, 22*(2), 439-449.

Fadare, D. (2009). Modelling of solar energy potential in Nigeria using an artificial neural network model. *Applied energy, 86*(9), 1410-1422.

Fathabadi, H. (2016a). Novel high accurate sensorless dual-axis solar tracking system controlled by maximum power point tracking unit of photovoltaic systems. *Applied Energy, 173*, 448-459.

Fathabadi, H. (2016b). Novel highly accurate universal maximum power point tracker for maximum power extraction from hybrid fuel cell/photovoltaic/wind power generation systems. *Energy, 116*, 402-416.

Gao, W., Hernández, R., & Engell, S. (2016). A Study of Explorative Moves during Modifier Adaptation with Quadratic Approximation. *Processes, 4*(4), 45.

Ghaffari, A., Krstić, M., & Nešić, D. (2012). Multivariable Newton-based extremum seeking. *Automatica, 48*(8), 1759-1767.

Ghaffari, A., Krstić, M., & Seshagiri, S. (2014). Power optimization for photovoltaic microconverters using multivariable newton-based extremum seeking. *IEEE Transactions on Control Systems Technology, 22*(6), 2141-2149.

Giovanni, P., Carlos Andres, R.-P., & Giovanni, S. (2016). PV Models. Dans Wiley-IEEE Press, *Photovoltaic Sources Modeling* (pp. 1-27). doi: 10.1002/9781118755877.ch1.

Golden, M. P., & Ydstie, B. E. (1989). Adaptive extremum control using approximate process models. *AIChE Journal, 35*(7), 1157-1169.

Guay, M., Dochain, D., & Perrier, M. (2004). Adaptive extremum seeking control of continuous stirred tank bioreactors with unknown growth kinetics. *Automatica, 40*(5), 881-888.

Guay, M., & Zhang, T. (2003). Adaptive extremum seeking control of nonlinear dynamic systems with parametric uncertainties. *Automatica, 39*(7), 1283-1293.

Guay, M. (2014). A time-varying extremum-seeking control approach for discrete-time systems. *Journal of Process Control, 24*(3), 98-112.

Guay, M. (2015). Proportional-integral extremum-seeking control. *IFAC-PapersOnLine, 48*(8), 675-680.

Guay, M., & Dochain, D. (2017). A proportional-integral extremum-seeking controller design technique. *Automatica, 77*, 61-67.

Gürgen, S., Ünver, B., & Altın, İ. (2018). Prediction of cyclic variability in a diesel engine fueled with n-butanol and diesel fuel blends using artificial neural network. *Renewable energy, 117*, 538-544.

Haber, R. (1986). Adaptive extremum value control based on the parametric Volterra model. *Meres es automatika, 34*(12), 463-469.

Haijun, L., Lucai, W., Zhaosheng, T., Houde, D., & Songhui, L. (2017). Optimization for a Neural Network Based on Input-Vectors Correlation and Its Application to a Truck Scale. *IEEE Transactions on Industrial Electronics*, *64*(6), 4917-4927.

Haring, M. A. (2016). *Extremum-seeking control: convergence improvements and asymptotic stability* (Thèse de doctorat, Norwegian University of Science and Technology, Norway).

Hatti, M. (2018). *Artificial Intelligence in Renewable Energetic Systems: Smart Sustainable Energy Systems* (Vol. 35). Springer.

Heng, S. Y., Asako, Y., Suwa, T., & Nagasaka, K. (2018). Transient thermal prediction methodology for parabolic trough solar collector tube using artificial neural network. *Renewable energy*.

Kato Marcus, A., Torres, C. I., & Rittmann, B. E. (2007). Conduction-based modeling of the biofilm anode of a microbial fuel cell. *Biotechnology and Bioengineering, 98*(6), 1171-1182.

Kazakevich, V. (1944). *On extremum seeking* (Thèse de doctorat, Moscow High Technical University, Moscow).

Kebir, A., Akhrif, O., & Woodward, L. (2016). Extremum-seeking control of a microbial fuel cell power using adaptive excitation. Dans *Industrial Electronics Society, IECON 2016-42nd Annual Conference of the IEEE* (pp. 4127-4132). IEEE.

Kebir, A., Woodward, L., & Akhrif, O. (2015). Extremum-seeking control with anticipative action of microbial fuel cell's power. Dans *Control and Automation (MED), 2015 23th Mediterranean Conference on* (pp. 933-939). IEEE.

Kebir, A., Woodward, L., & Akhrif, O. (2018). Extremum-seeking control with adaptive excitation: application to a photovoltaic system. *IEEE Transactions on Industrial Electronics, 65*(3), 2507-2517.

Khalil, H. K. (1996). *Nonlinear systems* (2nd ed. éd.). Upper Saddle River, N.J.: Prentice-Hall.

Khalil, H. K. (2002). *Nonlinear systems* (3rd ed. éd.). Upper Saddle River, N.J.: Prentice Hall.

Khan, O., & Xiao, W. (2016). Integration of Start–Stop Mechanism to Improve Maximum Power Point Tracking Performance in Steady State. *IEEE Transactions on Industrial Electronics, 63*(10), 6126-6135.

Khong, S. Z., Nešić, D., Manzie, C., & Tan, Y. (2013). Multidimensional global extremum seeking via the DIRECT optimisation algorithm. *Automatica, 49*(7), 1970-1978.

Khong, S. Z., NešIć, D., Tan, Y., & Manzie, C. (2013). Unified frameworks for sampled-data extremum seeking control: Global optimisation and multi-unit systems. *Automatica, 49*(9), 2720-2733.

Kohata, Y., Yamauchi, K., & Kurihara, M. (2010). High-Speed Maximum Power Point Tracker for Photovoltaic Systems Using Online Learning Neural Networks. *JACIII, 14*(6), 677-682.

Krstic, M. (2013). Extremum Seeking Control. Dans J. Baillieul & T. Samad (Éds.), *Encyclopedia of Systems and Control* (pp. 1-5). London: Springer London.

Krstić, M. (2000). Performance improvement and limitations in extremum seeking control. *Systems & Control Letters, 39*(5), 313-326.

Krstić, M., & Wang, H.-H. (2000). Stability of extremum seeking feedback for general nonlinear dynamic systems. *Automatica, 36*(4), 595-601.

Laaroussi, A., Ajana, S., Bakkali, S., Faraj, K., & Cherkaoui, O. (2017). E-learning Foresight for Renewable Energy Technology in Higher Education in Morocco. Dans *Europe and MENA Cooperation Advances in Information and Communication Technologies* (pp. 13-23). Springer.

Larsson, S. (2001). *Literature study on extremum control*. (Technical report). Göteborg: Control and Automation Laboratory Chalmers University of Technology.

Leblanc, M. (1922). Sur l'electrification des chemins de fer au moyen de courants alternatifs de fréquence élevée. *Revue générale de l'électricité, 12*(8), 275-277.

Leyva, R., Alonso, C., Queinnec, I., Cid-Pastor, A., Lagrange, D., & Martínez-Salamero, L. (2006). MPPT of photovoltaic systems using extremum-seeking control. *IEEE transactions on aerospace and electronic systems, 42*(1), 249-258.

Lin, H., Wang, L., Teng, Z., Dai, H., & Li, S. (2017). Optimization for a Neural Network Based on Input-Vectors Correlation and Its Application to a Truck Scale. *IEEE Transactions on Industrial Electronics*.

Liu, K., & Zhu, Z.-Q. (2015). Position-offset-based parameter estimation using the adaline NN for condition monitoring of permanent-magnet synchronous machines. *IEEE Transactions on Industrial Electronics, 62*(4), 2372-2383.

Liu, Y.-H., Liu, C.-L., Huang, J.-W., & Chen, J.-H. (2013). Neural-network-based maximum power point tracking methods for photovoltaic systems operating under fast changing environments. *Solar Energy, 89*, 42-53.

Mamarelis, E., Petrone, G., & Spagnuolo, G. (2014). A two-steps algorithm improving the P&O steady state MPPT efficiency. *Applied Energy, 113*, 414-421.

Manobel, B., Sehnke, F., Lazzús, J. A., Salfate, I., Felder, M., & Montecinos, S. (2018). Wind turbine power curve modeling based on Gaussian Processes and Artificial Neural Networks. *Renewable energy, 125*, 1015-1020.

Marinkov, S., de Jager, B., & Steinbuch, M. (2014). Extremum seeking control with data-based disturbance feedforward. Dans *American Control Conference (ACC), 2014* (pp. 3627-3632). IEEE.

Michalowsky, S., & Ebenbauer, C. (2015). Model-based extremum seeking for a class of nonlinear systems. Dans *American Control Conference (ACC), 2015* (pp. 2026-2031). IEEE.

Moase, W. H., & Manzie, C. (2012a). Fast extremum-seeking for Wiener–Hammerstein plants. *Automatica, 48*(10), 2433-2443.

Moase, W. H., & Manzie, C. (2012b). Semi-global stability analysis of observer-based extremum-seeking for Hammerstein plants. *IEEE Transactions on Automatic Control, 57*(7), 1685-1695.

Moase, W. H., Manzie, C., & Brear, M. J. (2009a). Newton-like extremum-seeking part I: Theory. Dans *Decision and Control, 2009 held jointly with the 2009 28th Chinese Control Conference. CDC/CCC 2009. Proceedings of the 48th IEEE Conference on* (pp. 3839-3844). IEEE.

Moase, W. H., Manzie, C., & Brear, M. J. (2009b). Newton-like extremum-seeking part II: Simulations and experiments. Dans *Decision and Control, 2009 held jointly with the 2009 28th Chinese Control Conference. CDC/CCC 2009. Proceedings of the 48th IEEE Conference on* (pp. 3845-3850). IEEE.

Moase, W. H., Manzie, C., & Brear, M. J. (2010). Newton-like extremum-seeking for the control of thermoacoustic instability. *IEEE Transactions on Automatic Control, 55*(9), 2094-2105.

Moshksar, E., Ghanbari, T., Samet, H., & Guay, M. (2018). Estimation-Based Extremum-Seeking Control: A Real-Time Approach for Improving Energy Efficiency in Photovoltaic Systems. *IEEE Systems Journal*, 1-12. doi: 10.1109/JSYST.2018.2868125

Moshksar, E., & Guay, M. (2016). Almost invariant manifold approach for adaptive estimation of periodic and aperiodic unknown time-varying parameters. *International Journal of Adaptive Control and Signal Processing, 30*(1), 76-92.

Mohammadi, A., Manzie, C., & Nešić, D. (2014). Online optimization of spark advance in alternative fueled engines using extremum seeking control. *Control Engineering Practice, 29*, 201-211.

Mohandes, M., Rehman, S., & Halawani, T. (1998). Estimation of global solar radiation using artificial neural networks. *Renewable energy, 14*(1-4), 179-184.

Moradi, M. H., & Reisi, A. R. (2011). A hybrid maximum power point tracking method for photovoltaic systems. *Solar Energy, 85*(11), 2965-2976.

Nesic, D., Mohammadi, A., & Manzie, C. (2013). A framework for extremum seeking control of systems with parameter uncertainties. *IEEE Transactions on Automatic Control, 58*(2), 435-448.

Nesic, D., Ying, T., Manzie, C., Mohammadi, A., & Moase, W. (2012). A unifying framework for analysis and design of extremum seeking controllers. Dans *2012 24th Chinese Control and Decision Conference (CCDC), 23-25 May 2012* (pp. 4274-4285). IEEE.

Nesic, D., Ying, T., & Mareels, I. (2006). On the choice of dither in extremum seeking systems: a case study. Dans *Proceedings of the 45th IEEE Conference on Decision and Control, 13-15 Dec. 2006* (pp. 6 pp.). IEEE.

Nesic, D., Tan, Y., Moase, W. H., & Manzie, C. (2010). A Unifying Approach to Extremum Seeking: Adaptive Schemes Based on Estimation of Derivatives. Dans *2010 49th IEEE Conference on Decision and Control (CDC 2010), 15-17 Dec. 2010* (pp. 4625-4630). IEEE.

Nikhil, G., Chaitanya, D. K., Srikanth, S., Swamy, Y., & Mohan, S. V. (2018). Applied resistance for power generation and energy distribution in microbial fuel cells with rationale for maximum power point. *Chemical Engineering Journal, 335*, 267-274.

Noguchi, T., Togashi, S., & Nakamoto, R. (2002). Short-current pulse-based maximum-power-point tracking method for multiple photovoltaic-and-converter module system. *IEEE Transactions on Industrial Electronics, 49*(1), 217-223.

Oliveira, T. R., Krstić, M., & Tsubakino, D. (2017). Extremum seeking for static maps with delays. *IEEE Transactions on Automatic Control, 62*(4), 1911-1926.

Ostrovskii, I. I. (1957). Extremum regulation. *Automatic and Remote Control, 18*, 900-907.

Peterson, K. S., & Stefanopoulou, A. G. (2004). Extremum seeking control for soft landing of an electromechanical valve actuator. *Automatica, 40*(6), 1063-1069.

Picioreanu, C., Katuri, K., Head, I., van Loosdrecht, M. C., & Scott, K. (2008). Mathematical model for microbial fuel cells with anodic biofilms and anaerobic digestion. *Water science and technology, 57*(7), 965-971.

Pinto, R., Srinivasan, B., Manuel, M.-F., & Tartakovsky, B. (2010). A two-population bio-electrochemical model of a microbial fuel cell. *Bioresource technology, 101*(14), 5256-5265.

Qi, W., Liu, J., Chen, X., & Christofides, P. D. (2011). Supervisory predictive control of standalone wind/solar energy generation systems. *IEEE transactions on control systems technology, 19*(1), 199-207.

Rahbar, K., Xu, J., & Zhang, R. (2015). Real-time energy storage management for renewable integration in microgrid: An off-line optimization approach. *IEEE Transactions on Smart Grid, 6*(1), 124-134.

Ram, J. P., Rajasekar, N., & Miyatake, M. (2017). Design and overview of maximum power point tracking techniques in wind and solar photovoltaic systems: A review. *Renewable and Sustainable Energy Reviews, 73*, 1138-1159.

Reisi, A. R., Moradi, M. H., & Jamasb, S. (2013). Classification and comparison of maximum power point tracking techniques for photovoltaic system: A review. *Renewable and Sustainable Energy Reviews, 19*, 433-443.

Roberts, P. (1979). An algorithm for steady-state system optimization and parameter estimation. *International Journal of Systems Science, 10*(7), 719-734.

Ryan, J. J. (2012). *A method of extremum seeking control based on a time varying Kalman filter and its application to formation flight* (Thèse de doctorat, University of California, Los Angeles).

Ryan, J. J., & Speyer, J. L. (2010). Peak-seeking control using gradient and hessian estimates. Dans *American Control Conference (ACC), 2010* (pp. 611-616). IEEE.

Salas, V., Olias, E., Lazaro, A., & Barrado, A. (2005). Evaluation of a new maximum power point tracker (MPPT) applied to the photovoltaic stand-alone systems. *Solar energy materials and solar cells, 87*(1), 807-815.

Scheinker, A., & Krstic, M. (2013). Minimum-seeking for CLFs: Universal semiglobally stabilizing feedback under unknown control directions. *IEEE Transactions on Automatic Control, 58*(5), 1107-1122.

Scheinker, A., & Krstić, M. (2014). Extremum seeking with bounded update rates. *Systems & Control Letters, 63*, 25-31.

Sharafi, J., Moase, W. H., & Manzie, C. (2015). Fast extremum seeking on Hammerstein plants: A model-based approach. *Automatica, 59*, 171-181.

Shorten, R., & Narendra, K. (1998). On the stability and existence of common Lyapunov functions for stable linear switching systems. Dans *Decision and Control, 1998. Proceedings of the 37th IEEE Conference on* (Vol. 4, pp. 3723-3724). IEEE.

Speyer, J., Banavar, R., Chichka, D., & Rhee, I. (2000). Extremum seeking loops with assumed functions. Dans *Decision and Control, 2000. Proceedings of the 39th IEEE Conference on* (Vol. 1, pp. 142-147). IEEE.

Shanmuganathan, S., & Samarasinghe, S. (2016). *Artificial neural network modelling* (Vol. 628). Warsaw: Springer.

Srinivasan, B. (2007). Real-time optimization of dynamic systems using multiple units. *International Journal of Robust and Nonlinear Control, 17*(13), 1183-1193.

Taha, H. A. (2017). *Operations Research: An Introduction* (10 éd.). London: Pearson.

Tan, Y., Moase, W., Manzie, C., Nešić, D., & Mareels, I. (2010). Extremum seeking from 1922 to 2010. Dans *Control Conference (CCC), 2010 29th Chinese* (pp. 14-26). IEEE.

Tan, Y., Nešić, D., & Mareels, I. (2006). On non-local stability properties of extremum seeking control. *Automatica, 42*(6), 889-903.

Tan, Y., Nešić, D., & Mareels, I. (2008). On the choice of dither in extremum seeking systems: A case study. *Automatica, 44*(5), 1446-1450.

Tan, Y., Nešić, D., Mareels, I. M., & Astolfi, A. (2009). On global extremum seeking in the presence of local extrema. *Automatica, 45*(1), 245-251.

Toloue, S. F., & Moallem, M. (2017). Multivariable sliding-mode extremum seeking control with application to MPPT of an alternator-based energy conversion system. *IEEE Transactions on Industrial Electronics, 64*(8), 6383-6391.

Verma, D., Nema, S., Shandilya, A., & Dash, S. K. (2016). Maximum power point tracking (MPPT) techniques: Recapitulation in solar photovoltaic systems. *Renewable and Sustainable Energy Reviews, 54*, 1018-1034.

Walsh, A., Forbes, J. R., Chee, S. A., & Ryan, J. J. (2017). Kalman-Filter-Based Unconstrained and Constrained Extremum-Seeking Guidance on SO (3). *Journal of Guidance, Control, and Dynamics*, 1-12.

Wang, Y., Li, Y., & Ruan, X. (2016). High-accuracy and fast-speed MPPT methods for PV string under partially shaded conditions. *IEEE Transactions on Industrial Electronics, 63*(1), 235-245.

Woodward, L., Perrier, M., & Srinivasan, B. (2009). Improved performance in the multi-unit optimization method with non-identical units. *Journal of Process Control, 19*(2), 205-215.

Woodward, L., Perrier, M., Srinivasan, B., Pinto, R., & Tartakovsky, B. (2010). Comparison of real-time methods for maximizing power output in microbial fuel cells. *AIChE Journal, 56*(10), 2742-2750.

Xia, C., Zhang, D., Pedrycz, W., Zhu, Y., & Guo, Y. (2018). Models for microbial fuel cells: a critical review. *Journal of Power Sources, 373*, 119-131.

Yadav, S. R., & Malik, A. K. Operations Research: Oxford University Press.

Yin, C., Chen, Y., & Zhong, S.-m. (2014). Fractional-order sliding mode based extremum seeking control of a class of nonlinear systems. *Automatica, 50*(12), 3173-3181.

Yu, G., Jung, Y., Choi, J., & Kim, G. (2004). A novel two-mode MPPT control algorithm based on comparative study of existing algorithms. *Solar Energy, 76*(4), 455-463.

Zhang, C., & Ordonez, R. (2007). Numerical optimization-based extremum seeking control with application to ABS design. *IEEE Transactions on Automatic Control, 52*(3), 454-467.

Zhang, C., & Ordónez, R. (2005). Numerical optimization-based extremum seeking control of LTI systems. Dans *Proceedings of the 44th IEEE Conference on Decision and Control* (pp. 4428-4433). IEEE.

Zhang, C., & Ordóñez, R. (2011). *Extremum-seeking control and applications: a numerical optimization-based approach*. London: Springer Science & Business Media.

Zhang, C., Siranosian, A., & Krstić, M. (2007). Extremum seeking for moderately unstable systems and for autonomous vehicle target tracking without position measurements. *Automatica, 43*(10), 1832-1839.

Zhang, R., & Tao, J. (2016). Data driven modeling using improved multi-objective optimization based neural network for coke furnace system. *IEEE Transactions on Industrial Electronics*.

Zhang, T., & Guay, M. (2005). Adaptive control of uncertain continuously stirred tank reactors with unknown actuator nonlinearities. *ISA transactions, 44*(1), 55-68.